TECHNICAL AND VOCATIONAL TRAINING INSTITUTE (TVTI)

School of Graduate Studies

FACULTY OF ELECTRICAL AND ELECTRONICS TECHNOLOGY AND INFORMATION AND COMMUNICATION TECHNOLOGY (DEPARTMENT OF ELECTRICAL AND ELECTRONICS TECHNOLOGY)

Pitch angle control of fixed wing airplane autopilot using artificial neural networks based model reference adaptive control

In partial fulfillment for the Degree

MASTER OF SCIENCE *in* ELECTRICAL AUTOMATION AND CONTROL TECHNOLOGY MANAGEMENT

By,

Bantalem Dagne (MTR/482/13)

Supervisor,

Dr. Lebsework Negash

AUGUST 2022

Addis Ababa, Ethiopia

PITCH ANGLE CONTROL OF FIXED WING AIRPLANE AUTOPILOT USING ARTIFICIAL NEURAL NETWORKS BASED MODEL REFERENCE ADAPTIVE CONTROL

A Thesis submitted to

TECHNICAL AND VOCATIONAL TRAINING INSTITUTE (TVTI)

FACULTY OF ELECTRICAL AND ELECTRONICS TECHNOLOGY AND INFORMATION AND COMMUNICATION TECHNOLOGY (DEPARTMENT OF ELECTRICAL AND ELECTRONICS TECHNOLOGY)

In partial fulfillment for the Degree

MASTER OF SCIENCE *in* ELECTRICAL AUTOMATION AND CONTROL TECHNOLOGY MANAGEMENT

By,

Bantalem Dagne (MTR/482/13)

Supervisor,

Lebsework Negash (PhD)

Declaration

I hereby declare that this thesis entitled; "**Pitch angle control of fixed wing airplane autopilot using artificial neural network based model reference adaptive control**" is the original work of my own, has not been presented for a master's thesis in this or other universities and all sources of materials used for this thesis work have been fully acknowledged.

Name: **Bantalem Dagne** (MTR/482/13)

Signature: 

Place: Addis Ababa, Ethiopia

Date of Submission: 31-08-2022

This thesis has been submitted to my Institute advisor for approval at TVTI advisor.

Name: Dr. **Lebsework Negash**

Signature: .....

Date: August 30/2022

TECHNICAL AND VOCATIONAL TRAINING INSTITUTE (TVTI)
SCHOOL OF POSTGRADUATE STUDIES

Thesis On

Pitch angle control of fixed wing airplane autopilot using Artificial Neural Network based model reference adaptive control

By,

Bantalem Dagne (MTR/482/13)

APPROVED BY THESIS ADVISOR COMMITTE

Name of the Advisor	Signature	Date
Dr. Lebsework Negash	----------	August 30/2022

Name of Examiner Internal	Signature	Date
Dr. Saravanakumar Gurusamy	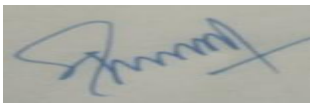	31-08-2022

Name of Examiner, Internal	Signature	Date
Seifu Getahun		30- 08-2022

Name of Examiner, External	Signature	Date
Dr. Eskinder Anteneh	----------	29/08/22

Acknowledgments

This thesis work would not be possible without the help of my advisor, Dr. Lebsework Negash who has supported me by giving his invaluable guidance, encouragement, advice and suggestions throughout my thesis work, and also who has given me the strength and ability to do this research. Also, I thank the academic members of the electrical automation& control technology department teacher for their comments and advice starting from the thesis proposal. The feedback inspired me to work diligently on my thesis. At last, I want to express my gratitude to my relatives for their encouragement, backing, and persistence.

ABSTRACT

This thesis investigates the advantages of an adaptive control based on the artificial neural network for the control of pitch angle of fixed-wing airplane autopilot systems. Flight control of a fixed-wing airplane is not suitable to work on due to unstable and time-varying conditions. Therefore, Lyapunov's stability analysis in a direct model reference based on artificial neural networks strategy has been applied, for the control of a fixed-wing airplane. The autopilot is one of the vital parts of flying airplanes which establishes stability and accomplishment of the desired flight control. The difference between the fixed-wing airplane response and the target application as provided by the reference model is used to train an adaptive neural network. This controller was investigated through the development of an appropriate reference model for the required airplane performance. The suggested neural net-based adaptive reference control system can be improved system behavior. The aerodynamic stability coefficients and longitudinal derivatives were used to determine the aircraft's dynamic equations. The outcomes demonstrate that the system structure that was built is suitable for testing the longitudinal controllers. By analyzing the findings, the effectiveness of the suggested control strategy is confirmed in MATLAB/Simulink software by assessing the various varieties of control parameters. In short period oscillation model, results show that the proposed controller is better than other controllers with a rise time of 0.1748 seconds & a settling time of 0.6633 seconds, compared to the classical model reference adaptive control's rise time of 0.7557 seconds and settling time of 1.3324 seconds, and the proportional integral & derivatives' rise time of 1.5895 seconds and settling time of 2.9289 seconds.

Keywords: *adaptive control, Artificial Neural Network (ANN), Lyapunov's, fixed wing airplane, autopilot, model reference adaptive control (MRAC)*

Table of Contents

List of tables

List of Figures

List of symbols

α_{ax} ,α_{ay}, α_{az}	X, Y,Z time derivative of the V_a in f_b dimension
a_{nx}	Z-body x, y & z gray scope production at CoG.
α_t	Angle of attack of the tail
C_L	lift coefficients
C_{Lwb}	Lift coefficient of the wing/body
C_{Lt}	Lift of the tail unit
C_D	drag coefficient
C_Y	Side force coefficient
$\overline{CF}^S$	Transformation from stability to wind frame
C_{wS}	Stability to wind
$\overline{c}$	aerodynamic chord
c	Mean aerodynamic chord
C_l	Rolling moment coefficient
C_m	Pitching moment coefficient due to angle of attack
C_n	Yawing moment coefficient
C_z	Normal force coefficient due to angle of attack
D	Air flow force along to X wind direction
E	Error
F	Flight envelope
F	Forces
F_b	Force in body frame
$F_{xA,}F_{yA}F_{zA}$	Air flow forces starting wind direction of (D,Y,L)
G	velocity due to gravitational force
h	Height
h_0	Aerodynamic center position on reference chord
H_{cg}	CoG direction on orientation chord
I_x I_y ,I_z	Rolling, Pitching, Yawing motion of inertia

K	Controller gain; Drag factor due to lift
L	Air flow force along the Z wind direction
l	Rolling moment in body axis
l_t	Gap of AC &f_b
M	pitching motion in body axis
M	Mass
$M_{\delta e}$, Mq, $M_{\Delta t}$	Pitching motion owing to pitch rate, Elevator Deflection , Derivative, Thrust Deflection
Mu	Compressible Effect Derivative
M	Pitching moment due to downward velocity
N	Yawing moment in body axis
N	Normal load factor per unit angle of attack
n_x	Airplane specific quantities
P	Equilibrium point
Q	Dynamic pressure
$Q_{aircraft}$	Present Dynamic Pressure of the Aircraft
R_{BV}	Transformation body-fixed
S	Wing reference area
s_t	Tail plan form area
U	velocity of body x axs
U_e	Axial component of steady equilibrium velocity
v	Total velocity
V	air speed
V_a	Vector airspeed
V_B	Body- fixed system
V_V	Velocity vector vertical frame
U	Axial velocity perturbation
u_c	Controller signal
V_B	Velocity the airplane

v_0	Steady equilibrium velocity
W	velocity of body z axs
W_g	Normal wind velocity perturbation
w_B	Wind velocity
X	track angle
Xu	Stability Derivative
Xw	Angle of Attack Derivative
Xq	Pitch Rate Derivative
$Xcg,\ Ycg,\ Zcg$	$X,Y,\ Z$ position of the COG in *fm*
$X_{APT1,2}$, $Y_{APT1,2}$, $Z_{APT1,2}$	X , Y,Z direction of engine 1st& 2nd application site of force in FM
y	Plant output
y_m	Reference output
Zu	Stability Derivative
Zw	Angle of Attack Derivative
Z_U	Normal force due to downward velocity
Z_q	Normal force due to pitch rate
$\delta_A, \delta_E, \delta_R, \delta_{Th}$	Deflection of aileron, elevator, rudder, Throttle

Greek letter

α	Angle of attack
β	Sideslip angle
q	Pitch rate
θ	Pitch angle
ϕ	Roll angle
δ_e	Elevator deflection
ζ	Damping ratio
ε	Down-wash
ψ	yaw Euler angle
γ	Flight path angle
ω	Rotational velocity

Abbreviations

AC	Aerodynamic Centre
AP	Autopilot
ANNs	Artificial neural networks
CoG	Centre of Gravity
MRAC(S)	Model reference adaptive control (system)
DMRAC(S)	Direct model reference adaptive control(system)
NNs	Neural networks
PID	Proportional integral derivatives
RNN	Recurrent neural network
RBF	Radial neural network
SPO	Short Period Oscillation
UAV	Unmanned Aerial Vehicle

CHAPTER ONE
INTRODUCTION

1.1. Background of the study

Fixed wing plane have increased its movement in the world nowadays. Implementations of this plane are incorporating inspection of disaster influenced regions, look and protect, inaccessible detecting, accuracy agribusiness, border watch, airborne photography, control line review, checking package, transportation, etc. to realize tall levels of independence the plane framework requires sensors, actuators, and computational gadget or autopilot. The autopilot must be modified with estimation and control calculations for handling sensor inputs and giving actuator yields. Instruction approximately an essential to encourage investigate and advancement of independent airplane. Understudies huge since inserted autopilots are complex to alter and common reenactment program does not constantly decipher the autopilot code [1]. MRAC Engineering was created within the 1950s for the plan of air-ship autopilot to bargain with vulnerabilities aimed the flight period. One of the most crucial techniques is model reference adaptive control plans utilized. Recently, MRAC has gotten impressive consideration, and numerous and unused approaches have been connected to the down to earth prepare [2]. Within model reference adaptive control system, the regulator is outlined to understand the airplane yield meets to orientation to demonstrate yield resting on presumption that airplane be able to be direct [3]. In later, a long time, ANN has ended up exceptionally well known in numerous controls applications because of their faster processing speeds and ability to work with irregular systems [4].

1.1.1. Fundamentals of Artificial Neural

The creator of the earliest neuron-computers, Robert Hecht Nielen, offers the clearest explanation of a neural net, which is further correctly referred to as an ANN. According to his definition, an artificial neural network (ANN) is a computing system made up of a number of simple but intricately coupled processing elements that analyze data in response to changes in their dynamic states. Artificial neural networks are processing systems that, though in much smaller dimensions, are based on the neural architecture of the mammalian cerebral cortex. Even though a man's mental mind has 1,000,000,000 neurons, because of matching rise in the size of its ability to respond and develop performance, a big artificial neural network may have a many number of processor units.

ANNs are frequently set in layers. Numerous nodes that are linked to one another and each have an activation function make up layers. The connection between the hidden neurons and the output neurons, in which the response is given, is shown in the following picture.

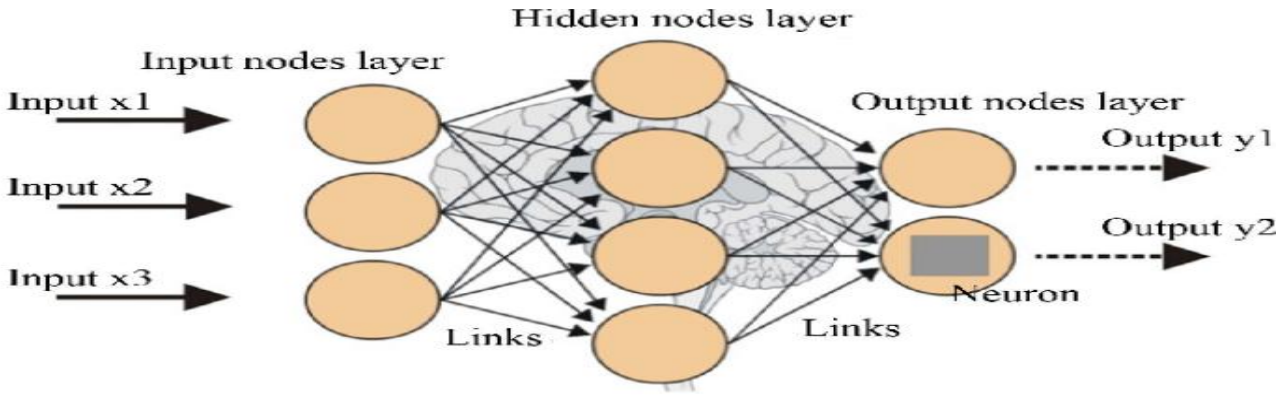

Figure 1.1 Artificial Neural network[4]

Most ANNs have a learning rule that adjusts links' weights in response to inputs. Although neural networks employ a wide number of learning rules, the delta rule is the only one that is addressed in this demonstration. The delta rule is frequently applied in BPNNs, the most prevalent kind of artificial neural network. Error backward propagation is referred to as back propagation. Learning occurs every cycle or epoch with the help of. Similarly, with other types of back propagation, a forward activation flow of outputs and a backwards error propagation of weight adjustments use the delta rule [4].

1.2. Statement of the Problem

Human mistakes are the primary cause of aircraft crashes. It is anticipated that the thesis will show independent flight in varying flight conditions and while being affected by outside disturbances. The fundamental elements that control the great result of a fixed wing airplane scheme consist of its stability, robustness, safety, its displacement improvement, accuracy, and reliability. Within, according to the MRAC system, the controller is created to recognize that the yields on an airplane that is flying straight correspond to the standard showing value. Adapting flying controllers using artificial neural network adaptability has been required to accomplish this independent navigation. Firstly, the availability of appropriate mathematical model models of the aircraft is required for the creation of an adaptation controller for the uncertain. ANN-based MRAC is suggested as a solution to the problem and as a means of advancing the data frameworks. The controller used ANN in combination with the standard direct MRAC framework to prepare.

1.3. Objective of the thesis

1.3.1. General Objective

The main objective of the thesis is to pitch angle control of fixed wing airplane autopilot using artificial neural networks based on model reference adaptive control**.**

1.3.2. Specific Objectives

- To develop fixed wing airplane mathematical model.
- Train NN using the error produced by the real output and reference model.
- To develop and analyze a direct model reference on adaptive control system based on artificial neural networks.
- To contrast the simulated results between the NN based MRAC fixed wing airplane autopilot and the old (PID and MRAC) autopilot.
- To analyze and examine the autopilot's effectiveness.

1.4. Importance of the Study

- To increase the reliability of fixed wing airplane autopilot, limit the uncertain condition between fixed wing airplane and autopilot.
- To increase its stability, robustness, safety profile, its displacement improvement, accuracy, and reliability of autopilot.

1.5. Scope and Limitations of the Study

The range of this thesis would be to train a neural network to follow a reference model to that same output of a fixed wing aircraft's AP while simulating its functionality using a MATLAB program. Additionally, a direct model reference adaptive controller based on artificial neural networks was created in the MATLAB program to assess the efficiency of the planned ANN plus MRAS to enhance the effectiveness of the system &pitch angle of a fixed wing airplane autopilot. This is done by analyzing a control model which is capable of stabilizing the system. The limitations of thesis both the short period oscillation pitch angle and phugoid oscillation model of pitch angle control of fixed wing airplane are not real implemented on all controllers. On the other hand, due to the company security (pattern) and asking for a premium, they did not get extreme resources, data and parameters were other limitations.

1.6. Methodology

The achievement of this research has been achieved using the following techniques.

1. The study of the thesis starts with a literature review that is relevant towards this thesis, and several ideas are used.
2. Based on mathematical modeling develops Proportional Integral and Derivatives (PID) & MRAC Lyapunov's stability criteria for control of fixed -wing airplane autopilot control.
3. Controller design: artificial neural networks based on adaptive control for pitch attitude hold autopilot has to be developed that is resistant to external disruptions and unpredictability of the parameters.
4. Using MATLAB algorithm, the simulation has compared the old autopilot (pitch attitude hold autopilot) and the neural net based on adaptive control of the pitch angle of fixed-wing airplane autopilot.
5. Finally, based on MATLAB simulation results, selecting the best performance from the old (pitch attitude hold) autopilot and artificial neural networks model reference adaptive control AP would be performed on a fixed wing airplane.

1.7. The Outlines of the thesis

Six chapters, including the introduction in the first one, make up this thesis.

Chapter 1 of this chapter is how the research is structured.

Chapter 2 presents an examination of the literature and conceptual understanding of the airplane, ANN & MRAC.

Chapter 3 presents modeling, dynamic modeling of the fixed-wing airplane using model reference adaptive control.

Chapter 4 presents controller design of pitch angle control of fixed-wing airplane autopilot.

Chapter 5 this chapter describes simulation studies and analysis of results.

Chapter 6 this chapter concludes the research conducted for this thesis, recommends of further research.

CHAPTER TWO

LITERATURE REVIEW

This chapter lays out the fundamental theoretical review of the interrelated work required for the advancement of the thesis & offers the key results of many investigators of intelligent devices &could they possibly be applied to control pitch angle control of fixed wing airplane autopilot using artificial neural network based on Lyapunov's stability criteria, the interrelated and comparable findings are cited. The standard data and guideline investigations that represent respectable appears to work, and academic studies carried out by professionals that are pertinent towards the artificial neural net based direct MRAS provide compelling motivation to continue the research, which is why it is presented inside this chapter. Based on the presumption that the plant can be linearized, the controller is built to ensure that a plant converges to reference model output. When operating around the operating point, the linear model reference adaptive control operates well; in this case, the linear model can approximate the plant. Therefore, in the ideal scenario, this approach is efficient for operating a linear plant with unknown parameters. The performance of the linear model reference adaptive control, however, may decrease due to the fact that the majority manufacturing methods be extremely not linear, non-zero, & by different types of unpredictability & load disruptions, and it may be necessary to employ suitable nonlinear control [5]. An attractive area for additional studying would include examine 2^{nd} order systems by means of together Massachusetts Institute of Technology and Lyapunov's stability criteria & concentrate on modifying the reference model's characteristics. This article analyzes the consequences of adaptation gain for a 2^{nd} order structure using the Massachusetts Institute of Technology stability criteria [6]. A neural net could be successfully trained to recognize process forward dynamic behavior and make predictions to system behavior for predictable control and design going to follow control, or to understand system reverse dynamics for inverted operation, with the right artificial neural constructions, having trained methods, and just enough past and present both input and output information. Due to the maximum non-linearity of the neural net & the absence of response, the stability, error converges, and resilience for all this machine - learning controllers with off-line training have not been fully provided [7]. In order to improve system performance measures including stability, convergence, and robustness, a RBFNN based adaptive regulator has

been designed to compensate for the results of method uncertainties. A RBFNN is more complex to use after training is finished, since more calculations are needed to produce an output [8]. Demonstrates how to apply adaptive control to a direct current machine; the errors include variable fluctuations in the varying overtime problem. For the adaptation mechanism, we opted to employ model reference adaptive control with the MIT rule technique, and we estimated the controller variable to meet the reference representation. The project attempts to develop a robust adaptive architecture by using Simulink to describe the system dynamics. Without performing too many computations on the difficult mathematical equations, it is simple to come up with a modeling solution [9]. Using the model reference adaptive control approach, describe how artificial neural networks are used to automatically tune PID controllers. The method involves building a plant simulator initially using a multiplayer perceptron network. The PID parameters are then adjusted by this emulator in combination with an online-trained neural network, minimizing the difference between the reference set point and plant response. An NN connection creates the necessary PID controller settings by taking into account the previous process output amount, control sign, and desired set signal as inputs [10].

2.1. Fixed-wing airplane

Fixed wing plane are aircraft driven by aerodynamic forces acting on a fixed surface, which are frequently utilized to achieve an errand that requires tall elevation and tall speed since of their quick flight speed, long flight removal and solid stack capacity characteristics [11]. Fixed- wing aircraft can have several distinctive wings types, the primary and most common configurations known as monoplane or one wing plane, low wing, shoulder wing, parasol wing are a few of the wing types that are utilized within the conventional monoplane aircraft [12]. Drones with fixed wings are heavier than air drones that can fly recognition to the lift produced by their forward motion through the air [1]. In later a long time, small fixed-wing airplane has been attracting increasing importance, because fixed wings planes are versatile, disposable and flexibility. With a short wing span and light weight, small fixed wing airplanes can be built effectively worked by, as if it were one or two people and can be carried and launched by hand [13]. Finding stability and control derivatives for any kind of aircraft (airplane) is the first step in creating an accurate mathematical model. These derivatives would have impact on flying characteristics and would be used to control surfaces, design flight control systems and program devices [14]. Aerodynamic stability coefficients and longitudinal

derivatives were used to determine the aircraft's dynamic equations. A set of linear differential equations characterize the longitudinal equations of motion. The most important concept in analysis and design of control systems is the transfer function [15]. The many automatic longitudinal flight control modes are shown here. Autopilots that use the pitch attitude hold, altitude hold, and vertical speed hold modes are used, and each of these modes has a specific controller. The efficiency of the model is enhanced by using this PID controller [16].

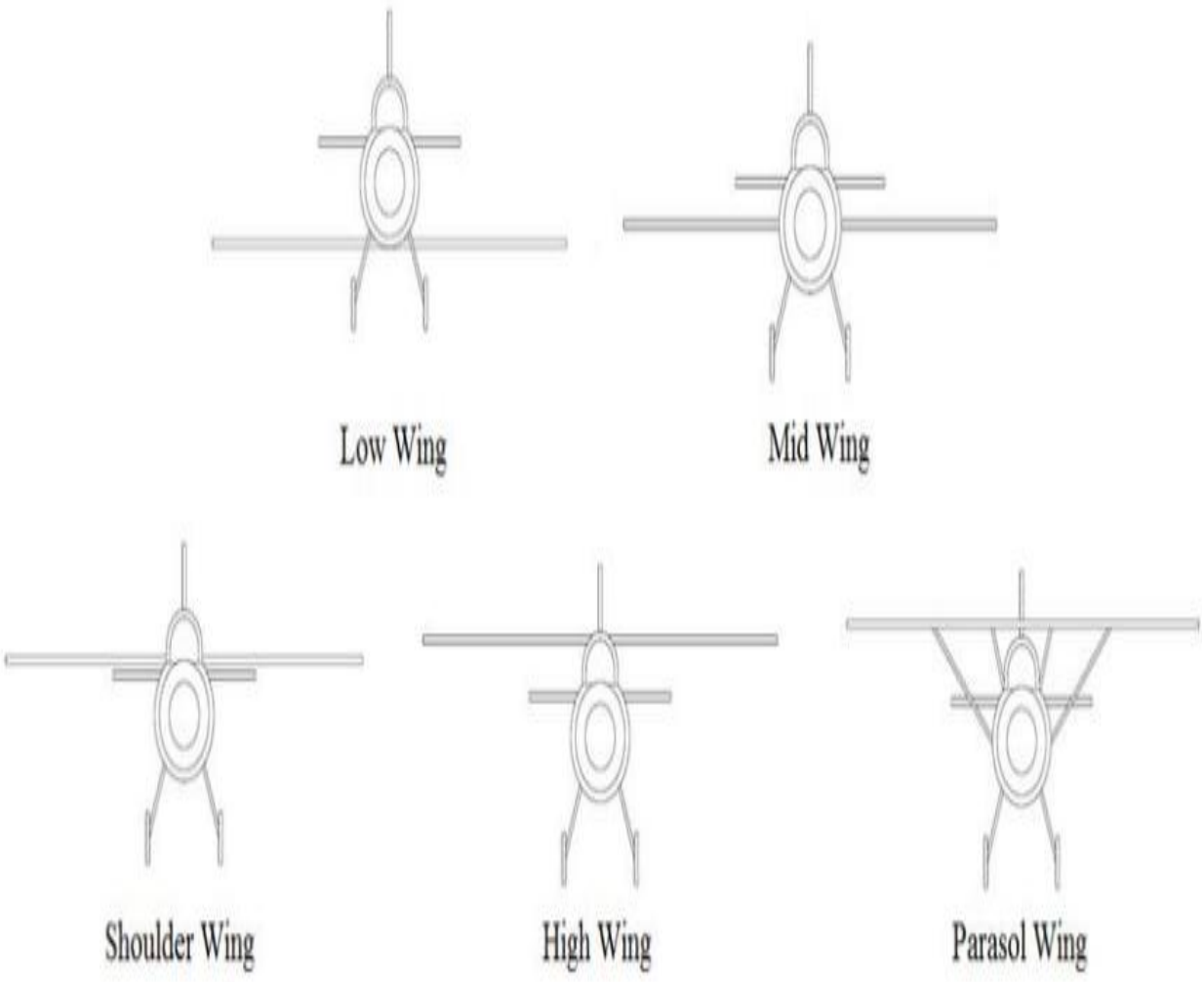

Figure 2.1 Wings type of monoplanes [12].

2.2. Artificial neural networks

Neural network as a computing system made up of a number of simple, highly interconnected processing elements, which process information by their dynamic state response to external inputs [4].

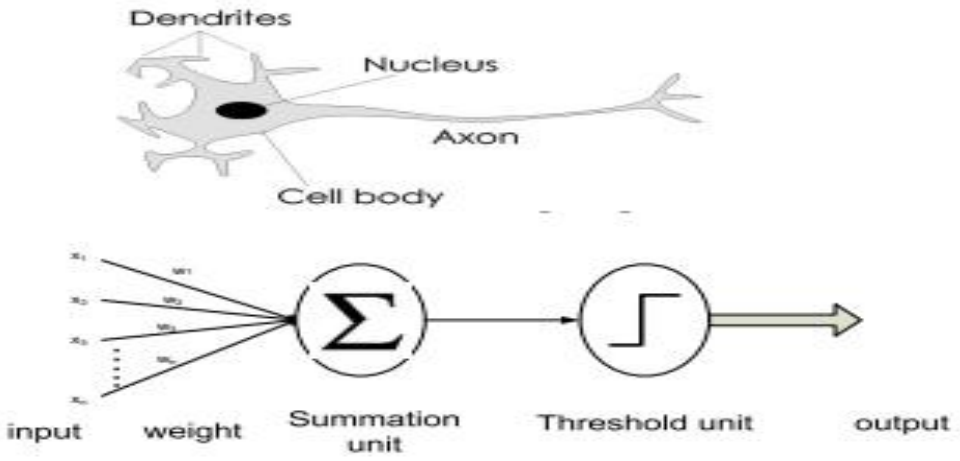

Figure 2.2 Arithmetical models for ordinary natural neuron [4]

The fundamental element of computation in a neuron arrangement is the neuron, regularly known as a hub. It gets input by starting a few additional hubs or an outside basis and computes a yield. All data has a related weight (w), which is allowed due to its importance in relation to other data. Its hub performs work on the inputs that are weighted collectively. The idea is that connection characteristics, or "weights," can be learned and regulate whether a neuron's action on another will be stimulating (positive weight) or inhibiting (negative weight). The signal is carried by the dendrites to the cell body during the basic display, where it is added. In the unlikely event that the final sum exceeds a predetermined threshold, the neuron may activate, transfer a spike through its axon. We hope that in the computing display, the precise duration of the spikes won't matter because the data is communicated to the finishing nodes repeatedly. They use an implementation (such as the Sigmoid function) that indicates the regularity of spikes along the axon to show the neuron's termination rate [7].

2.2.1. Types of Neural Networks

Here are the most popular categories of neural networks that make learning them easier. Neural networks can be divided into numerous distinct categories, many of which also include sub – categories [17].

2.2.1.1. Feed forward Neural Network

A feed forward neural network is an artificial neural network in which there are no cycles formed by the connections between the units. In this organization, the data moves as if it were one heading, forward, from the input hubs, through the covered up hubs (in case any) and to the yield hubs. The network is devoid of cycles and circles.

2.2.1.1.1. Single-layer Perceptron

Since there are no hidden layers in this feed forward neural network, it only has one layer of output nodes, making it the simplest one.

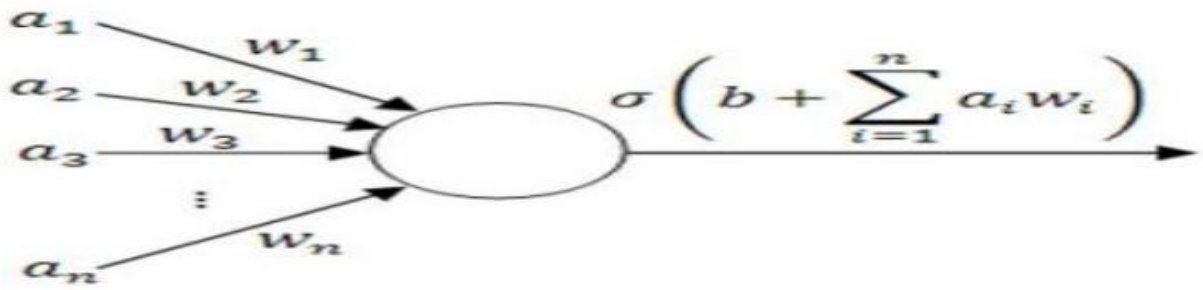

Figure 2.3 one layer perceptron [17].

2.2.1.1.2. Many-layer perceptron (MLP)

The majority of the time, this group of devices consists of multiple layers of feed-forward-connected computing units. All neurons at one level have made it easier for them to affiliate with neurons at the level below them.

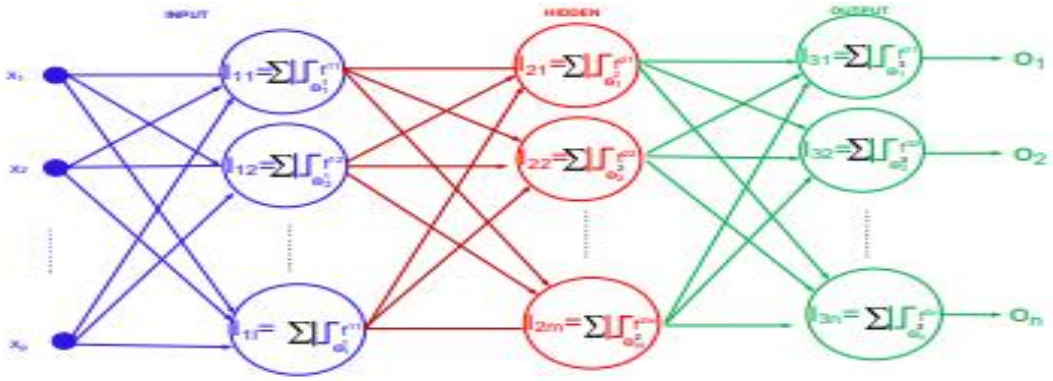

.

Figure 2.4 Many perceptron model [17].

2.2.1.2. Recurrent Neural Networks

The connection between units and the RNN arrangement indicate a synchronized cycle.

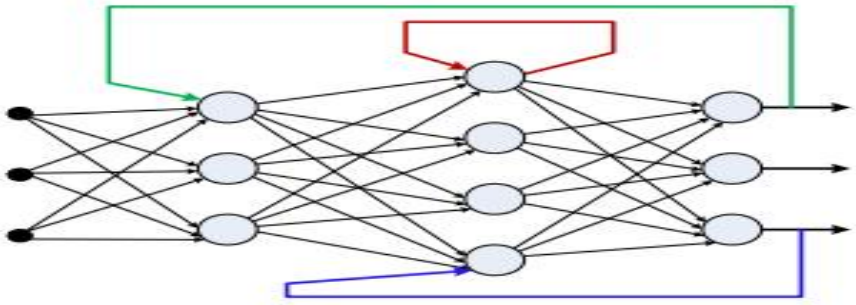

Figure 2.5 Multi layer re current neuron model [17]

2.2.1.3. Radial Basis Function Network

An RBF net could be a supervised learning program similar to multi layer models that it takes after in a few methods. In any case, the RBF is organized by a single covered up layer. Studying of RBF decides the number of cells within the covered up layer. Similar to several outspread capacities, their centers, radii and coefficients. To execute a natural arrangement (plan, prepare) the taking after. To compare the steps that must be followed, a reenactment comes about of the ancient settled plane and neural net based coordinate model reference adaptive control system on diverse fixed wing plane ramble to autopilot. Access and analyze the execution of the autopilot [4].

2.3. Classification of neural network Learning

Most typical neural net training techniques include, [18].

Supervised learning: Here, it uses a "teacher" to provide the machine with examples of inputs and the desired results. Its objective is to discover a generic rule that connects inputs and outputs. One use of supervised learning is spam filtering. Email communications marked as "spam" or "not spam" in particular, includes a learning system for classification.

Unsupervised Learning: In this, the learning algorithm is not given labels; instead, it is left to cluster similar inputs together (clustering), estimate densities, or project highly dimensional data that may be efficiently shown. Finding hidden patterns in data via the training process may be the objective in and of itself, or income to a finish. In issue modeling, an algorithm is given a collection of human-language papers and instructed to identify the papers that design related themes. The topic of modeling is an example of unsupervised learning.

Reinforcement Learning: This involves the interaction of a machine's algorithm with a real-time atmosphere. This should do a specific action in this with no the trainer explicitly indicating whether

it has achieved the task or not. Let's take robotic navigation as an example. A robot is capable of doing tasks with extremely accurate motion. However, the robot must practice these actions repeatedly in order to master them. It uses the information learned from this to increase its effectiveness. The foundation of reinforced learning is this. The output is not limited to a single action in robotic navigation systems and other systems that are similar to them, including self-driving cars and sensor doors. It could include a series of activities.

Workflow for neural network design

The actions listed below must be taken in order to implement a neural network (design process).

- Gather information.
- Neuron of net information.
- Choice of network structural design
- Set the biases and weights to zero.
- Teach the net.
- Assess the results.
- Just use the net.

Procedure steps for many layer neuron net in software

- Before choosing activation functions and initializing weights and biases, the network's structure is initially determined.
- The parameters for the training method, such as the largest number of epochs (repetitions) and error objective are specified.
- Start the program for learning.
- Simulate the neural network's response using the measured input data. Compare this to the observed response.
- Independent information must be used for the final confirmation.

2.4. Back propagation neural network

A few researchers utilize the thought of setting up back propagation based on neural systems to anticipate Spare Parts. The rule of back propagation is based on neural systems as appeared within. The reason is that this thought can compare the input with the qualified yield and calculate the cruel square blunder. The cruel square mistake is proliferated in reverse through the organized, and the

circle is rehashed to diminish the forecast mistake esteem underneath the set foreordained the edge to control the ideal save parts forecast arrangement utilized mimicked information of saving parts request to prepare back engendering neural organize (BPNN) as a tool for requesting forecasts. Setup a three BPNN demonstrates to anticipate save part demand. In arrange to supply a reference for saving parts stock control [19].

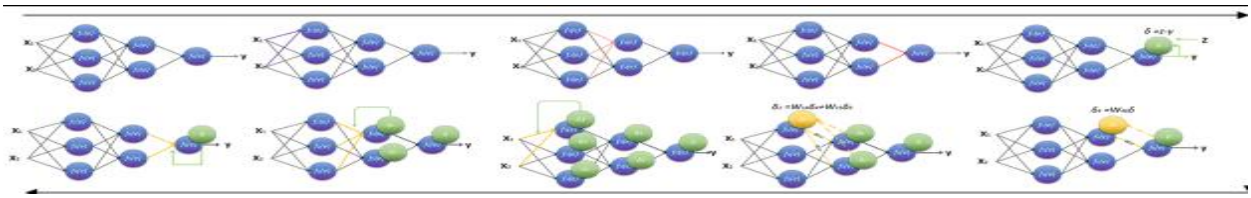

Figure 2.6 Back propagation neural network [19]

2.5. Typical adaptive control

An adaptive control framework consequently compensates for varieties of framework elements by altering the controller characteristics so that the general framework execution remains the same or maybe kept up at an ideal level. This control system beneath thought any debasement in plant execution with time. The common ways of assessing execution are by showing comparison and execution criteria. Within to demonstrate comparison framework, to demonstrate is chosen that bears a likeness to the required framework characteristics. In it, all impacts of framework characters and influence are known [2].

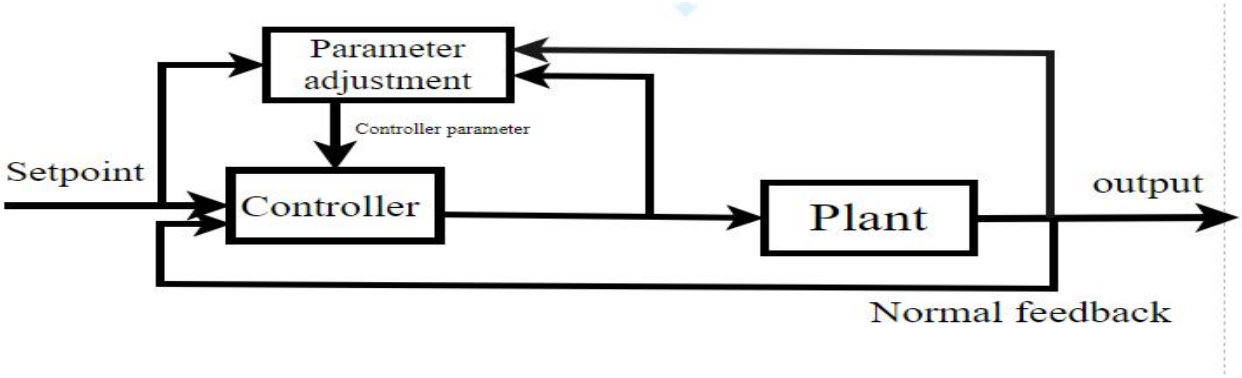

Figure 2.7 Typical adaptive controls

2.5.1. Model Reference Adaptive Control

Model reference adaptive control is one of the adaptive control schemes. A control designer typically wants to know how a system behaves physically when designing a controller for it. This knowledge is typically represented by a numerical form. Practical model building cannot be perfect

for many application areas because systems may include parameter changes caused by non-linearity, variable uncertainty caused by modeling inaccuracies or imprecision, and so on; uncertainty in measurements, external perturbations from the working environment, or other factors. A modeling professional's task is to create a system as unpredictable as possible. Once the device unpredictability may increase beyond the specified tolerance level and negatively impact a controller's efficiency, the performance of the controller can be significantly impacted by system uncertainty, although adaptive control can help to mitigate this effect. Direct adaptive control and indirect adaptive controller are the two main types of control scheme [2].

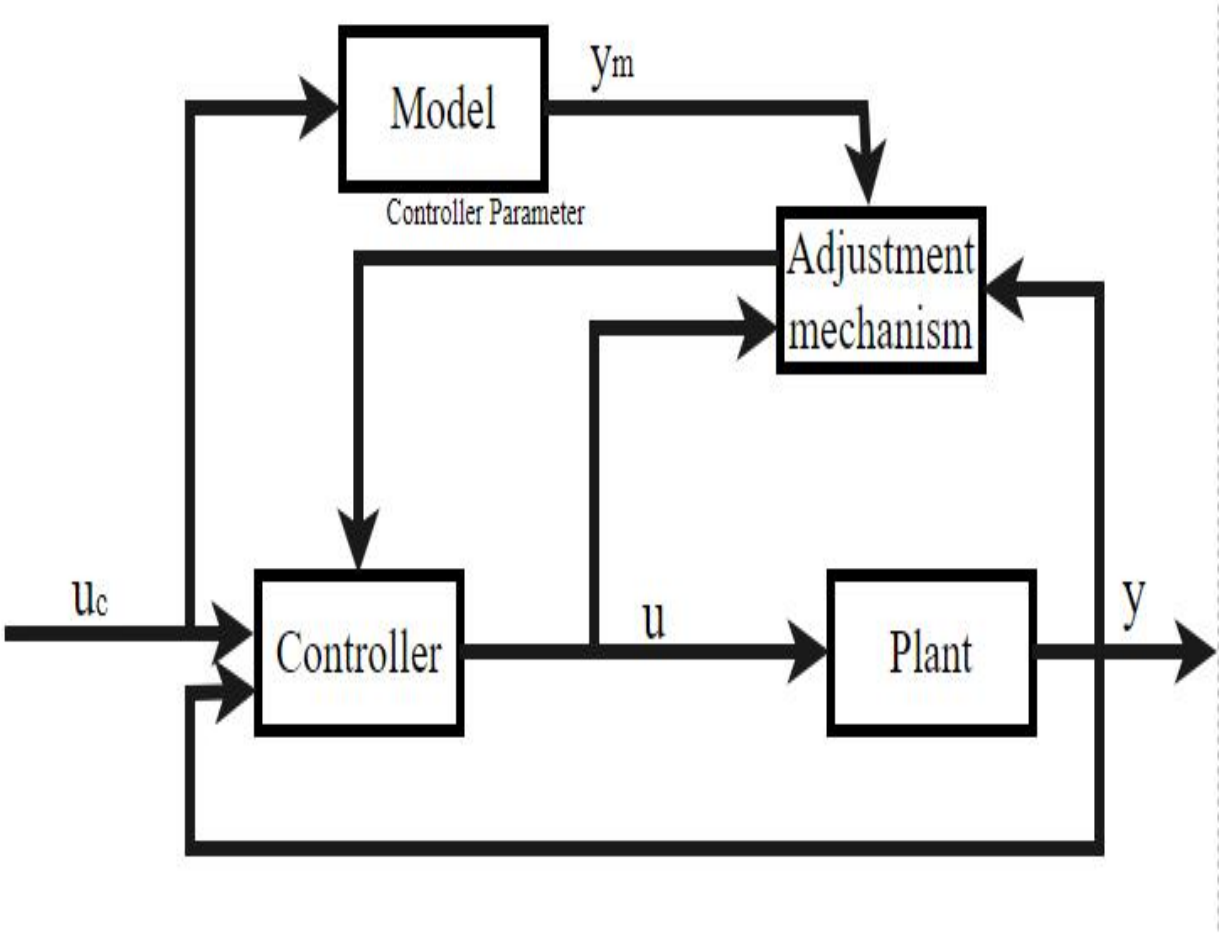

Figure 2.8 Model Reference Adaptive Control

2.6. Conceptual Framework

The tangible example of performance fixed wing airplane autopilot system by ANN based adaptive control is used for this thesis so that researchers can connect with the work and use it to inform future research. The task an accomplished to achieve a fixed wing airplane system with an increased

performance by the artificial neural networks based on an adaptive control system. Designing a model system to direct on fixed wing airplane model and verified the effectiveness of the model through the use of computer simulations.

2.7. Research gap

From the above literature, we find control of DC motor by neural net on model reference adaptive control, PID control on the fixed wing UAV autopilot, design of longitudinal model of fixed wing airplane, model reference control of simple pendulum. Shows that autonomous flight is possible in varying flight conditions and while being influenced by outside disturbances. Some fundamental elements that control the great result of a fixed-wing airplane plant contain its stability, robustness, safety of flying profile, its displacement improvement, accuracy, and reliability. The regulator for MRAC technique was created to ensure that the airplane's autopilot direct yield conforms to the reference display value. According to [2],the controller is then developed by the control engineer using a mathematical representation of the system. Evaluation criteria and stability margins can be used to determine models of fixed-wing airplanes, parameters of plants, types of controllers etc. In order to achieve this autonomous flight, MRAC flight controllers with the ability to adapt to the artificial neural networks used under the supervised learning algorithm are necessary.

CHAPTER THREE
MODELING

A collection of equations that accurately or at least pretty well captures the dynamics of the system is referred to as a mathematical model of a dynamic system. A mathematical model can be applied to any system. Numerous diverse systems' dynamics can be described using differential equations. These differential equations might be created utilizing the physical rules that control a specific system. After that, a mathematical formulation of a process is created, several statistical and numerical methods can be used for evaluation and synthesis [20].A vital element in the creation and management of a dynamic system is dynamic modeling. Dynamic models are simplified mathematically or computer code representations of some real world entity. Furthermore, the design of controls frequently uses dynamic models.

3.1. Boeing 757-200 a commercial transport aircraft

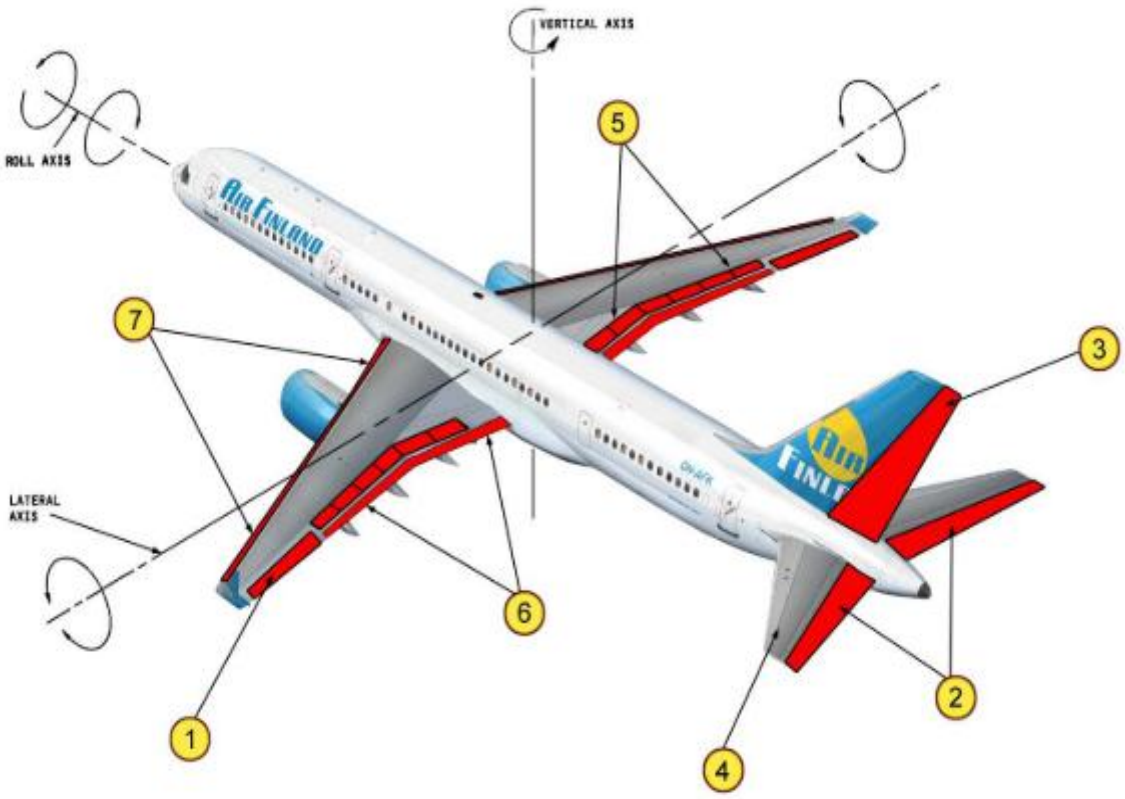

Figure 3.1 Boeing 757- 200 [21]

Table 3.1 Boeing 757-200 parameter definitions [21]

Sign	Alphanumeric	Name	Standard	Unit
Dimensions of mass				
M	Mass	Airplane full mass	*120000*	*kg*
Aerodynamic factors				
$\bar{c}$	CBAR	Average chord for aerodynamics	*6.6*	*m*
l_t	LTAIL	Length between the AC of the tip $(Act)$and the flap fuselage $(ACwb)$	*24.8*	*m*
S	S	wings make region layout	*260.0*	m^2
s_t	STAIL	tip layout form area	*64.0*	m^2
Xcg	X_{CG}	*CoG* X location in fm	$0.23\bar{c}$	*m*
Ycg	Y_{CG}	*CoG* Y location in fm	$0.0\bar{c}$	*m*
Zcg	Z_{CG}	*CoG* Z location in fm	$0.10\bar{c}$	*m*

Table 3.2 possible parameter choice [21]

Variables		Ranges	Standard average
M	*Mass*	*100000kg* < *m* < *150000kg*	*120000kg*
Xcg	*XCG*	$0.15\bar{c} < xcg < 0.13\bar{c}$	$0.23\bar{c}$
Ycg	*YCG*	$-0.03\bar{c} < ycg < 0.03\bar{c}$	$0.0\bar{c}$
Zcg	*ZCG*	$0.00\bar{c} < zcg < 0.21\bar{c}$	$0.10\bar{c}$

3.2. Body equation of motion

The force equation is used to generate the formulas for transitional movement in body-fixed coordinates.

$$F = ma \tag{3.1}$$

$$a = a_B + \omega * v_B \tag{3.2}$$

The airplane's mass is given by the notation *m*, its velocity by *v*, and *ω* its angular speed by in body-fixed dimensions. All combined forces of gravitation, airflow, as well as the engine are represented by the letter F. Acceleration is really the time derivative of velocity (in a body-fixed system).

$$\alpha B = \frac{dV_B}{dt} = \frac{d}{dt}\begin{bmatrix} u_B \\ v_B \\ w_B \end{bmatrix} \tag{3.3}$$

And the velocity is the vertical frame carried by the vehicle's position vector's time derivative.

$$V_V = \frac{dX_v}{dt} = \frac{d}{dt} = \begin{bmatrix} x \\ y \\ z \end{bmatrix} \tag{3.4}$$

In addition, the airplane stated parameters are precise.

$$n_x = \frac{a_{nx}}{g} \tag{3.5}$$

Where a_{nx} is show result of the *z*direction gyroscope at CoG.

The height *h*, which is the negative *z*coordinate in the vehicle carried system.

$$h = - z \tag{3.6}$$

Flight path angle γ

$$tan\gamma = - \frac{wv}{\sqrt{uv^2 + vu^2}} \tag{3.7}$$

Shown as a function of the velocity elements in coordinates transported by the airplane

The track angle x

$$tanx = - \frac{u_V}{V_V} \tag{3.8}$$

3.3. Rotational movement

Moment's formula is used to obtain the formulas for the rotational motion in body fixed coordinates.

$$M = I\dot{\omega} + \omega * I\omega \tag{3.9}$$

M is the total motion caused by the engine and aerodynamics with regard to the center of gravity. Inside a body-fixed system, is ω the rotation motion, and $\dot{\omega}$ is the rotational acceleration.

$$\dot{\omega} = \begin{bmatrix} \dot{p} \\ \dot{q} \\ \dot{r} \end{bmatrix} = \frac{d}{dt} \begin{bmatrix} p \\ q \\ r \end{bmatrix} \tag{3.10}$$

The rotation velocity and the Euler angles have the following relationship.

$$\frac{d\Phi}{dt} = \begin{bmatrix} \dot{\emptyset} \\ \dot{\theta} \\ \dot{\Psi} \end{bmatrix} = \begin{bmatrix} 1 & sin\emptyset tan\theta & cos\emptyset tan\theta \\ 0 & cos\theta & -Sin\emptyset \\ 0 & \frac{sin\emptyset}{cos\theta} & \frac{cos\emptyset}{cos\theta} \end{bmatrix} \begin{bmatrix} p \\ q \\ r \end{bmatrix} \tag{3.11}$$

The aircraft inertia tensor I defined in the body frame is.

$$I = \begin{bmatrix} I_x & 0 & -I_{xz} \\ 0 & I_y & 0 \\ -I_{xz} & 0 & I_z \end{bmatrix} = m \begin{bmatrix} 40.07 & 0 & 2.098 \\ 0 & 64 & 0 \\ 2.098 & 0 & 99.92 \end{bmatrix} \tag{3.12}$$

Where all numbers are expressed in m^2

3.4. Coordinate conversion (F_B)

The transformations between both the airplane carried coordinate system and the body-fixed coordinate are shown in

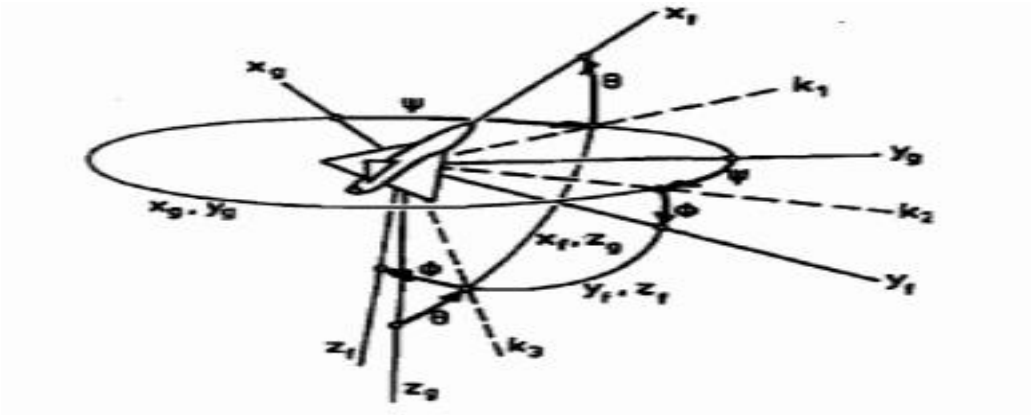

Figure 3.2 coordinate conversions body-fixed (vehicle-carried) [22]

The airplane's location is represented; using a conversion with Euler angles $\emptyset$, θ and Ψ becomes necessary. For the transformation, the vehicle carried system is rotated about z-axis by the bearing angleΨ. The after that, rotary motion is done through the pitch angle θ about k_2 and lastly in the roll

angle ∅ on the x-axis. The conversation matrix between body fixed and vehicle-carried axis system results in.

$$R_{BV} = \begin{bmatrix} 1 & 0 & 0 \\ 0 & cos\emptyset & sin\emptyset \\ 0 & -sin\emptyset & cos\emptyset \end{bmatrix} \begin{bmatrix} cos\theta & 0 & -sin\theta \\ 0 & 1 & 0 \\ sin\theta & 0 & cos\theta \end{bmatrix} \begin{bmatrix} cos\Psi & sin\Psi & 0 \\ -sin\Psi & cos\Psi & 0 \\ 0 & 0 & 1 \end{bmatrix} \quad (3.13)$$

Note that $R_{BV} = R_{VB}^{T}$

Multiplying the three matrices yields

$$R_{BV} = \begin{bmatrix} cos\psi cos\theta & +sin\psi cos\theta & -sin\theta \\ cos\psi sin\theta sin\phi - sin\psi cos\phi & sin\psi sin\theta sin\phi + cos\psi cos\phi & cos\theta sin\phi \\ cos\psi sin\theta cos\phi + sin\psi sin\phi & sin\psi sin\theta cos\phi - cos\psi sin\phi & cos\theta cos\phi \end{bmatrix} \quad (3.14)$$

The conversion of velocity between body-fixed dimensions and those conveyed by airplane

$$V_B = R_{BV} V_v \quad (3.15)$$

With

$$V_B = \begin{bmatrix} u_B \\ v_B \\ w_B \end{bmatrix} \quad (3.16)$$

$$V_V = \begin{bmatrix} u_V \\ v_V \\ w_V \end{bmatrix} \quad (3.17)$$

3.5. Calculate airspeed

The vector airspeed V_a(expressed in body axis) is the gap of the kinematic velocity of the air-plane V_B, &the airstream velocity w_B expressed in body-fixed coordinates.

$$V_a = V_B - w_B \quad (3.18)$$

With

$$V_a = \begin{bmatrix} u_a \\ v_a \\ w_a \end{bmatrix} \quad (3.19)$$

And v is the total velocity

$$v = \sqrt{u_a^2 + v_a^2 + w_a^2} \quad (3.20)$$

The angle of attack α & the angle of sideslip β be

$$\alpha = tan^{-1}\left(\frac{w_a}{u_a}\right) = \text{angle of attack (AOA)} \quad (3.21)$$

$$\beta = \sin^{-1}\left(\frac{v_a}{V}\right) \text{ side slip of angle} \tag{3.22}$$

The derivatives of α and β with respect to time are,

$$\dot{\alpha} = \frac{\alpha_{az} u_a - \alpha_{ax} w_a}{u_a^2 + w_a^2} \tag{3.23}$$

$$\dot{\beta} = \frac{a_{a_y}(u_a^2 + w_a^2) - v_a\left(a_{a_x} v_a + a_{a_x} w_a\right)}{u_a^2 + \ v_a^2 \ + w_a^2} \tag{3.24}$$

Where $\alpha_{ax}, \alpha_{ay}\ and\ \alpha_{az}$ are the *x, y, z* time derivatives of the airspeed in body-fixed coordinates.

$$\alpha_{ax} = du_a/dt$$

3.6. Aerodynamics

As a function of the aerodynamic moments, the aerodynamic forces are represented in the wind axes. Factors $(\bar{q}s)$, aerodynamic coefficients (C_D, C_Y, C_L) and angle of attack (α) and the sideslip angle (β).

$$\bar{q} = \frac{1}{2}\rho V^2 \tag{3.25}$$

With V as the total air speed.

The aerodynamic lift coefficients $C_L$are defined as

$$C_L = C_{Lwb} + C_{Lt} \tag{3.26}$$

C_{Lwb} Is the lift factor for just the flap and fuselage, and is given by,

$$C_{Lwb} = 5.5(\alpha - \alpha_0) \tag{3.27}$$

$$\alpha_0 = \frac{11.5}{180/\pi} \tag{3.28}$$

α_0 Is the attack degree at which the lift becomes none.

The lift of the tail unit C_{Lt} is,

$$C_{Lt} = \frac{S_t}{s} 3.1\ \alpha_t \tag{3.29}$$

Where α_t denotes the angle of attack of the tail unit

$$\alpha_t = \alpha - \varepsilon + \delta_E + 1.3\ \frac{q l_t}{V} \tag{3.30}$$

$$\varepsilon = \frac{d\varepsilon}{d\alpha} * (\alpha - \alpha_0) \tag{3.31}$$

$$\frac{d\varepsilon}{d\alpha} = 0.25$$

With ε the down-wash angle $\delta_{E,}$ the elevator deflection q, the pitch ratio and l_t,the horizontal separation between the airplane's center of gravity and the aerodynamic axis of the rear section.

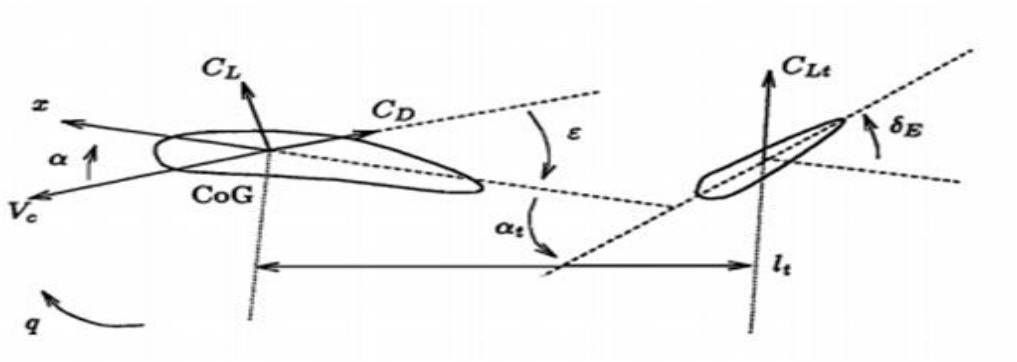

Figure 3.3 Aerodynamic forces [22].

The drag factor for an airplane C_D is given as purpose of its aerodynamic lift coefficient of the wing/body C_{Lwb} without the tail.

$$C_D = 0.13 + 0.07(C_{Lwb} - 0.45)^2 \tag{3.32}$$

The aerodynamic side force coefficientC_Y can be written as follows,

$$C_Y = -1.6\beta + 0.24\delta_R \tag{3.33}$$

With β as the angle of sideslip and δ_R as the rudder deflection

The equations for the moment coefficients C_l, C_m, C_n expressed in body axes are given by

$$\begin{bmatrix} C_l \\ C_m \\ C_n \end{bmatrix} = \begin{bmatrix} -1.4\beta \\ -0.59 - 3.1 * S_t l_t s/s\bar{c}\,(\alpha - \mathcal{E}) \\ (1 - \partial 180/15\pi)\beta \end{bmatrix} + \begin{bmatrix} -11 & 0 & s \\ 0 & -4.03 * S_t l_t/s\bar{c} & 0 \\ 1.7 & 0 & -11.5 \end{bmatrix} + \frac{l}{V}\begin{bmatrix} p \\ q \\ r \end{bmatrix} + \begin{bmatrix} -0.6 & 0 & 0.22 \\ 0 & -3.1 * S_t l_t/s\bar{c} & 0 \\ 0 & 0 & -0.63 \end{bmatrix}\begin{bmatrix} \delta_A \\ \delta_E \\ \delta_R \end{bmatrix} \tag{3.34}$$

α: Angle of attack

β : Angle of sideslip

S: wing plan form area

S_t : Tail unit plan form area

l: generalized length

l_t: Distance between the CoG and aerodynamic center of the tail

V: Total airspeed

$p, q, and\ r$: Rotational rates (body axes)

δ_A, $\delta_E and \delta_R$: Deflection of aileron, elevator, and rudder

In order to calculate dimensional forces and moments, the following expressions must be applied.

Aerodynamic pressure on the air's X direction

$$D = C_D \frac{1}{2} \rho V^2 S \tag{3.35}$$

Aerodynamic pressure on the air's *Y* direction

$$Y = C_Y \frac{1}{2} \rho V^2 S \tag{3.36}$$

Aerodynamic pressure on the air's *Z* direction

$$L = C_L \frac{1}{2} \rho V^2 S \tag{3.37}$$

Rolling moment in body axis

$$l = C_l \frac{1}{2} \rho V^2 S b \tag{3.38}$$

Pitching moment in body axes

$$m = C_l \frac{1}{2} \rho V^2 S \bar{c} \tag{3.39}$$

Yawing moment in body axes

$$N = C_n \frac{1}{2} \rho V^2 S b \tag{3.40}$$

L =lift

D =Drag

b=wingspan =44.8m

$\bar{c}$ = mean aerodynamic chord =6.6m

In order to transform the aerodynamic forces from wind axes (*D, Y, L*) in to the body axes frame ($F_{xA,}F_{yA}\ F_{zA}$) the following expressions are used,

$$F_{xA,} = Lsin\alpha - Dcos\alpha\, cos\,\beta - Y\, cos\alpha sin\,\beta \tag{3.41}$$

$$F_{yA} = -Dsin\beta + Y\, cos\beta \tag{3.42}$$

$$F_{zA} = -Lcos\alpha - Dsin\alpha cos\beta - Y\, sin\alpha sin\beta \tag{3.43}$$

3.6.1. Rotate from F_S to F_W

The transformation from stability to wind frame is given by

$$\overline{CF}^S = \begin{bmatrix} force\ in\ x_s\ axis \\ force\ in\ y_s\ axis \\ force\ in\ z_s\ axis \end{bmatrix} = \begin{bmatrix} -c_D^S \\ c_Y^S \\ -c_L^S \end{bmatrix} = \begin{bmatrix} -(0.13 + 0.07(5.5a + 0.654)2) \\ -1.6\beta + 0.24u_3 \\ -(CL_{wb} + CL_t) \end{bmatrix} \tag{3.44}$$

$$\overline{C}F^W = C_{wS}\beta\overline{C}F^S \tag{3.45}$$

Where

$$C_{wS}\beta = \begin{bmatrix} Cos\beta & sin\beta & 0 \\ -sin\beta & cos\beta & 0 \\ 0 & 0 & 1 \end{bmatrix} \tag{3.46}$$

3.6.2. Aerodynamic force in F_b

An airfoil-shaped streamline body is what generates the aerodynamic force on an airplane. For a body to be considered a streamline, the fluid's viscous or skin friction action on the body must account for the majority of the drag force in the free stream direction. A thin flat plate, for instance, laying parallel to and edge of the approaching flow is an example of a streamline body because the flow is kept attached to the surface and skin friction accounts for up to 90 per cent of the total drag. Aerodynamic forces and moments on the body are due to two basic sources: pressure distribution throughout the surface of the body distribution of shear stress throughout the body's surface. Aircraft forces shear stress and pressure apply tangential and normal forces, respectively, to the surface. The "tugging action" on a surface that results from friction between a body and the air is known as shear

stress. The resulting aerodynamic force R and moment M just on the body is the net result of the pressure and shear stress distributions integrated over the entire body surface.

$$\overline{F}_A^S = \begin{bmatrix} -DS \\ Y \\ -L \end{bmatrix} = \begin{bmatrix} -C_{D,} & Q, & S \\ C_Y, & Q, & S \\ -C_L, & Q, & S \end{bmatrix} S \tag{3.47}$$

Rotate to

$$F_A^{-b} = C_{\underline{b}}(\alpha)\overline{F}_A^S \tag{3.48}$$

Where

$$c_{\underline{\boldsymbol{b}}}(\alpha) = \begin{bmatrix} cos\alpha & 0 & -sin(\alpha) \\ 0 & 1 & 0 \\ sin(\alpha) & 0 & cos\alpha \end{bmatrix} \tag{3.49}$$

Aero moment about AC in F_b

$$M_{Aac}^{-b} = C_{mac}^{-b} * qs\overline{c} \tag{3.50}$$

Aero moment about CoG in F_b

$$m_{AcG}^{-b} = m_{\boldsymbol{Aac}}^{-\boldsymbol{b}} + F_{\boldsymbol{A}}^{-\boldsymbol{b}} * \overline{r}_{cg}^{b} - \overline{r}_{ac}^{b} \tag{3.51}$$

$$\overline{r}_{cg}^{b} = \begin{bmatrix} X_{CG} \\ Y_{CG} \\ Z_{CG} \end{bmatrix} = \begin{bmatrix} 0.23\,\overline{C} \\ 0 \\ 0.1\overline{C} \end{bmatrix} \tag{3.52}$$

$$\overline{r}_{ac}^{b} = \begin{bmatrix} X_{ac} \\ Y_{ac} \\ Z_{ac} \end{bmatrix} = \begin{bmatrix} 0.12\overline{C} \\ 0 \\ 0 \end{bmatrix} \tag{3.53}$$

3.7. Engine model

The thrust F provided by each of the two engines $(\pi 1, \pi 2)$ is described by;

$$F = \delta_{TH} i\, mg \tag{3.54}$$

Where$\delta_{TH} = 0$means zero thrust and, $\delta_{TH} = 1$ means a thrust equal to the gravity force (mg),acting toward the aircraft. The engines' force vector is parallel to the forward-facing x-body axis.

$$F_{xT} = F \tag{3.55}$$

$$F_{yT} = F_{xT} = 0 \tag{3.56}$$

The moments from engine about the center of gravity $T_E$are,

$$T_{Ei} = \begin{bmatrix} X_{APTi} \\ Y_{APTi} \\ Z_{APTi} \end{bmatrix} * (F, 0,0)^{'} (i = 1,2) \tag{3.57}$$

These are brought on by how far the engine is from the center of gravity.$\pi 1 \text{and } \pi 2$ are the locations at which push is applied.

Table 3.3 Descriptions of engine specifications [21].

Engine specifications				
X_{APT1}	*XAPT1*	X direction of engine 1's application site of force in *FM*	0.0	*m*
Y_{APT1}	*YAPT1*	Y direction of engine 1's application site of force in *FM*	-7.94	*m*
Z_{APT1}	*ZAPT1*	Z direction of engine 1's application site of force in *FM*	-1.9	*m*
X_{APT2}	*XAPT2*	X direction of engine 2nd application site of force in *FM*	0.0	*m*
Y_{APT2}	*YAPT2*	Y direction of engine 2nd application site of force in *FM*	7.94	*m*
Z_{APT2}	*ZAPT2*	Z direction of engine 2nd application site of force in *FM*	-1.9	*m*

Recall *U4, U5*$\leq 10\pi/180$ at maximum thrust *U4=U5*=$10\pi/180(F_1 max + F_2 max)/mg = 0.35$

$$F_{Ei}^{-b} = \begin{bmatrix} F_i \\ 0 \\ 0 \end{bmatrix} bF_{Ei}^{-b} = F_{E1}^{-b} + F_{E2}^{-b} \text{ Propulsive / engine force in } Fb \tag{3.58}$$

$$\bar{m}_{ECGi}^{b} = \mu_{\boldsymbol{i}}^{-b} * F_{Ei}^{-b} \quad \text{Where} \quad \mu_{\boldsymbol{i}} = \text{left}\frac{\text{engine}}{\text{right}} \tag{3.59}$$

$$\bar{\mu}_{i}^{b} = \begin{bmatrix} X_{cog} - X_{APTi} \\ Y_{APTI} - Y_{cog} \\ Z_{cog} - Z_{APTi} \end{bmatrix} \tag{3.60}$$

$$\bar{m}_{ECG}^{b} = \bar{m}_{ECG1}^{b} + \bar{m}_{ECG2}^{b} \text{ propulsive engine moment about CoG in} F_b \tag{3.61}$$

3.8. Atmosphere

No matter the height or location, the atmosphere is thought to be constant.

$$\rho = 1.225\frac{kg}{m^3} \quad , \; p = 101325.0\frac{N}{m^2} \; , T = 288.15k^0$$

Whereas, ρ stands for air density, p for static pressure, and T for actual temperature.

3.9. Model of gravitation

At the airplane center of gravity, gravitational force operates. In this paradigm, gravity is not thought to depend on altitude;

$$w = mg \tag{3.62}$$

$$F^{-e}{}_{g} = m.\bar{g} \; easy\, frame \; \bar{F}_{g}^{e} = \begin{bmatrix} 0 \\ 0 \\ g \end{bmatrix} * m \tag{3.63}$$

Need to rotate to F_b

$$\bar{F}_{g}^{b} = C_{be}(\Phi\Theta\Psi)F^{-e}{}_{g} \tag{3.64}$$

$$\bar{F}_{g}^{b} = \begin{bmatrix} -gsin(X_8) \\ gcos(X_8)sin(X_7) \\ gcos(X_8)cos(X_7) \end{bmatrix} * M \; (M \text{ assume constant}) \tag{3.65}$$

The acceleration caused by gravity close to the earth's surface is assumed to be constant.$g = 9.81\frac{\boldsymbol{m}}{\boldsymbol{s^2}}$

3.10. Actuator model

The throttle motion speed restrictions are

Increased slew rate $1.6 * (\frac{\pi}{180})\ rad/s$failing slew rate $= -1.6 * \pi/180$ rad/s

Throttle limits/ saturation are$0.5 * \pi/180\ rad \leq \delta_Th1 \leq 10 * \pi/180\ rad$

We can assume that in the event of engine problem, the throttle level for the damaged engine decreases to $\delta_{Th1} = 0.5 * \pi/180$ rad/s using transfer function-based first degree dynamic behavior *1/ (1+3.3s)*

Fixed rates of elevator deflection $-25 * \pi/180 \leq \delta_e \leq 25 * \pi/180$

Concentration (saturation) levels of elevator deflection$-25 * \pi/180 \leq \delta_e \leq 25 * \pi/180$

Rate limits for tail plane deviation $-15 * \pi/180 \leq \delta_T \leq 15 * \pi/180\ rad/s$

Concentration levels of tail plane deflection $-25 * \pi/180 \leq \delta_T \leq 10 * \pi/180\ rad$

Fixed rates of rudder deflection $-25 * \pi/180 \leq \delta_R \leq 25 * \pi/180\ rad/s$

Saturation of rudder deflection is $-30 * \pi/180 \leq \delta_R \leq 30 * \pi/180$ rad/s [21].

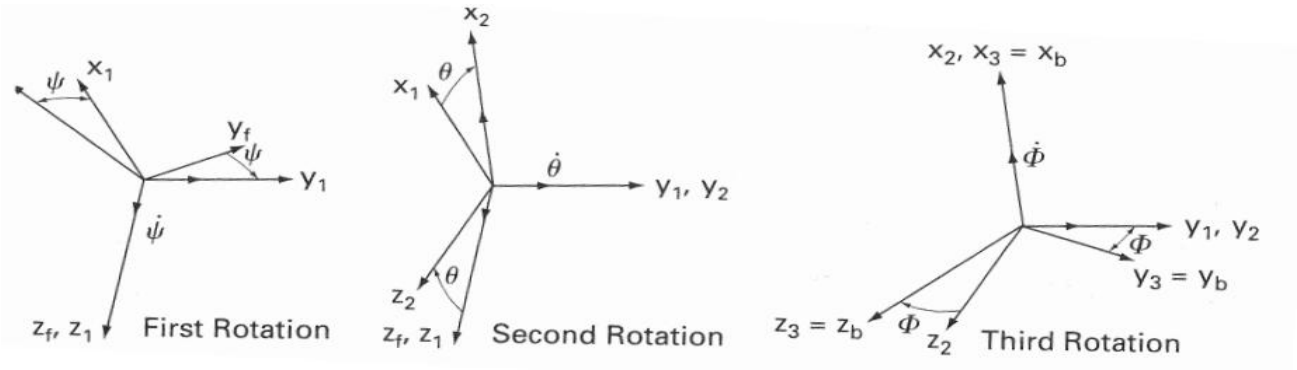

Figure 3.4 Euler angles [21]

Generally model formula

$$\begin{bmatrix}\dot{X}_1\\ \dot{X}_2\\ \dot{X}_3\end{bmatrix} = \begin{bmatrix}\dot{u}\\ \dot{v}\\ \dot{w}\end{bmatrix} = \frac{1}{m}\overline{F}^b - \overline{w}^b_{be} * \overline{v}^b \tag{3.66}$$

$$\text{Where } \overline{F}^b = \overline{F}^b_g + \overline{F}^b_E + \overline{F}^b_a \tag{3.67}$$

$$\begin{bmatrix}\dot{X}_4\\ \dot{X}_5\\ \dot{X}_6\end{bmatrix} = \overline{I}^1_b(\overline{M}^b_{CG} - \overline{w}^b_{be} * Ib\overline{w}^b_{be}), \text{ Note } I_b \text{ is constant} \tag{3.68}$$

$$\text{Where} \qquad \overline{M}^b_{CG} = \overline{M}^b_{ECG} + \overline{M}^b_{ACG} \tag{3.69}$$

$$\frac{d\Phi}{dt} = \begin{bmatrix}\dot{X}_7\\ \dot{X}_8\\ \dot{X}_9\end{bmatrix}\begin{bmatrix}1 & sin\emptyset tan\theta & cos\emptyset tan\theta\\ 0 & cos\theta & -Sin\emptyset\\ 0 & \frac{sin\emptyset}{cos\theta} & \frac{cos\emptyset}{cos\theta}\end{bmatrix}\begin{bmatrix}p\\ q\\ r\end{bmatrix} \tag{3.70}$$

$$F(\overline{X},\overline{U}) = \begin{bmatrix}\frac{1}{m}\overline{F}^b - \overline{w}^b_{be} * \overline{v}^b\\ \overline{I}^1_b(\overline{M}^b_{CG} - \overline{w}^b_{be} * Ib\overline{w}^b_{be}\\ \frac{d\Phi}{dt}\end{bmatrix} \tag{3.71}$$

3.11. Model verification airplane

The aforementioned aircraft design, like all designs, comprises physical characteristics that require accurate knowledge. These parameters are also *m, I_x, I_y, I_z* and all the aerodynamic coefficients C_L, C_y & C_D, it is dependent upon both the speed and the attack angle. It is possible to calculate these numbers using software, but there is little doubt that a direct measurement of the forces and torques acting on a section of a wing within a wind tunnel is preferable [22].

3.11. Longitudinal dynamics

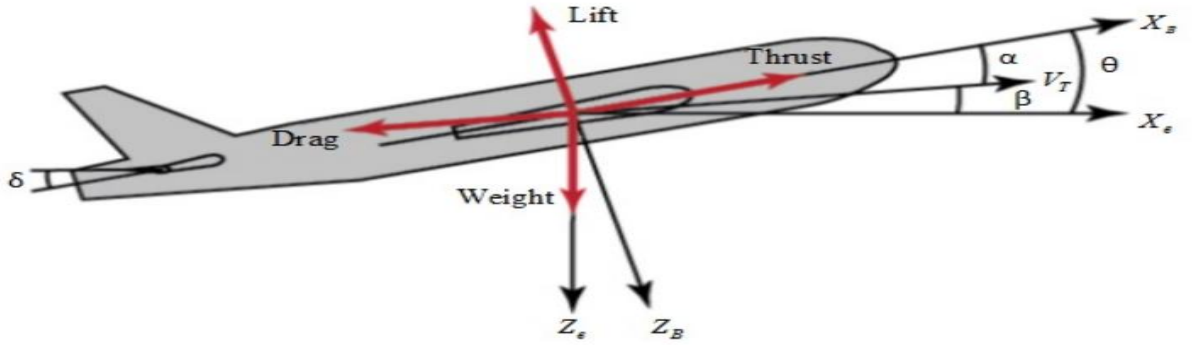

Figure 3.5 pitch angle with the direction of an aircraft [23]

The longitudinal equations of motion were described by a set of linear differential equations. A very useful concept in analysis and design of control system is the transfer function. In the context of dynamics, it describes the connection between both the control input and the motion parameters. The longitudinal transfer functions can be obtained from the equation of motion in the following manner. First, we simplify the equations of motion by assuming that [22].

$\theta 0 = 0, cos\theta 0 = 1,$ and $sin\theta = 0$

Dimensional stability derivatives of longitudinal motion

$$X_U = -(CD_U + 2CD)QS/MU_0 \tag{3.72}$$

$$Z_U = -(CL_U + 2CD)QS/MU_0 \tag{3.73}$$

$$M_U = CM_U * QS\overline{C}/MU_0 \tag{3.74}$$

$$X_W = -(CD_\alpha - CL)QS/MU_0 \tag{3.75}$$

$$X_{\delta e} = -CD_{\delta e} * QS/M \tag{3.76}$$

$$Z_q = -CL_q * \frac{\overline{C}}{2uo} * \frac{QS}{M} \tag{3.77}$$

$$M_q = CM_q * \frac{\overline{C}}{2uo} * \frac{QS\overline{C}}{I_Y} \tag{3.78}$$

$$M_{\delta e} = C_{M\delta e} * \frac{QS\overline{C}}{I_Y} \tag{3.79}$$

$$Z_W = -\left(C_{L\delta e} * QS/m\right. \tag{3.80}$$

$$M_w = CM_{m\alpha} * \frac{\overline{C}}{2uo} * \frac{QS\overline{C}}{uoI_Y} \tag{3.81}$$

The following set of longitudinal differential equations [23].

$$\left(\frac{d}{dt} - x_u\right)\Delta u - x_w\Delta w + x_q + w_0 - gcos\Delta\theta = x\delta\Delta\delta \tag{3.82}$$

$$-z_u\Delta u + \left(\frac{d}{dt} - z_u\right)\Delta w + z_q + w_0 - gsin\Delta\theta = z\delta\Delta\delta \tag{3.83}$$

$$-m_u\Delta u - (m(w\,d/dt + m_w))\,\Delta w + d/dt(d/dt - m_q)\Delta\theta = m\delta\Delta\delta \tag{3.84}$$

$$\theta\Delta q = q\delta\Delta\delta \tag{3.85}$$

Whereas $\frac{d}{dt} = s$

We can determine the transfer functions by performing an equation's Laplace transformation, then dividing the result by the control deflection. $\Delta u/\Delta\delta$, $\Delta\theta/\Delta\delta$, $\Delta w/\Delta\delta$. It's crucial to remember that $\Delta\delta$ stands for the elevator deflection. Crammers rule can be used to find solutions to these equations [23].

3.12. Longitudinal Directional SS System

Since the aircraft's longitudinal motion involves the four state variables *u, w, q*, and θ four transfer functions are required. However, we turned to the pitch angle transfer function. The longitudinal equation of motion can therefore be expressed using the state space mode [15],[22],[23].

$$\begin{bmatrix}\Delta u'\\ \Delta w'\\ \Delta q'\\ \Delta\Theta'\end{bmatrix} = \begin{bmatrix} s - x_u & -x_w & x_q + w_0 & -gcos\theta 0\\ z_u & s - z_w & z_q + w_0 & -gsin\theta 0\\ m_u & m_w & s(s - m_q) & 0\\ 0 & 0 & 1 & 0\end{bmatrix}\begin{bmatrix}\Delta u\\ \Delta w\\ \Delta q\\ \Delta\Theta\end{bmatrix} + \begin{bmatrix}X\,\Delta\delta_e\\ Z\,\Delta\delta_e\\ M\,\Delta\delta_e\\ 0\end{bmatrix}[\Delta\delta_e] \tag{3.86}$$

Whereas

Elevator deflections angle δ_e = 25

Rolling moment of inertia I_X = 40.07

Pitching moment of inertia I_Y = 64

Yawing moment of inertia I_Z = 99.92

Stability Derivative, X_U = -0.4502

Angle of Attack Derivative, X_W = 4.3112

Elevator Deflection, $X\delta_e$ = -2.8812

Compressible Effect Derivative, M_U = -0.2486

Dimensional Pitching Moment, Derivative, M_W = 0.1319

Pitching moment (Elevator Deflection), $M\delta_e$ = 3.706

Dimensionless Pitching Moment Derivative, M_q = -0.721

Pitching moment (Thrust Deflection), $M\delta_T$ = 0

Pitch Rate Derivative, X_q = -1.16

Stability Derivative, Z_u = -8.9092

Angle of Attack Derivative, Z_w = -9.4786

Elevator Deflection, $Z\delta_e$ = -83.8474

$$\begin{bmatrix} \Delta\dot{u} \\ \Delta\dot{w} \\ \Delta\dot{q} \\ \Delta\dot{\theta} \end{bmatrix} = \begin{bmatrix} -0.4502 & 4.3112 & 0 & -9.81 \\ -8.9092 & -9.4786 & 10 & 0 \\ 0.2486 & 0.1319 & -0.721 & 0 \\ 0 & 0 & 1 & 0 \end{bmatrix} \begin{bmatrix} \Delta u \\ \Delta w \\ \Delta q \\ \Delta\theta \end{bmatrix} + \begin{bmatrix} -2.8812 \\ -83.8474 \\ 3.706 \\ 0 \end{bmatrix} [\Delta\delta e]$$

$$G(s) = \frac{3.706s^2 + 25.0204s + 59.9124}{s^4 + 10.65\,s^3 + 48.52\,s^2 + 21.9\,s + 11.59}$$

To find Eigen value

$$s^4 + 10.65\,s^3 + 48.52\,s^2 + 21.9\,s + 11.59 = 0$$

$$(s^2 + 10.2114\,s + 43.7746)(s^2 + 0.4386s + 0.2644)$$

The two-second order equations in the denominator term describe the short period &phugoid modes of aircraft response. The damping ratios and natural frequency parameter for both short period

oscillations and phugoid mode can be determined by looking at the denominator equation. The elevator dynamics are used to control the aircraft's pitch attitude [15], [22], [23], [24].

3.13.1. Phugoid mode

The response in states u and $\theta$are dominated by the phugoid mode, which is sluggish and well damped. This mode can be illustrated thus [23], [24].

$$\begin{bmatrix} \dot{u} \\ \dot{\theta} \end{bmatrix} = \begin{bmatrix} x_u & x_\theta \\ -z_{u/u_0} & 0 \end{bmatrix} \begin{bmatrix} u \\ \theta \end{bmatrix} + \begin{bmatrix} Z_\eta \\ M_\eta \end{bmatrix} [\Delta\delta e] \tag{3.87}$$

The characteristic equation for the phugoid form

$$\lambda_{ph}^2 - x_u\lambda_{ph} - \frac{x_\theta}{u_o}z_u = 0, \; = \lambda_{ph}^2 - x_u\lambda_{ph} - \frac{x_\theta}{u_o}z_u = 0 \tag{3.88}$$

$\lambda_{ph} = \lambda_R \pm \lambda_I = \lambda_R \pm \lambda_I \; = \; -0.219239 \pm j0.465467$

The third term directly yields the natural frequencyω_n, for the phugoid mode, which is generally written as,

$$\omega_{n_{ph}} = \sqrt{-\frac{x_\theta}{u_\theta}Z_u} \; = \sqrt{\lambda_R + \lambda_I} \; = \; 5.14e^{-01}HZ$$

The period of the phugoid oscillation is on the order of one minute. Thus, the phugoid era was chosen for this investigation τ_{ph} was computed as,

$$\tau_{ph} = \frac{2\pi}{\omega_{n_{ph}}} = \; 4.56e^{+00}s$$

It's damping factor $\zeta_{ph} = -\frac{x_u}{2\omega_{n_{ph}}} = -\frac{\lambda_R}{\omega_n} = \; 4.26e^{-01}$

3.13.2. Short period mode pitch angle control

The reaction in states $w \; and \; q$ is typically rapid, mildly damped, and dominated by the short-period mode. The aircraft's stability characteristics and pilot handling characteristics are significantly

influenced by the dynamics of the short period mode. The short period model is expressed as [23], [24].

$$\begin{bmatrix}\dot{w}\\ \dot{q}\end{bmatrix} = \begin{bmatrix}Z_w\, Z_q\\ M_w m_q\end{bmatrix}\begin{bmatrix}w\\ q\end{bmatrix} + \begin{bmatrix}Z_\eta\\ M_\eta\end{bmatrix}\eta \tag{3.89}$$

The characteristic equation for the short period mode is

$$\lambda_{sh}^2 - m_q\lambda_{sh} + Z_w\lambda_{sh} + z_w m_q + m_q z_w = 0 \tag{3.90}$$

$\lambda_{sh} = -\lambda_R \pm \lambda_I - 5.10566 \pm j\ 4.20789$

The following is a representation and computation of the short period mode's natural frequency;$\omega_{n_{Sh}} = \sqrt{z_w m_q + m_w z_q}\ \ = 6.62e^{+00} HZ$

In this research, short period oscillation, which has a period of little more than a few seconds, was calculated as;

$$\tau_{sh} = \frac{2\pi}{\omega_{n_{sh}}} = \ \ 1.96e^{-01} s$$

The short period oscillation is typically significantly and strongly dampened.

The damping factor is calculated as follows,

$$\zeta_{sh} = \frac{m_q + z_w}{2\omega_{n_{sh}}} = 7.72e^{-01} \tag{3.91}$$

The standard transfer function of an elevator servo can be visualized as a first order lag. In used, servo transfer function for elevators is $\delta e/e = \frac{10}{s+10}$[15].

3.13. Model analysis of system

Model analysis of a plant, both short period oscillation and phugoid period oscillation pitch angle control of a fixed wing airplane has a single input and a single output system. The elevator of an airplane is the input and the pitch angle of the plane is the output. This model analysis represents our damping ratio, frequency, pole, overshoot and gain. These systems are represented by a linear

deferential equation of SISO. In figure 3. 6, A and B show that the open loop control root locus system of phugoid period oscillation and short period oscillation pitch angle of a fixed wing airplane respectively with p lot root locus data. In figure 3.7 A and B show that the closed loop control root locus system of short period oscillation and phugoid period oscillation pitch angle of a fixed wing airplane respectively with plot root locus data.

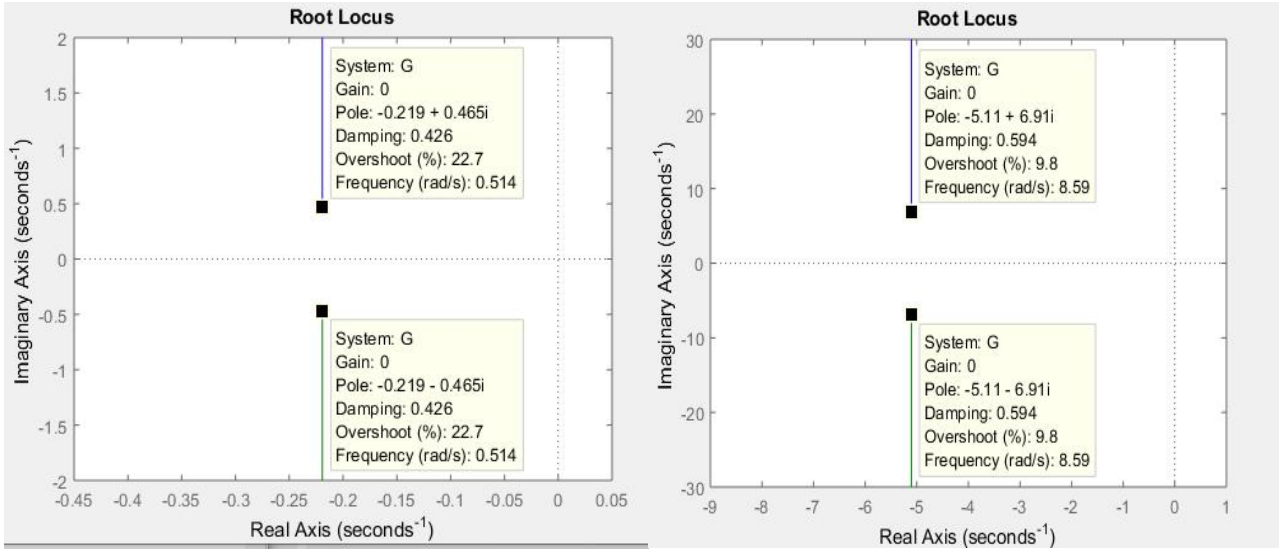

A B

Figure 3. 6 Response open loop root locus

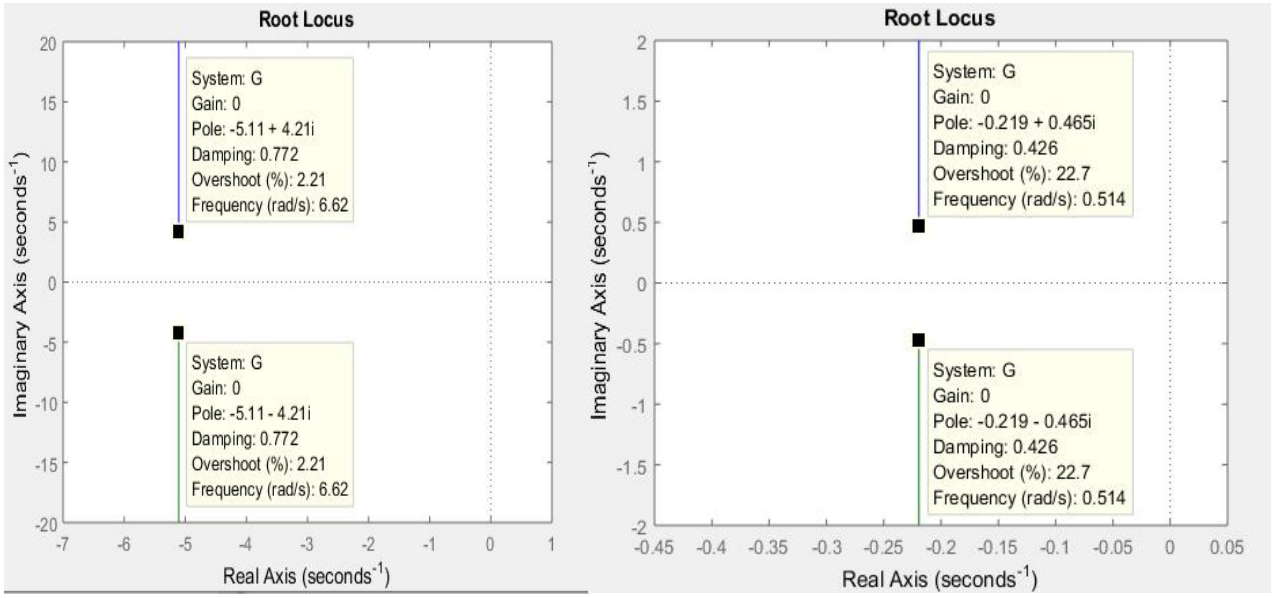

A B

Figure 3.7 Response closed loop root locus

CHAPTER 4
CONTROLLER DESIGN

The controller should be planned to give overall system performance & plant stability without uncertainty. Therefore, it can be thought of as the basis or control of self-expression. The goal of the control method determines the kind of measures. This is possible for the controller to be totally flexible or self-contained with versatility.

4.1. Autopilot Controllers Design

The four control loops that make up the longitudinal control are the position of height, elevation, direct speed, and forward speed. In autopilot pitch attitude, the pitch angle is compared to the height angle required to create the error angle. The longitudinal transfer function of the line works between the pitch angle and the elevator representation of the target plane model. In this thesis, three types of controls are used as the PID controller, the MRAC compliant model reference controller and the MRAC based ANN. The purpose of this control is to control the short period and phugoid oscillation mode [2], [15], [25].

Simulink model of the open loop short period oscillation and phugoid period oscillation pitch angle control.

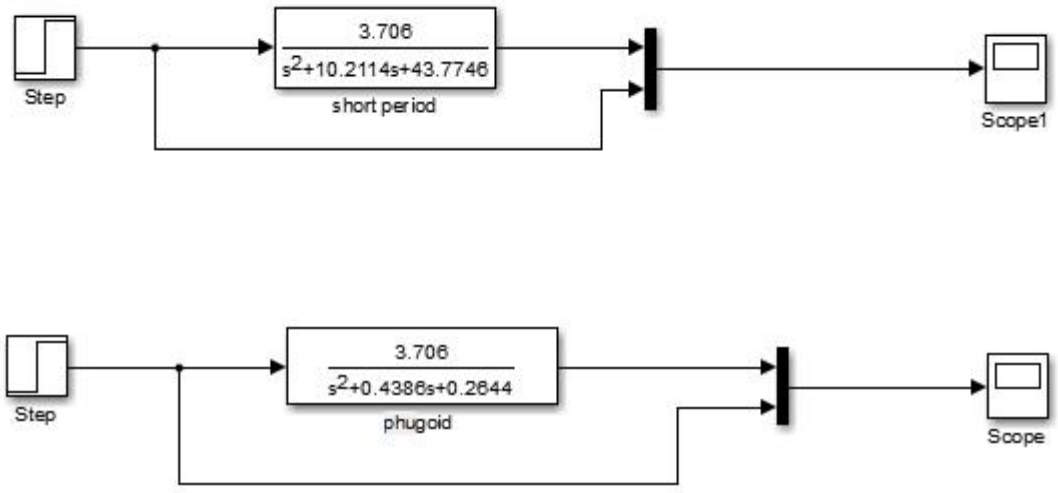

Figure 4.1 Short period and phugoid period oscillation control without controller

4.2. PID controller

PID control is an acronym for proportional integral derivative control. A response technique utilized in the control system is PID control. These types of controls are called three term controls and are made of PID control. By calculating and controlling the equation parameters, combined with the result of another, is how the variable process deviates from the set point value [26].

Proportional term (p): refer to the presents of error. The proportional control often operates with what is known as the steady state error, since it needs a non-zero mistake to drive it[26].The measurement time is given by;

$$P_{out} = k_p e(t) \tag{4.1}$$

Integral term (I): recounts past error values. The size of both the error and the length of the error are equal to the integral term contribution. The key term is provided by;

$$I_{out} = k_i \int 0te(\tau)d\tau \tag{4.2}$$

The integral term speeds up the process by moving to a fixed location and eliminate the remaining conditional error that occurs with a pure proportional control [26].

Derivative term (D): refer to future values of error, based on the rate of change at present. Calculating the effects of a process fault involves finding its slope over time and multiplying this rate of change by a derivative benefit [26].The term derivative is provided by;

$$D_{out} = K_d \frac{de(t)}{dt} \tag{4.3}$$

By forecasting system behavior, derivative action increases stability of the system and settling time.

Table 4.1 Effects of independently increasing PID controller gains

Control response	Rise time	Settling time	Overshoot	Steady state error
K_p	Reduce	little changes	Increase	Reduce
K_d	little changes	Reduce	Reduce	No change
K_i	Reduce	Increase	Increase	Remove

PID control combines the advantage of proportional, derivative and integral regulating acts. It is a 3 term controller, whose transfer function is generally written in the parallel form as in equation.

$$C = P\left(1 + \frac{1}{S} + \frac{DS}{\frac{S}{N} + 1}\right) \tag{4.4}$$

All three value coefficients need to be positive in a stable controller. Ni being positive requires that $iN > 0$ be I and be positive. Negative D, however, still generates a stable controller as long as $DN > -1$because the only restrictions are$D(1 + DN) > 0$,. When N filters, P are the estimated profit, $I$is the total profit, and D is the derivative. There are various approaches. Instead of adjusting a PID controller, automatic PID tuning using MATLAB/ Simulink is used in this thesis. A PID controller can be tuned in a variety of methods; in this thesis, Automatic PID tuning using MATLAB/Simulink is used.

Short period pitch angle control

The congested ring plant for single input single output of fixed wing airplane short period with PID controller is developed in MATLAB/Simulink as exposed in Figure 4-2. The gain values obtained through automated PID tuning are, robustness=0.86, K_p=2.099K_i=13.999, K_d=0.389 and N=70[27].

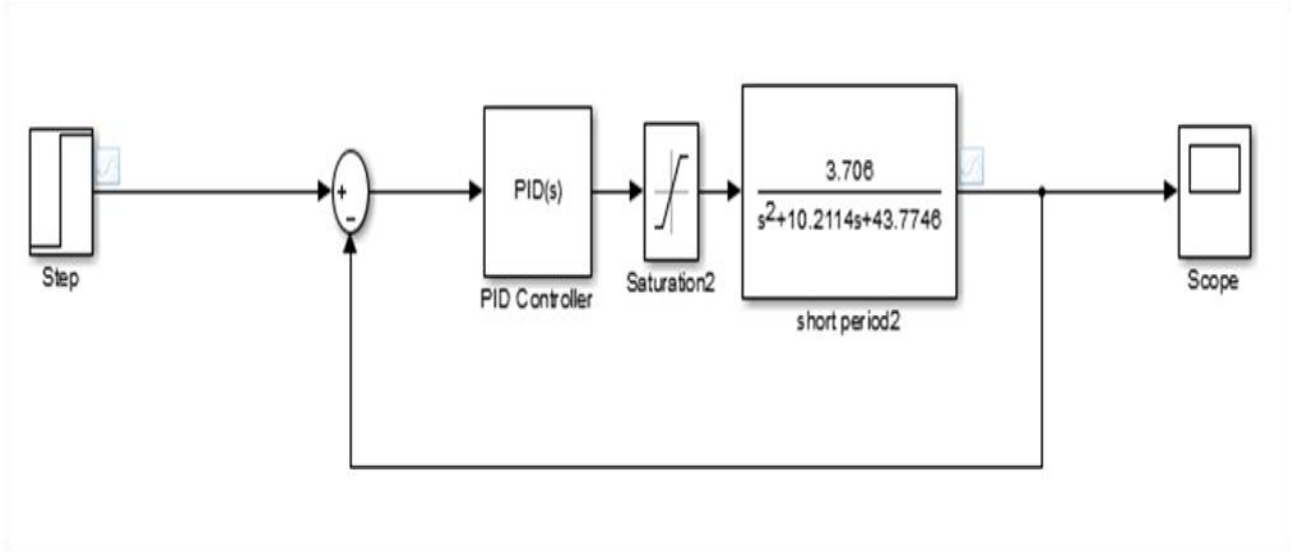

Figure 4.2 PID short periods pitch angle control

Phugoid mode pitch angle control

The of closed loop fixed wing airplane for single input single output of phugoid mode with PID controller is developed in MATLAB/ Simulink as shown in Figure 4-3. The values of gain obtained using automated tuning of PID are, robustness 0.86 K_p=0.01617297 K_i=0.005664, K_d=0.0126336 and N=60.

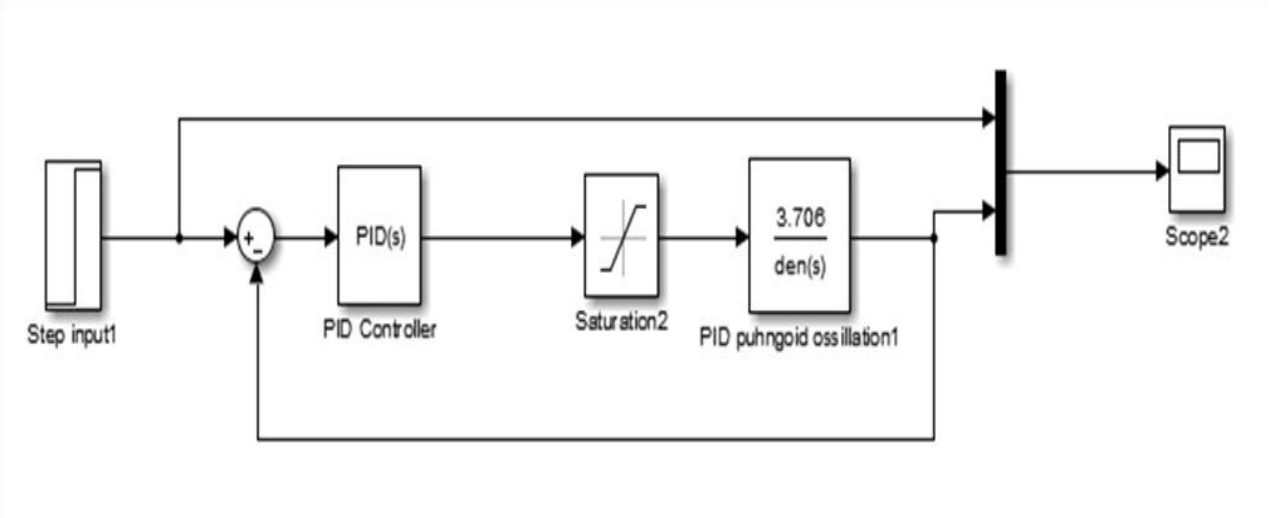

Figure 4.3 PID controller phugoid mode pitch angle

4.3. Classical MRAC Design

4.3.1. Lyapunov's stability method

The class of adaptive control known as the Lyapunov's stability approach is significant. In order to reduce the difference between the model and the plant to zero, this strategy seeks to identify the Lyapunov's function and an adaptation mechanism. Additionally, this approach guarantees the stability of the system's control settings. In this thesis, we examine Lyapunov's stability-based design (Lyapunov's rule). The reference model, controller structure, and tuning gains for the adjustment mechanism are all chosen when developing a model reference adaptive control utilizing the Lyapunov's rule. In this method, the control structure illustrated below is driven by a reference model that is typically believed to be a 1st order system with a differential equation[2].

$$\frac{d_{ym}}{dt} = - a_m y_m + b_m u_c \tag{4.5}$$

A 1st order model is used to define the procedure that needs to be regulated.

$$\frac{d_y}{dt} = -a_y + b_u \tag{4.6}$$

For the control law, it is chosen a combination of feed forward and feedback of the form and the error is.

$$u = \theta_1 u_c - \theta_2 y \tag{4.7}$$

$$e = y - y_m \tag{4.8}$$

Where;

y- Is the fixed wing airplane output

y_m –is the reference model output

θ_1& θ_2- are the controller's parameters due for an update.

u_c – is the reference set point

e - is the difference between actual fixed wing airplane output and reference model output

u - is the signal from the controller.

As a result, since it is necessary to reduce the error to zero as much as feasible, the following differential equation should be used to calculate the error.

$$e = y - y_m \tag{4.9}$$

$$= -a_y + b_u - (-a_m y_m + b_m u_c) \tag{4.10}$$

$$= -a_y + b_u + a_m y_m - b_m u_c \tag{4.11}$$

Replacement u by the above.

$$\dot{e} = -a_y + b(\theta_1 u_c - \theta_2 y) + a_m y_m - b_m u_c \tag{4.12}$$

$$= -a_y - b\theta_2 y + a_m y_m + (b\theta_1 - b_m)uc \tag{4.13}$$

$$= -a_m e - (b\theta_2 + a - a_m)y + (b\theta_1 - b_m)uc \tag{4.14}$$

A quadratic function is used as the Lyapunov's function in order to determine the Lyapunov's criterion while the parameter adjustment mechanism drives the parameters $\theta_1 \& \theta_2$ to their desired values;

$$V(e, \theta_1, \theta_2) = 1/2\ [e^2 + \frac{1}{b\gamma}(b\theta_2 + a - a_m)2 + \frac{1}{b\gamma}(b\theta_1 - b_m)^2] \quad (4.15)$$

When e (error) is zero and the controller settings are identical to the right values, this Lyapunov's function is zero. The result of V's complete derivation is;

$$\dot{V} = e\frac{de}{dt} + \frac{1}{\gamma}(b\theta_2 + a - a_m)\frac{d\theta_2}{dt} + \frac{1}{\gamma}(b\theta_1 - bm)\frac{d\theta_1}{dt} \quad (4.16)$$

$$= - a_{me^2} + \frac{1}{\gamma}(b\theta_2 + a - a_m)(\frac{d\theta_2}{dt} - \gamma ye) + \frac{1}{\gamma}(b\theta_1 - bm)(\frac{d\theta_1}{dt} - \gamma u_c e) \quad (4.17)$$

When negative, the quadratic function given above is a Lyapunov's function. When the parameters have been modified,

$$\frac{d\theta_1}{dt} = -\gamma u_c e \quad (4.18)$$

$$\theta_1 = -\frac{\gamma u_c e}{s} \quad (4.19)$$

$$\frac{d\theta_2}{dt} = \gamma ye \quad (4.20)$$

$$\theta_2 = \frac{\gamma ye}{s} \quad (4.21)$$

Wherever γ is the derivative gained through adaption

$$V = - a_m e^2 \quad (4.22)$$

Is negative therefore semi-definite? This suggests that $(t) \leq (0)$ and that θ_1 & θ_2 must thus be bounded. The output of the system $y = e + y_m$ is therefore also bounded. The instability issues in gradient techniques or the (Massachusetts Institute of Technology) MIT principle are avoided by the Lyapunov's stability based method.

In this thesis under damped second order method is selected as reference model y_m with damping ratio 7.49e-01, time constant 6.67e-02 and natural frequency 2.00e+01 which is a transfer function of

$$Y_m = \frac{400.9}{s^2 + 30s + 400.9}$$

Simulink model of MRAC for the short period

Simulink model of Single input single output system of short period pitch angle design is given as follows. The approximated transfer function for SISO short period pitch angle is given by

$$\frac{\theta}{\delta_e} = \frac{3.706}{s^2 + 10.2114\,s + 43.7746}$$

The MRAC developed in MATLAB/ Simulink for short period pitch angle is given in Figure4.4.

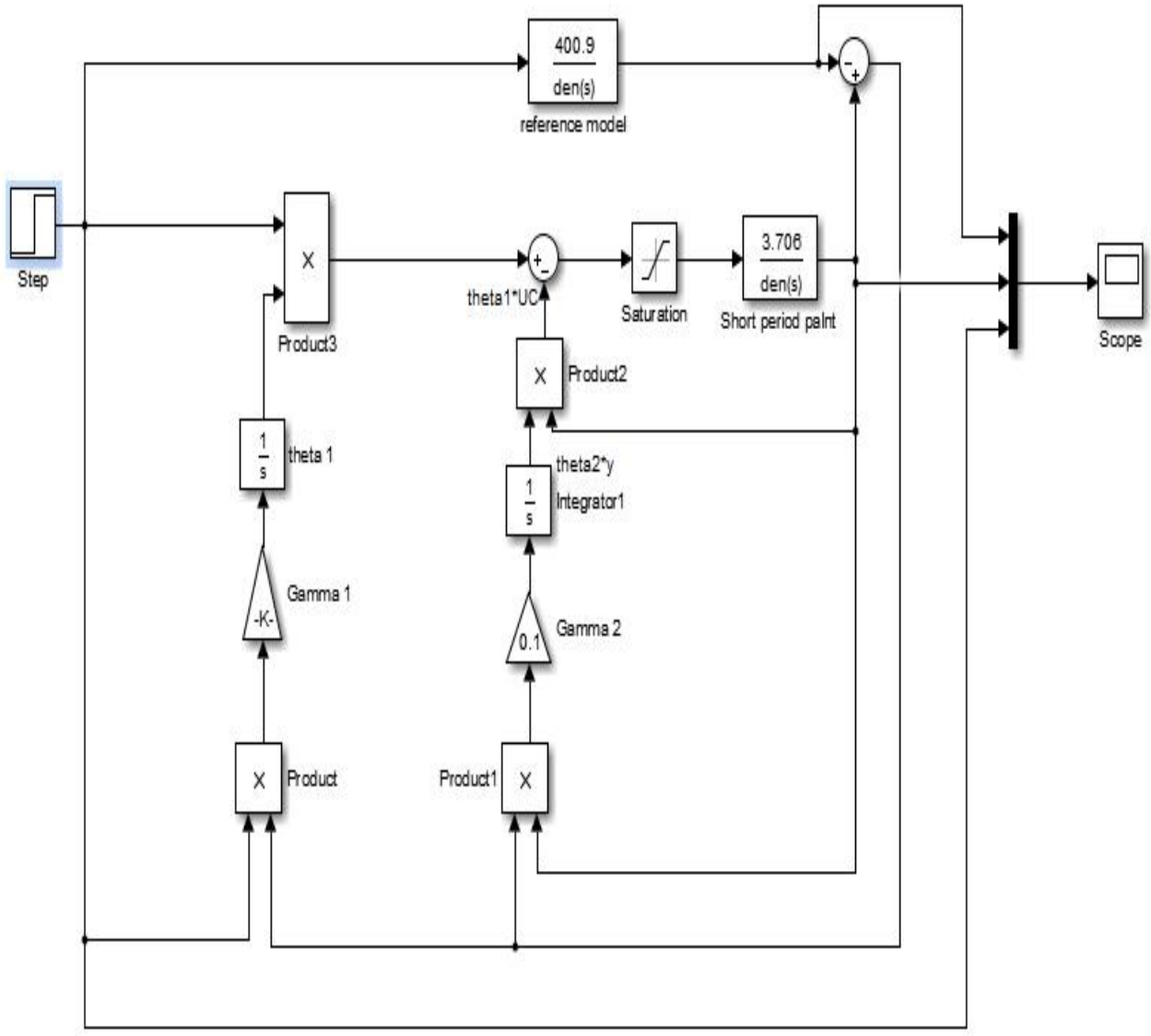

Figure 4.4 MRAC for the short period pitches angle control

Simulink model of DMRAC for the phugoid mode pitch angle control

Simulink model of each single input single output scheme of phugoid mode oscillation pitch angle design is provided below. The approximated transfer function for SISO phugoid mode pitch angle is given by.

$$\frac{\theta}{\delta_e} = \frac{3.706}{s^2 + 0.4386\,s + 0.2644}$$

The MRAC developed in MATLAB Simulink for phugoid mode pitch angle control is given in Figure 4.5

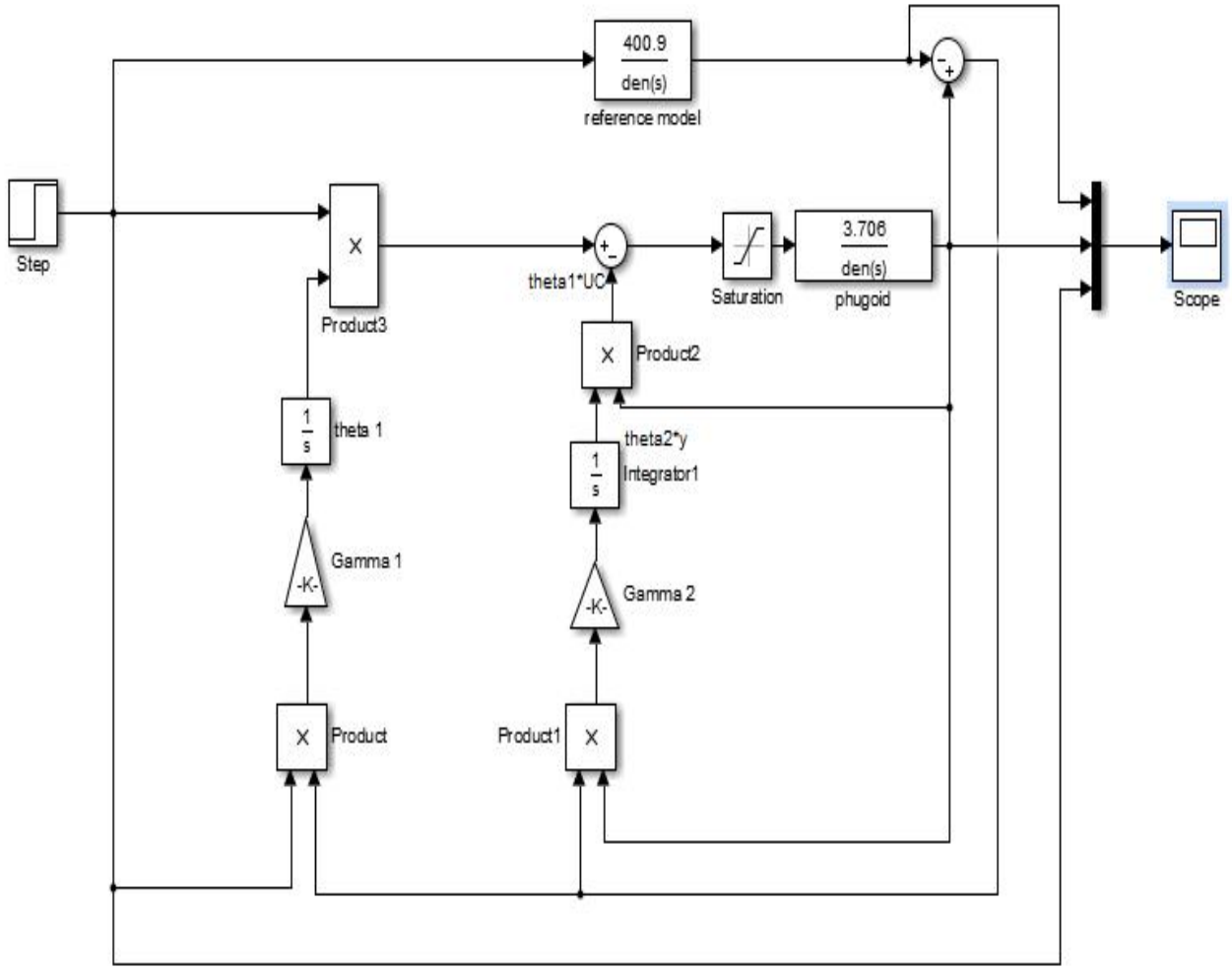

Figure 4.5 MRAC phugoid modes pitches angle control

4.4. Neural network controller

A neural network is a sequence of algorithms that actions to distinguish uncovering the original relations in a piece of information using a method that simulates how the human being mind works. It consists of inputs and outputs neuron with hidden layers. The base of the neural network training is back propagation. It is a method for modifying the weights of a neural network in accordance with the error rate observed in the previous epoch.

4.4.1. Algorithm for back-propagation training

Back-propagation is a popular technique for training neural networks, and it aims to optimize the weights so that the network can learn how to accurately map different inputs to outputs[19].

Back-propagation method contains the following steps:

Step1 initialization: - put all the weights and threshold values of the network to uniformly dispersed arbitrary numbers within a range.

$$\left(-\frac{2{,}4}{Fi}+\frac{2{,}4}{Fi}\right) \tag{4.23}$$

Where Fi is the whole quantity of inputs of the neuron i in the networks.

Step2activation: -Applying inputs will trigger the back-propagation neural network.

$x_1(p), x_2(p), \ldots\ldots x_n(p)$ and preferred outputs $y_{d1}(p), y_{d2}(p), \ldots\ldots y_{dn}(p)$, forward pass.

Determine the hidden layer's neurons' actual outputs.

$$y_j(p) = sigmoid\left[\sum_{i=1}^{n} x_i(p).w_{ij}(p) - \theta_j\right] \tag{4.24}$$

Where *n* is the number of inputs of neuron *j* in the hidden layer.

Determine the neurons' real outputs in the output layer.

$$y_k(p) = sigmoid\left[\sum_{j=1}^{m} x_j(p).w_{jk}(p) - \theta_k\right] \tag{4.25}$$

Where *m* is the number of inputs of neuron *k* in the output layer.

Step3 Weight training (back-propagation): This technique updates the weights in the back-propagation network, which causes the errors caused by output neurons to be propagated backward.

Determine the error gradient for the output layer's neurons.

$$\delta_k(p) = y_k(p).[1 - y_k(p)].e_k(p) \tag{4.26}$$

Where,

$$e_k(p) = y_{dk}(p) - y_k(p) \tag{4.27}$$

Make the necessary weight modifications.

$$\Delta W_{jk}(p) = a.y_j(p).\delta_k(p) \tag{4.28}$$

Modernize the weight at the output neurons;

$$W_{jk}(p+1) = w_{jk}(p) + \Delta W_{jk}(p) \tag{4.29}$$

Determine the neurons' error gradient in the deep layer

$$\delta_j(p) = \ y_j(p).\left[1 - y_j(p)\right].\sum_{j=1}^{m} \delta_k(p).w_{jk}(p) \tag{4.30}$$

Work out the weight correction

$$W_{ij}(p) = a.x_j(p).\delta_j(p) \tag{4.30}$$

Modernize the weights at the hidden neurons;

$$W_{ij}(p+1) = W_{ij}(p) + \Delta W_{ij}(p) \tag{4.31}$$

Step 4 iteration As soon as the chosen mistake is satisfied, increase iteration p by one, go back to step 2, and continue the procedure.

4.5. Compound controller design

Fixed-wing aircraft are mathematically represented by a SISO, which is non-linear, strongly coupled, and disturbance-sensitive. The model is faulty since numerous terms were left out throughout the modeling process. The model's unknown parameters make it challenging to construct a controller,

yet MRAC is appropriate for models with unknown parameters. Despite the fact that MRAC has numerous benefits, it views complex models as simple reduced order constructs. Unmodeled dynamics also refers to the higher order dynamics that were excluded. An excess reaction of unmodeled dynamics or even the instability of an adaptive control system will be brought on by high-frequency noise or an excessive amount of adaptive gain. When MRAC encounters complex nonlinear systems, the implementation is particularly challenging. This study blends MRAC with neural networks to prevent the negative impact of unorganized uncertainties of the fixed wing airplane model [25].

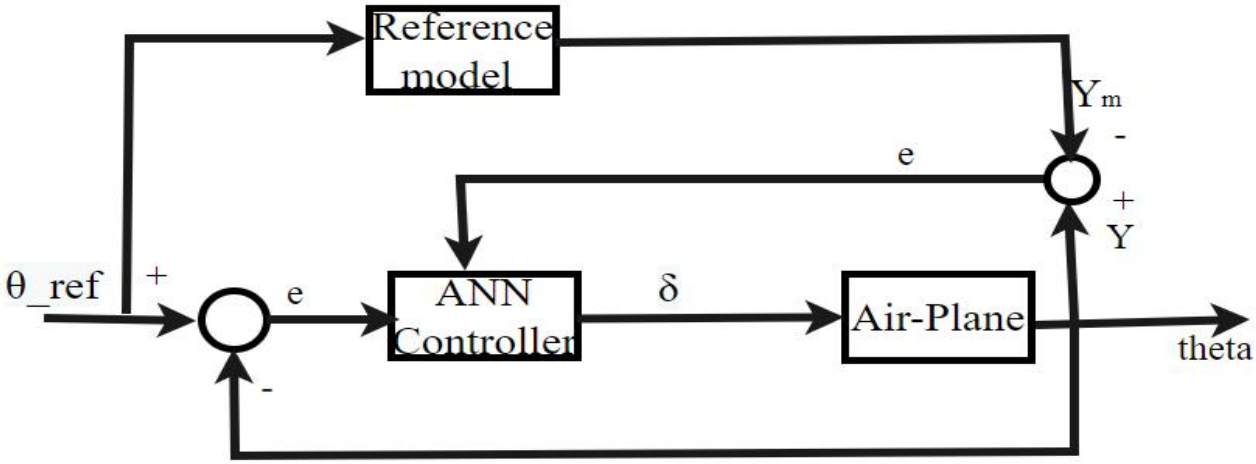

Figure 4.6 General ANN based on MRAC pitch angle controller

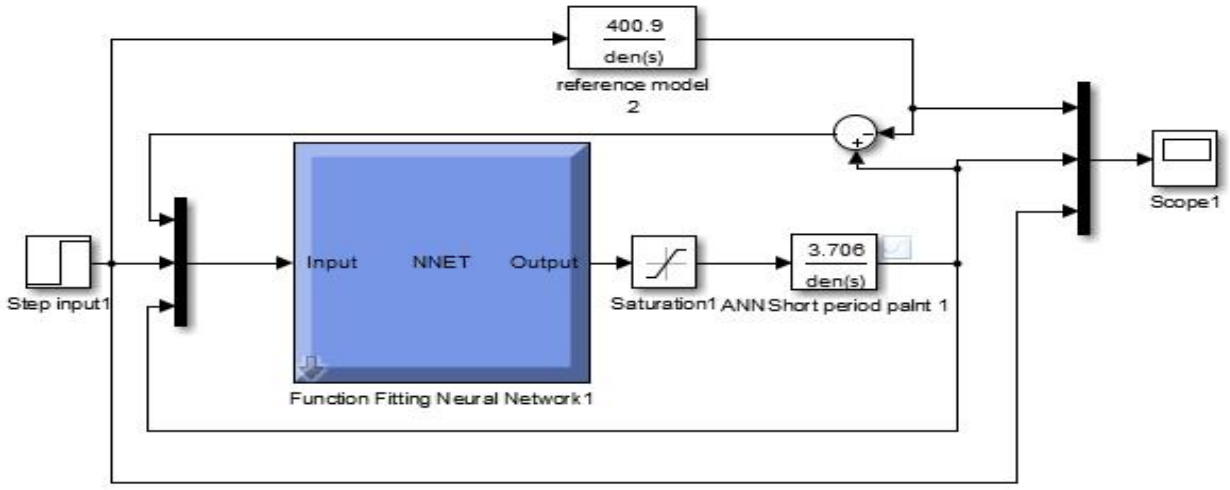

Figure 4.7 ANN based on MRAC short period pitch angle controller

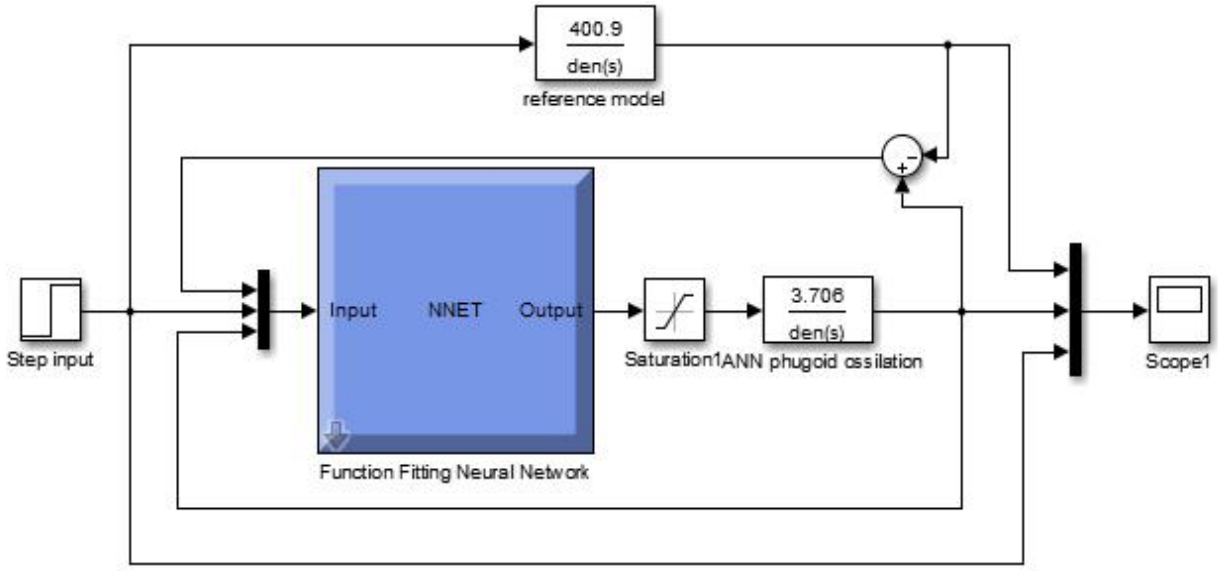

Figure 4.8 ANN based on MRAC phugoid mode pitch angle controller

The artificial neural network's error index for training weights is provided in b.

$$e(K) = \frac{1}{2}e(k)^2 \tag{4.32}$$

CHAPTER 5

RESULTS AND DISCUSSION

In chapter 3, the mathematical model of fixed wing airplane longitudinal dynamics and design of pitch angle of short period model and phugoid mode oscillation autopilot are presented and analyzed in depth. Moreover, in the chapter 4 designs of PID controller, classical MRAC and ANN based MRAC for pitch angle control of fixed wing airplane autopilot be completed. The system's simulations are the subject of this chapter. Initially, simulations results of without controller second PID controller, and then classical MRAC finally ANN based MRAC respectively.

5.1. Without controller MATLAB result

We can determine the response of fixed wing airplane short period oscillation and phugoid (long) period oscillation pitch angle with and without controller in unit step input.

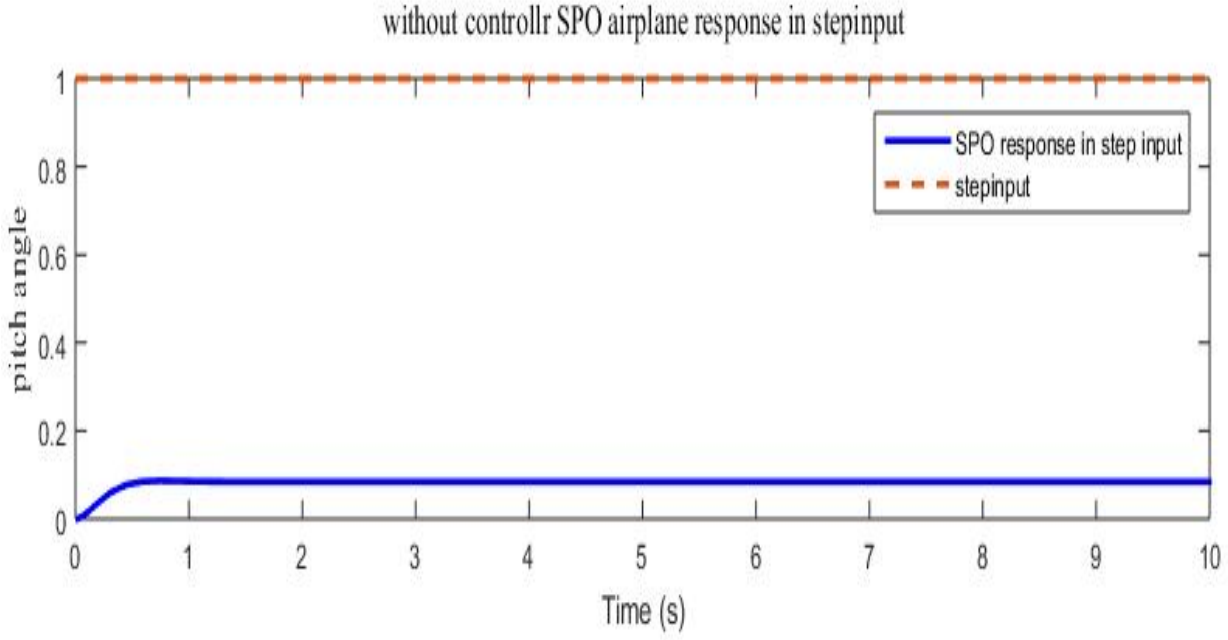

Figure 5.1 Response of short period pitch angle without controller

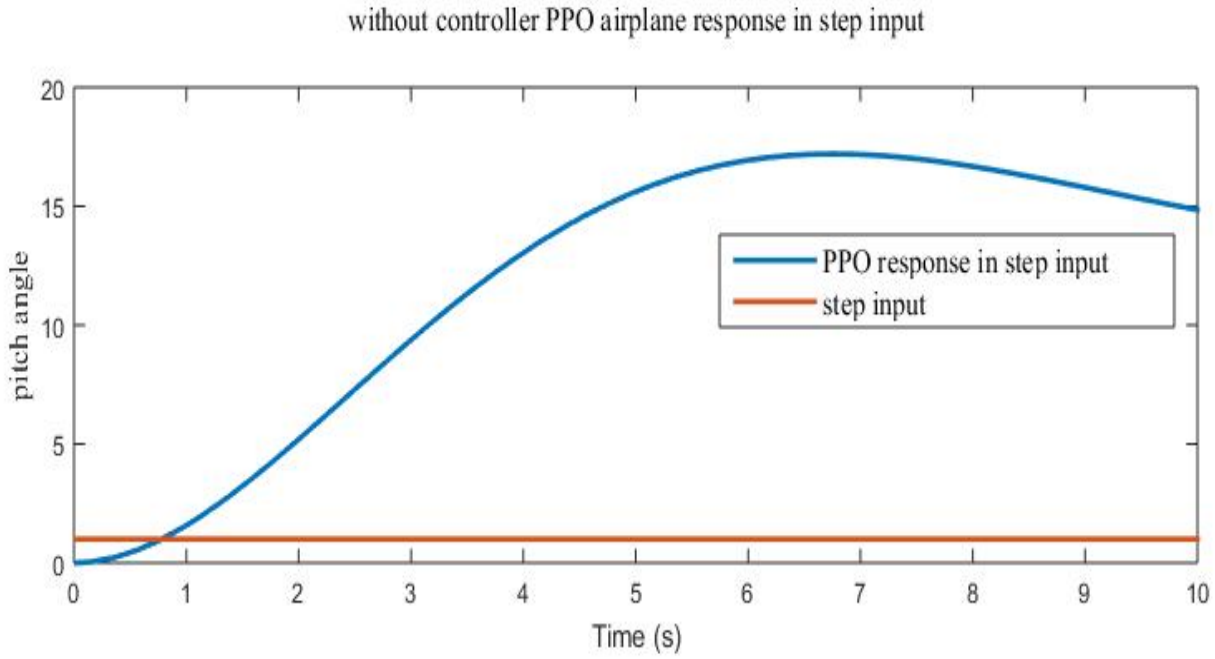

Figure 5.2 Responses of phugoid model pitch angle control without controller

5.2. Response using PID controller

In this thesis, PID controller is used to contrast the performance of the classical Lyapunov's criteria control and ANN using MRAC pitch angle control of fixed wing airplanes.

Response short period mode pitch angle control using PID controller

The PID controller results of the single input single output system of short period pitch angle control in fixed wing aircraft in Figure 5.3 been derived from the single input single output system's MATLAB/Simulink to govern short period pitch angle control of fixed wing aircraft. The outcome is displayed in Figure 5.3.With the following time domain specifications; rise time = 1.5895 second, settling time = 2.9289 second, overshoot = 0 %, peak = 1, closed loop stability =stable.

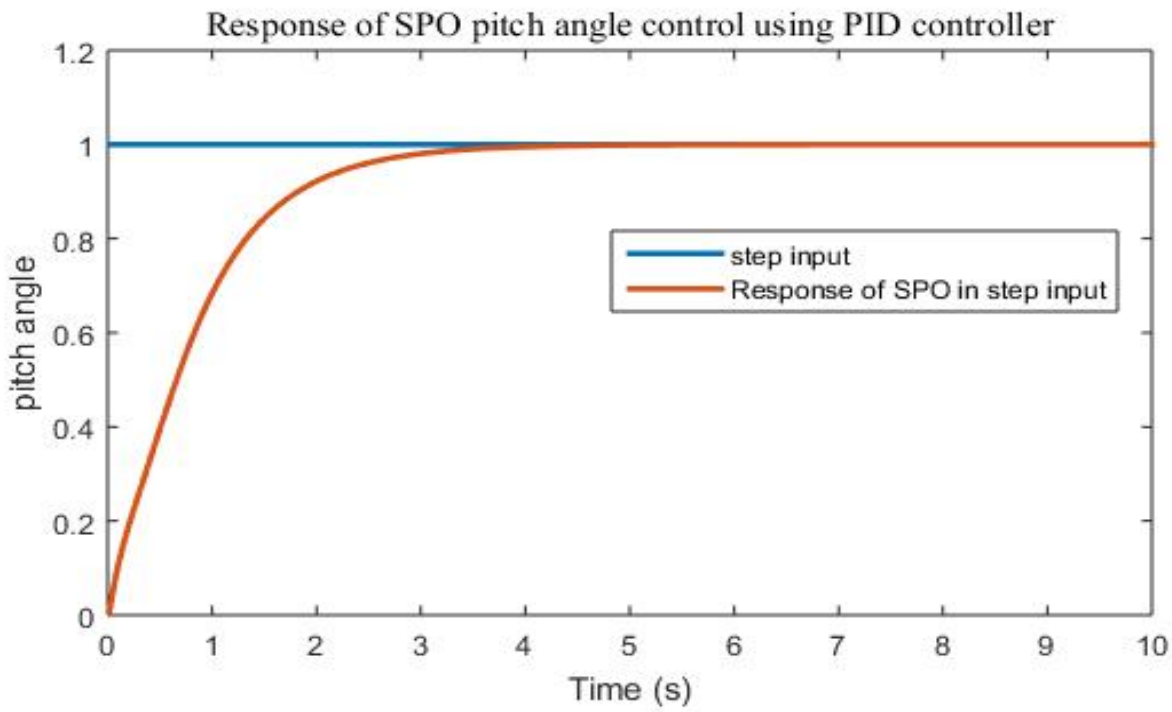

Figure 5.3 Responses short period pitch angle control using PID controller

Response of SISO phugoid model oscillation pitch angle using PID controller

The PID controller results of the single input single output system of phugoid model oscillation pitch angle control in fixed wing aircraft in Figure 5.4 was obtained from the Simulink model of single input single output system to control phugoid model oscillation pitch angle control of fixed wing aircraft. The response is shown in Figure 5.4. With the following time domain specifications: rise time =28.47 second, settling time=53.0312second, overshoot= 0 %, peak = 1, closed loop stability =stable

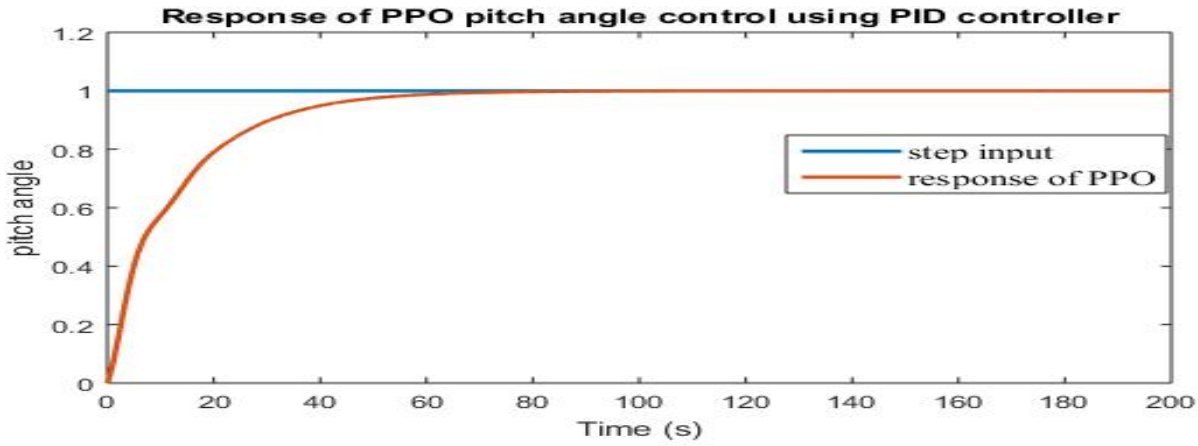

Figure 5.4 Responses of phugoid model oscillation pitch angle control using PID controller

5.3. Results using model reference adaptive control

Response of SISO short period pitch angle control using MRAC

The model reference adaptive control results of the single input single output system of short period pitch angle control of fixed wing aircraft in figure 5.5 in -19.8 and 0.1 gamma value was obtained from the Simulink model for single input single output system to control short period pitch angle control fixed wing aircraft. The results have shown in figure 5.5 perfectly follow the model reference and quickly attended the preferred short period pitch angle. Model reference adaptive control systems therefore exhibit better answer than the created PID controller.

The response of appendix II (A) table 5.1 Short period MRAC different gamma value.

Selection Criteria	Reference model	Short period mode gamma value				
		-19.8	-23.8	-15.8	-10	-33
Rise Time	0.1177	0.7557	0.6065	1.0646	2.0494	0.4407
Settling Time	0.2847	1.3324	1.6753	2.1106	3.9374	2.1042
Overshoot	2.7658	0.3150	4.4342	3.1388e-04	0	15.8360
Undershoot	0	0	0	0	0	0
Peak:	1.0277	1.0031	1.0443	1.0000	1.0000	1.1584

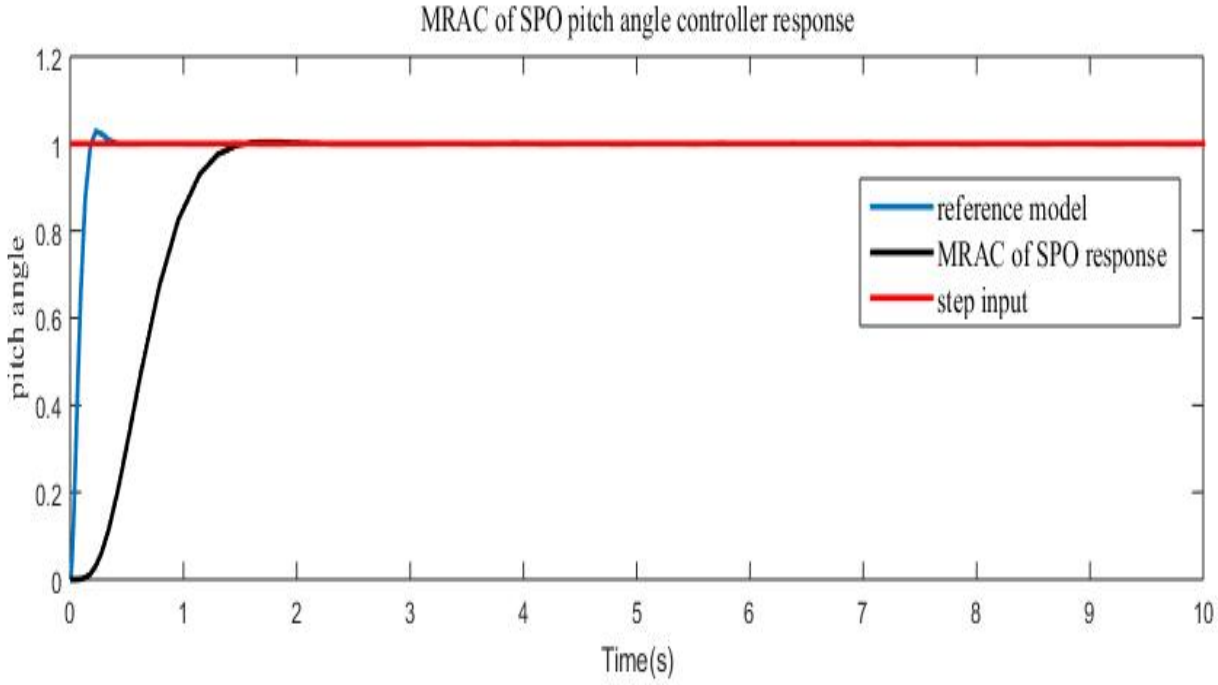

Figure 5.5 Response short periods pitch angle control using MRAC

Response of SISO phugoid model oscillation pitch angle control using MRAC

The model reference adaptive control of Lyapunov's stability response of the single input single output system of phugoid model oscillation pitch angle control of fixed wing aircraft in using -0.039 and 0.039 gamma value figure 5.6 was obtained from the MATLAB results for single input single output system to control phugoid model oscillation pitch angle control fixed wing aircraft. The results have shown in figure 5.6 perfectly follows the model reference and quickly attended the desired phugoid model oscillation pitch angle. So, MRAC have good results than the PID controller.

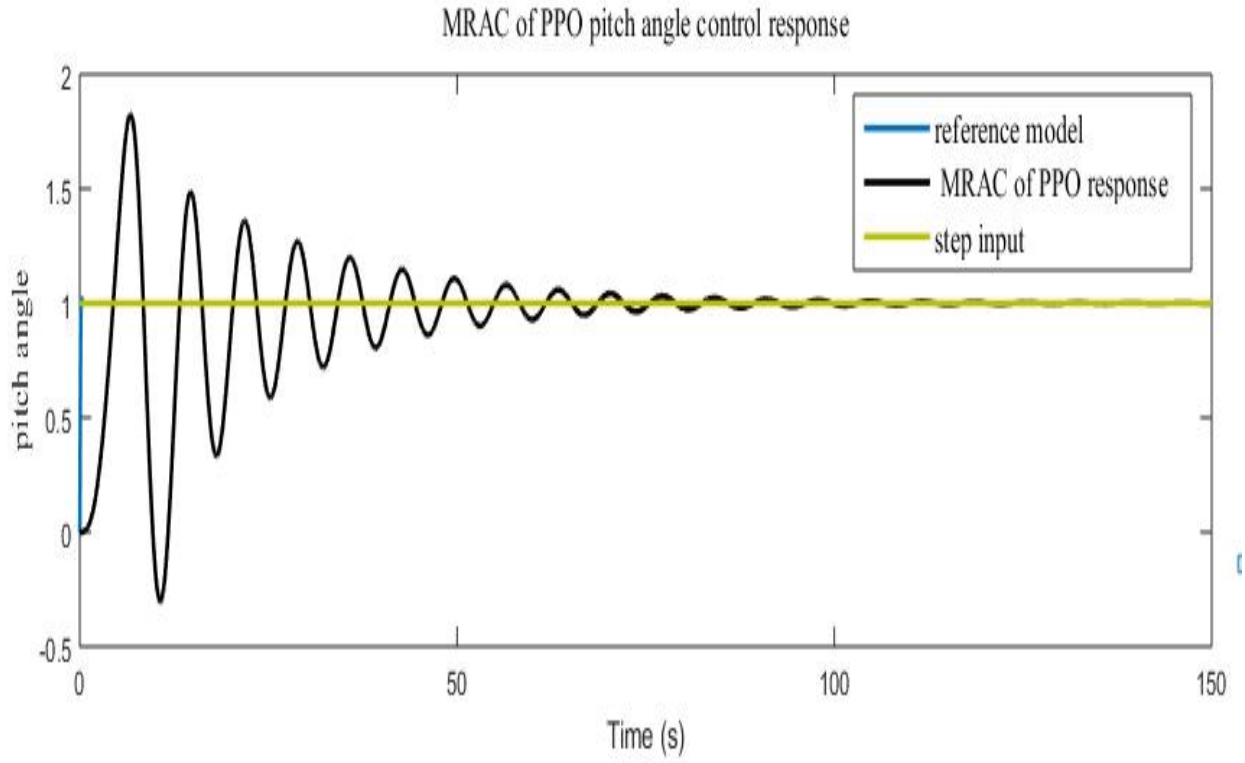

Figure 5.6 Response phugoid mode oscillation pitch angle control using MRAC

The response of appendix II (B) table 5.2 Different gamma value of phugoid mode oscillation pitch angle control using MRAC

Selection Criteria	Reference model	Phugoid mode gamma value			
		-0.039	-0.01	-1	-0.0001
Rise Time	0.1177	2.0258	3.0202	0.6492	3.0950
Settling Time	0.2847	34.6395	41.2926	33.3524	48.7552
Overshoot	2.7658	49.1570	0	750.9702	0
Undershoot	0	0	0	565.9779	0
Peak:	1.0277	1.4928	0.9892	8.5104	0.8222

5.4. Response ANN based MRAC

Response Short period pitch angle control using ANN based MRAC

The artificial neural network based model reference adaptive control of the single input single output system of short period pitch angle control of fixed wing airplane in figure 5.7 was obtained from the Simulink model for single input single output system to control short period pitch angle control fixed wing aircraft. The results as shown in figure 5.7 perfectly follows the ANN based MRAC quickly attended the desired short period pitch angle. Rise Time: 0.1748 second, Settling Time: 0.6633 second, Overshoot: 8.156 Undershoot: 0, So, ANN based MRAC have good results than model reference adaptive controls and proportional integral derivative's controller.

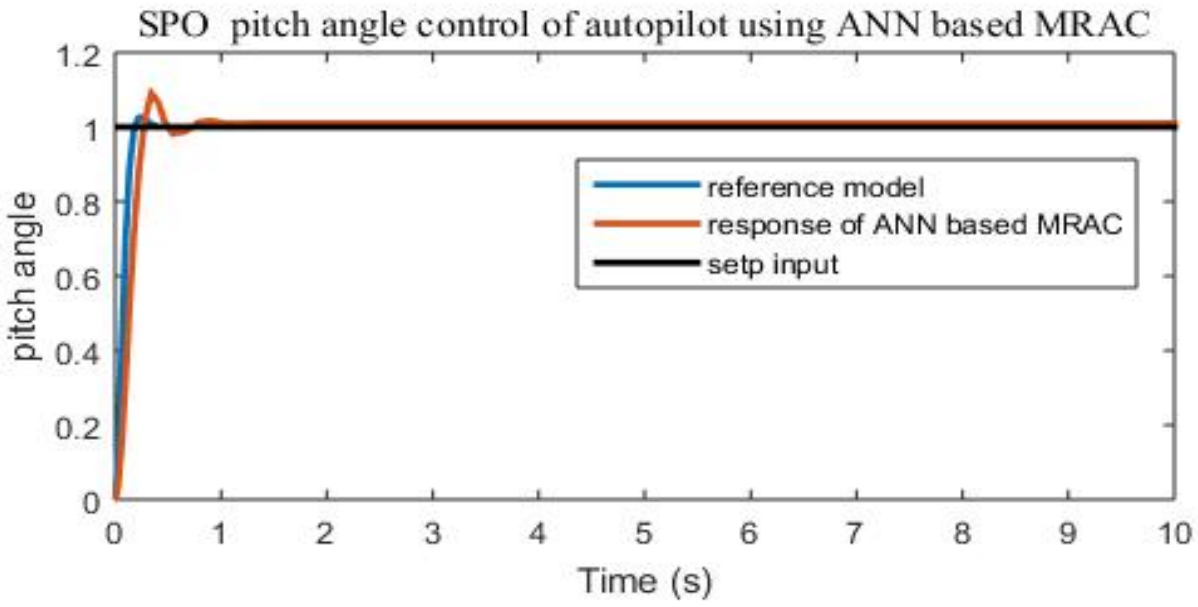

Figure 5.7 Response Short periods pitch angle control using ANN based MRAC

Phugoid model oscillation pitch angle control using ANN based MRAC

The closed loop response of ANN based MRAC the single input single output system of phugoid model oscillation pitch angle control of fixed wing airplane in figure 5.8 was obtained from the Simulink model for single input single output system to control phugoid model oscillation pitch angle control fixed wing aircraft. The response as shown in figure 5.8 perfectly follows the ANN based MRAC quickly attended the desired phugoid model oscillation pitch angle; rise Time:

0.7080 second, settling time: 17.8862 second, overshoot: 72.296, undershoot: 0. So, ANN based MRAC have good response than model reference adaptive controls and proportional integral derivative's controller.

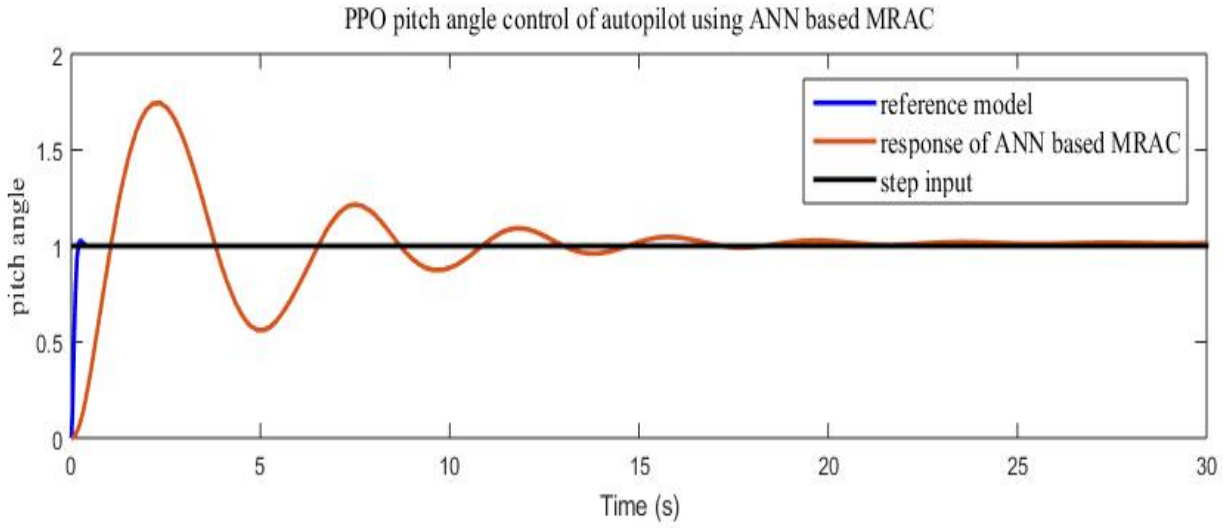

Figure 5.8 Response of Phugoid oscillation pitch angle control using ANN based MRAC

The figure 5.9 shows short period oscillation pitch angle autopilot different controllers have different response.

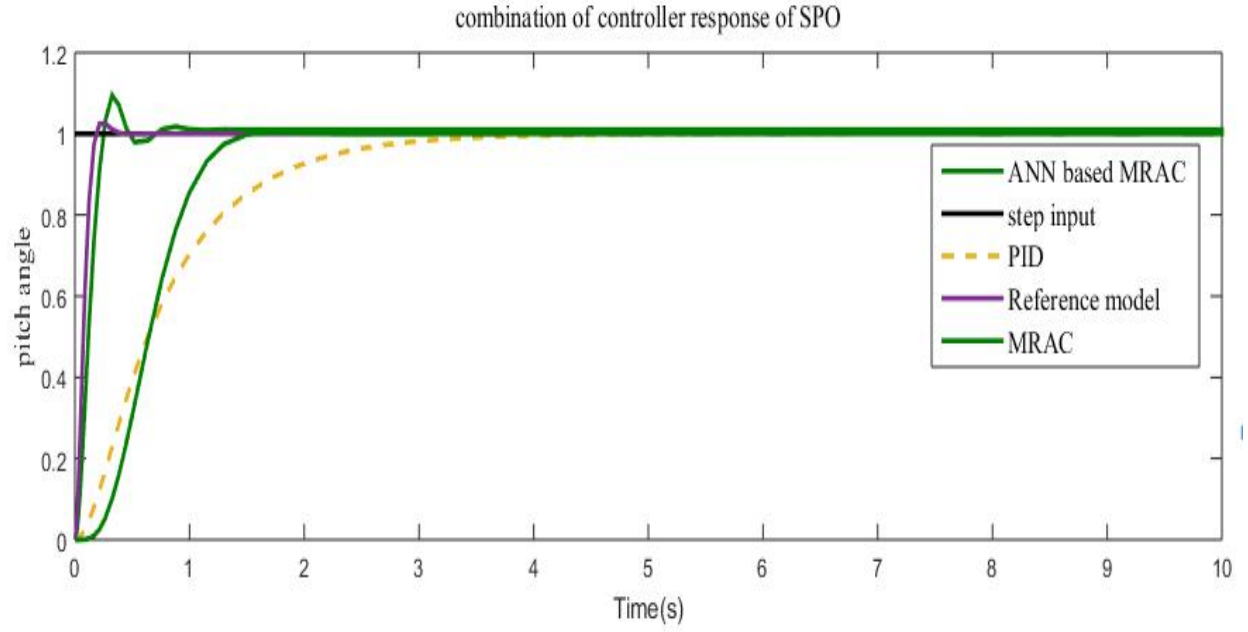

Figure 5.9 Response of combination of controller short period

The figure 5-10 shows phugoid period oscillation pitch angle autopilot different controllers have different response.

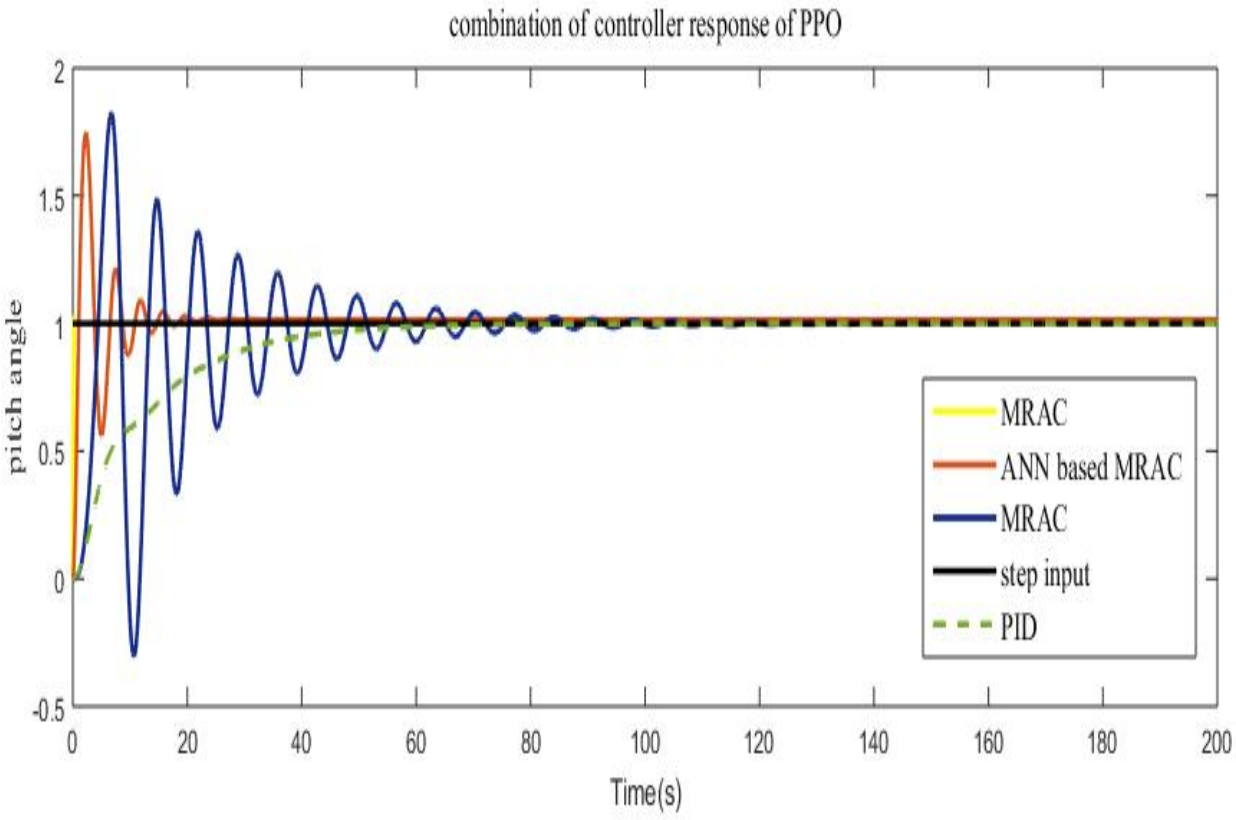

Figure 5.10 Response of combination of controller phugoid oscillation pitch angle

In this thesis, the ANN is utilized to enhance system performance by instructing the controllers to enhance the system by quickly estimating from uncertain and undetermined variables to optimum values. The current neural network (NN) is divided into 3 layers: an output layer with one neuron, a hidden layer with 30 neurons, and an input layer with three neurons. The network is trained using the back-propagation learning technique (Levenberg Marquardt). Samples of artificial neural network training information are gathered from the controller's step input, error and fixed wing airplane output (input) and u_c (output). Sigmoid activation function is used to stimulate the neurons in the hidden layer, while a simple linear activation function is employed for output.

The subsequent actions must be taken in order to implement a neural network;

- Gather information.
- Neuron of net information.
- Choice of network structural design
- Set the biases and weights to zero.
- Teach the net.
- Assess the results.
- Just use the net.

The figure below shows the regression graph under plots after training the ANN.

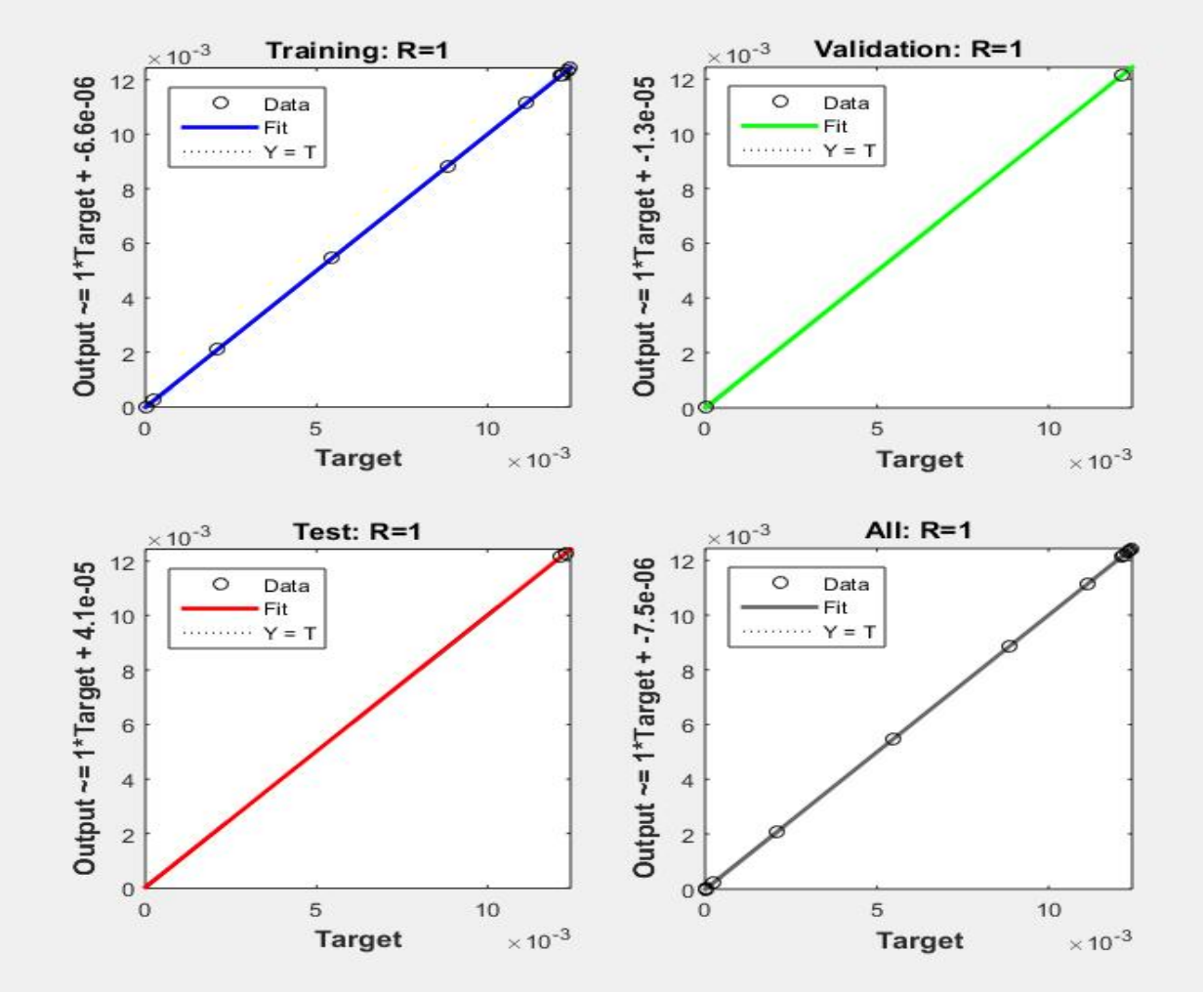

Figure 5. 11 Regression graph for short period ANN training

Performance characteristics for the short period oscillation pitch angle system all PID controller, Classical MRAC and artificial neural network base DMRAC.

From the above figures and table, we can draw the conclusion that the artificial neural network's ability to generalize, adaptively alter the network parameters, and learn makes it superior to PID and conventional mode MRAC for varied step reference input to the nonlinear airplane. Because the airplanes respond more slowly to PID and conventional MRAC than to ANN-based DMRAC with variable reference signal,

In general, we can see from the graphs and table above that an ANN controller is more effective than PID and traditional MRAC at controlling the pitch angle of a fixed-wing aircraft.

CHAPTER 6

CONCLUSION AND FUTURE SCOPE

6.1. Conclusion

In this paper, modeling & designing a fixed wing airplane pitch angle controller by means of the PID controller, classical MRAC controller & combine classical MRAC technique with neural networks have been checked. Lyapunov's stability criteria have been used to create an adaptive rule intended for changing the controller parameters online.

To demonstrate the advantages of the NN based DMRAC over traditional MRAC controller and PID controller, computational domain has been used. Through simulation tests utilized MATLAB/Simulink software, the proposed NN based DMRAC, Conventional MRAC, and PID are evaluated for performance**.**

- For PID 28.47, 53.0312 MRAC, 2.0258, 34.6395, and ANN utilizing MRAC 0.7080, 17.8862, rise time and settling time in phugoid model oscillations are shown. Every unit is in seconds.
- In SPO contrast to traditional MRAC, which has a rise time of 0.7557 seconds, settling time of 1.3324 seconds, and PID, which has a rise time of 1.5895 seconds, settling time of 2.9289 seconds, It is clear after the simulation outcome SPO that the proposed artificial neural network-based direct model reference adaptive control has rise time of 0.1748 seconds and settling time of 0.6633 seconds.

The simulation result intended for the neural network based DMRAC control shows good performance compared to classical MRAC and PID for regulating output. The results of short period oscillation both classical MRAC and PID controller are good accuracy arise time, settling time. Phugoid model oscillations results of NN using MRAC, PID and MRAC controllers are not acceptable in real applications due to rise time, settling time and purpose.

6.2. Future Scope

The simulation findings show that, when compared to the ANN based MRAC, classical model reference adaptive controller and PID controller, the ANN based MRAC controller for pitch angle fixed wing airplane autopilot performed best. Hence, it is advised to install the short period pitch angle ANN based DMRAC on the actual operation of a fixed wing airplane autopilot in to verify these MATLAB software & not implement phugoid mode oscillation pitch angle ANN based MRAC on the real use of an autopilot in a fixed wing aircraft. Phugoid oscillation cannot happen if the pitch angle or attitude is not allowed to change; otherwise, the autopilot's pitch angle holding feature would crush the phugoid and lower the transfer function. Further investigation should concentrate on trying to extend this scheme to a higher order model such as lateral automatic pilot, longitudinal, quad copters, robotics, ship automatic pilot, and electrical machine modeling.

REFERENCE

[1] T. Elijah, R. S. Jamisola, Z. Tjiparuro, and M. Namoshe, "A review on control and maneuvering of cooperative fixed-wing drones," *Int. J. Dyn. Control*, vol. 9, no. 3, pp. 1332–1349, 2021, doi: 10.1007/s40435-020-00710-2.

[2] N. T. N. AG, *"'Model- Reference Adaptive Control'" springer international publishing*. 2018.

[3] K. B. Pathak and D. M. Adhyaru, "Survey of model reference adaptive control," *3rd Nirma Univ. Int. Conf. Eng. NUiCONE 2012*, vol. 2, pp. 6–8, 2012, doi: 10.1109/NUICONE.2012.6493284.

[4] U. Bern, P. V. Koubi, and A. Room, "Dr. Qadri Hamarsheh."Lectures for Neural networks and Fuzzy logic" at Philadelphia University on 2015/2016.," *Philadelphia Univ.*, vol. 35, no. 1991, pp. 2008–2009, 2015.

[5] R. R. Gupta and V. V. Chalam, "Lyapunov Redesign of Model Reference Adaptive Control Systems - 1,2.," *J. Inst. Electron. Telecommun. Eng.*, vol. 25, no. 11, pp. 456–461, 2020, doi: 10.1080/03772063.1979.11451981.

[6] P. Swarnkar, S. Jain, and R. K. Nema, "Effect of Adaptation Gain in Model Reference Adaptive Controlled Second Order System," *Eng. Technol. Appl. Sci. Res.*, vol. 1, no. 3, pp. 70–75, 2011, doi: 10.48084/etasr.11.

[7] R. Zbikowski. and P. J. Gawthrop. K. J. HUNT, t D. SBARBARO and Neural, "Neural Networks for Control Systems A Survey *," *Surv. Pap.*, vol. 28, no. 6, pp. 1083–1112, 2016.

[8] Z. Man, H. R. Wu, K. Eshraghian, and M. Palaniswami, "Adaptive tracking controller using neural networks for nonlinear systems," *IEEE Int. Conf. Neural Networks - Conf. Proc.*, vol. 1, pp. 314–319, 2014, doi: 10.1109/icnn.1995.488116.

[9] Munadi, M. A. Akbar, T. Naniwa, and Y. Taniai, "Model Reference Adaptive Control for DC motor based on Simulink," *Proc. - 2016 6th Int. Annu. Eng. Semin. Ina. 2016*, pp. 101–106, 2017, doi: 10.1109/INAES.2016.7821915.

[10] K. Pirabakaran and V. M. Becerra, “PID autotuning using neural networks and Model Reference Adaptive Control,” *IFAC Proc. Vol.*, vol. 35, no. 1, pp. 451–456, 2020, doi: 10.3182/20020721-6-es-1901.00728.

[11] C. Bao and Y. Guo, “Design of a Fixed-Wing UAV Controller Based on Adaptive Backstepping Sliding Mode Control Method,” *IEEE Access*, vol. 9, pp. 157825–157841, 2021, doi: 10.1109/ACCESS.2021.3130296.

[12] U. C. Yayli, C. Kimet, A. Duru, O. Cetir, and U. Torun, “Design optimization of a fixed wing aircraft,” *flght tester*, no.1 November 2016, 2017, doi: 10.12989/aas.2017.4.1.065.

[13] R. Zhai, Z. Zhou, W. Zhang, S. Sang, and P. Li, “Control and navigation system for a fixed-wing unmanned aerial vehicle,” *AIP Adv.*, vol. 4, no. 3, 2014, doi: 10.1063/1.4866169.

[14] A. Gupta, “Modeling and Control of an Aircraft System (for Aerospace Applications),” *Natl. Inst. Technol. Rourkela Rourkela-769008, Odisha, India. Certif.*, no.2 May, 2015, [Online]. Available: http://ethesis.nitrkl.ac.in/7821/

[15] S. R. Barros Dos Santos and N. M. F. De Oliveira, “Longitudinal autopilot controllers test platform hardware in the loop,” *2011 IEEE Int. Syst. Conf. SysCon 2011 - Proc.*, pp. 379–386, 2011, doi: 10.1109/SYSCON.2011.5929071.

[16] K. D. Solomon Raj and P. R. Kumar, “Design and simulation of longitudinal autopilot modes for a conventional aircraft,” *2nd Int. Conf. Electron. Commun. Syst. ICECS 2015*, no. Icecs, pp. 1040–1045, 2015, doi: 10.1109/ECS.2015.7124738.

[17] M. T. Hagan, *Neural networks 2nd edtion by PWS*. 2018. doi: 10.1007/1-84628-303-5.

[18] W. C. Parke, *Neural Networks and Brains*, Thrid Edit. Biophysis, 2020. doi: 10.1007/978-3-030-44146-3_14.

[19] A. J. I, O. A. Ezechukwu, and P. C. Uwaechi, “Analysis of Neural Network Back-Propagation Algorithm,” *IRE 1700753 ICONIC Res. Eng. JOURNALS*, vol. 2, no. 4, pp. 33–37, 2018.

[20] T. I. Fossen, “Mathematical Models for Control of Aircraft and Satellites,” *Nor. Univ. Sience Technol.*, no.1 January, pp. 1–31, 2011.

[21] RTI, “User ’ s Manual User ’ s air crafts modeling,” vol. 2886, no. 408, 2012, pp. 1–38.

[22] M. V. Cook, *Flight Dynamics Principles*, Second edi. ELSEVIER, 2017. doi: 10.1016/B978-0-7506-6927-6.X5000-4.

[23] HACKER T, “Neutral Dynamic Stability of Aircraft,” *Rev Roum. des Sci. Tech. Mec. Appl.*, vol. 13, no. 5, pp. 861–870, 2017.

[24] M. V. Cook, “Longitudinal Dynamics,” in *Flight Dynamics Principles*, Second edi., ELSEVIER, 2013, pp. 147–181. doi: 10.1016/b978-0-08-098242-7.00006-7.

[25] M. Liu, X. Dong, Q. Li, and Z. Ren, “Model Reference Adaptive Control of a Quadrotor UAV based on RBF Neural Networks,” *IEEE CSAA Guid. Navig. Control Conf. CGNCC 2018*, 2018, doi: 10.1109/GNCC42960.2018.9019021.

[26] K. J. H. Astrom and Tore, “PID controllers: theory, design, and tuning,” vol. 2. instrument socity of America, 2016.

[27] T. Win, H. T. C. Nyunt, and H. M. Tun, “Pitch Attitude Hold Autopilot for YTU EC-001 Fixed-Wing Unmanned Aerial Vehicle,” *2019 1st Int. Symp. Instrumentation, Control. Artif. Intell. Robot. ICA-SYMP 2019*, no.2 May, pp. 78–81, 2019, doi: 10.1109/ICA-SYMP.2019.8646286.

APPENDIX I

Neural network training code

```
x = input'; % error, set point and fixed wing airplane output.
t = output'; % saturation of control signal.
% Select a Training Function
% 'trainlm' is mostly take small time.
trainFcn ='trainlm'; % Levenberg-Marquardt learning.
% Create a appropriate Net
inputlayersize=3;
hiddenLayerSize = 30;%By changing the amount of hidden layer dimensions.
% We will observe how the matching works.
net = fitnet(hiddenLayerSize,trainFcn);
% Setup Divided of Data for Training, Validation, Testing
net.divideParam.trainRatio = 0.9
net.divideParam.valRatio = 0.05;
net.divideParam.testRatio = 0.05;
net.trainparam.epochs=10000;
% Training the Net
[net,tr] = train(net,x ,t);
% check the Net
y = net(x);
e = gsubtract (t,y);%gates 2 transfer function and minus those system.
Performance = perform (net,t,y)
% showthe Net
% show (net)
net = configure(net,x,t)
gensim (net)
```

APPENDIX II

Short period MRAC different gamma value

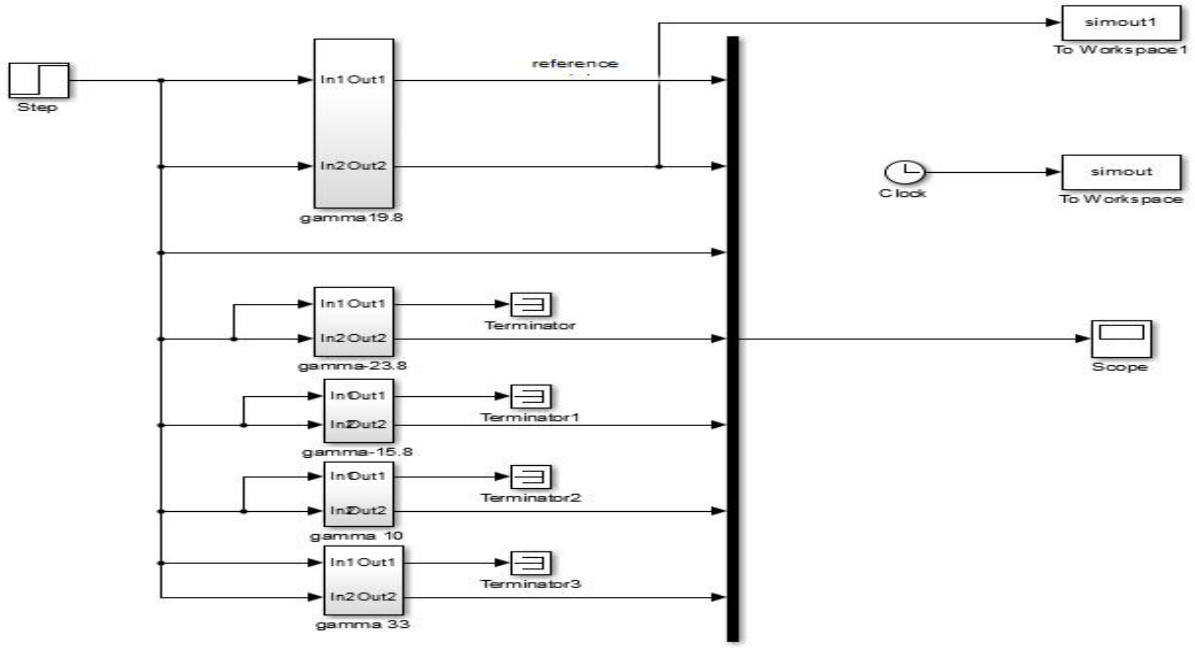

Phugoid mode oscillation MRAC different gamma value

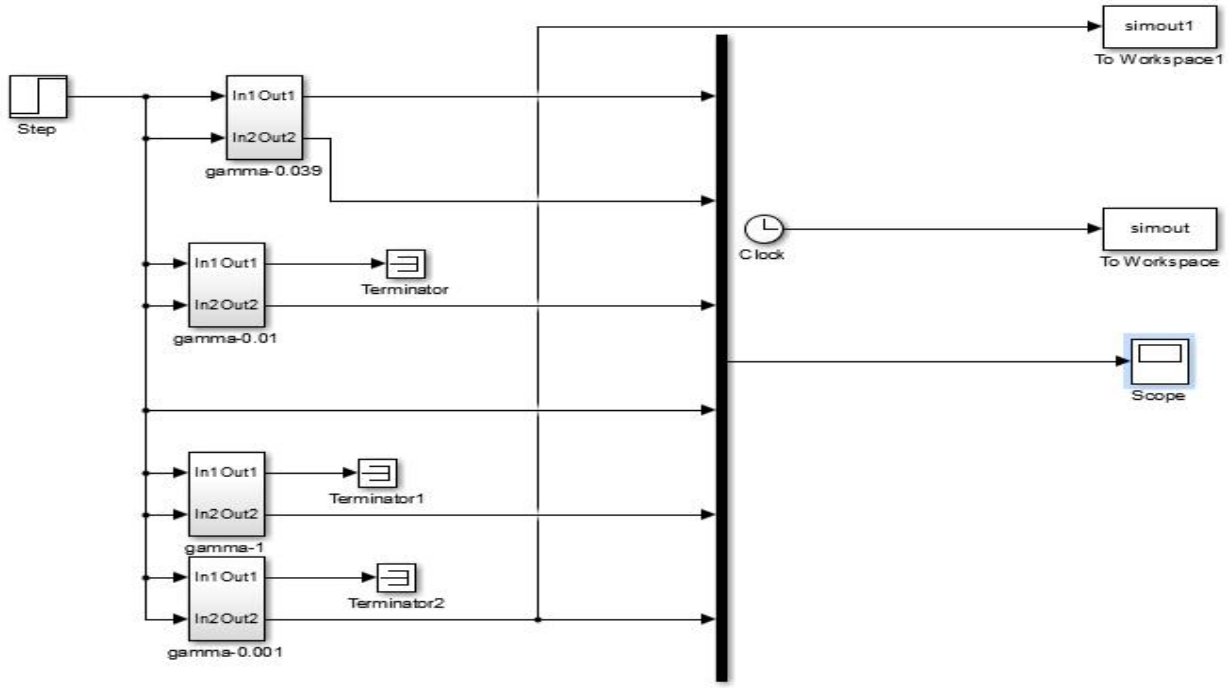

Comparison of Different controller short period oscillations

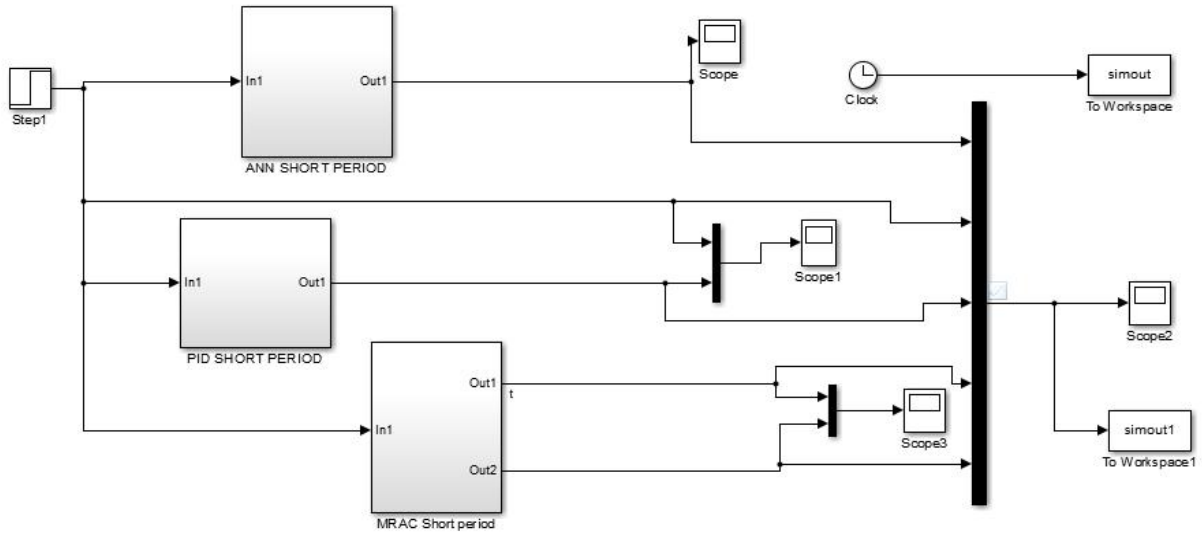

Comparison of Different controller phugoid mode oscillations

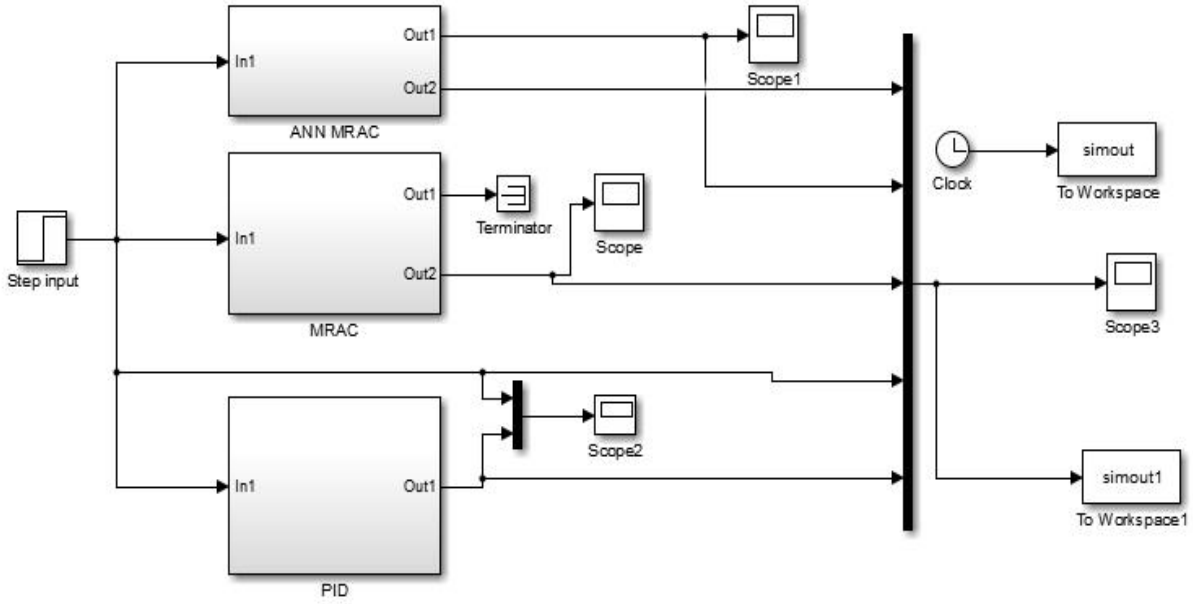

APPENDIX III

Train data of Short period oscillation pitch angle control

No	Input train data			Output train data
1.	0	0	1	0
2.	-1.99584545869906e-57	2.92514606337708e-68	1	3.92321333466018e-66
3.	-8.07817335011363e-06	7.85795353782590e-17	1	1.05027227746890e-08
4.	-0.000287903496262826	6.06761465265887e-13	1	2.25154705270931e-06
5.	-0.00730662473185849	2.15558526987281e-09	1	0.000299019517628339
6.	-0.0451854734692767	2.47799868455009e-07	1	0.00496967944658738
7.	-0.134578244998036	4.95306944780555e-06	1	0.0285150257131563
8.	-0.279324717236056	4.32504397356778e-05	1	0.0982925995805076
9.	-0.447492917741370	0.000205436773113018	1	0.233787368574056
10.	-0.659755455244645	0.000930326138088306	1	0.526213134144641
11.	-0.869921503793691	0.00399524623713300	1	1.10728097771089
12.	-0.981690343786429	0.0128234586901609	1	1.93497009387095
13.	-0.997633791093042	0.0302203628068154	1	2.84531543057344
14.	-0.961257893974692	0.0610763959397542	1	3.84646528065166
15.	-0.893685160490649	0.114080740838977	1	4.98705447564351
16.	-0.794035884976035	0.205691829103154	1	6.35713167771390
17.	-0.673196246965631	0.326096920965015	1	7.69170498333006
18.	-0.535009966053032	0.464927170849972	1	8.90663915261447
19.	-0.337158298832834	0.663016318289603	1	10.2801775861028
20.	-0.182974019133443	0.817064719975311	1	11.1261417809614
21.	-0.0772132776469567	0.922256633673060	1	11.5888373525904
22.	-0.0313279182537969	0.968667645563855	1	11.7486985019818
23.	-0.00860342407943904	0.991878361245229	1	11.8079251840822
24.	-0.000494022779124026	0.999467494989869	1	11.8186194458727
25.	0.00226962098423456	1.00186357676621	1	11.8147214990983
26.	0.00125382310709066	1.00136496120400	1	11.8090196477009
27.	-0.000141745928506465	1.00036691359390	1	11.8060821281192
28.	-4.29462003935788e-05	0.999810732358902	1	11.8063897402346
29.	-0.000208257447218640	0.999540868275131	1	11.8073187665447
30.	-0.000593820773741149	0.999536605804290	1	11.8084562550300
31.	-0.000583593571555907	0.999660085536623	1	11.8100731304461
32.	3.95530731114313e-05	0.999782443017154	1	11.8112959454537
33.	7.13247702711639e-05	0.999882008832772	1	11.8114537492222
34.	-0.000250399080838237	0.999949497998928	1	11.8115242250631
35.	-8.71779848329313e-05	0.999985930231621	1	11.8118953634015
36.	0.000235163327112375	0.999998497478950	1	11.8120782453442
37.	7.41628269554928e-05	1.00000171993285	1	11.8117068637390
38.	-0.000418314589419655	1.00000822132242	1	11.8114817616290
39.	-1.03325285341072e-05	1.00000473713673	1	11.8119865725845
40.	0.000364969111626978	0.999996857199566	1	11.8120742486341

41.	-3.23116789774369e-05	0.999998585531945	1	11.8116371341163
42.	-0.000150075355311419	1.00000164383776	1	11.8117294400881
43.	3.27924782593803e-05	1.00000000637165	1	11.8119002877300
44.	0.000306404718255604	0.999995356927559	1	11.8119560467119
45.	-0.000262166907949224	0.999998770989846	1	11.8113019358118
46.	-0.000163877898218923	1.00000250351032	1	11.8117659520267
47.	4.00015934534093e-05	0.999999930109311	1	11.8118818608046
48.	0.000169387097331608	0.999997005219885	1	11.8118477513267
49.	-0.000471068019286536	1.00000141102905	1	11.8111663178208
50.	-0.000143714456584121	1.00000285658596	1	11.8118200544673
51.	5.69146427655820e-05	0.999999717375566	1	11.8118876895828
52.	6.55088617705912e-05	0.999998490929971	1	11.8118003964607
53.	-0.000359792532323988	1.00000237011210	1	11.8114276428628
54.	-8.48098434929057e-05	1.00000249730912	1	11.8118869649360
55.	0.000111556689755266	0.999999043243712	1	11.8119215348650
56.	2.69144958936485e-05	0.999998699328718	1	11.8117549580571
57.	-0.000441969591321367	1.00000432531099	1	11.8114554909419
58.	-4.09486605166265e-05	1.00000540845661	1	11.8121995302858
59.	0.000217195721851859	0.999997597298989	1	11.8119742298894
60.	-7.76887914288871e-06	0.999999511042078	1	11.8117655301441
61.	-0.000246807632084067	1.00000301803636	1	11.8116657397551
62.	0.000146255734088663	1.00000316793815	1	11.8123195552305
63.	0.000184217537666065	0.999997558057260	1	11.8119171620010
64.	-2.02896980827649e-05	0.999999789755354	1	11.8117681636568
65.	-0.000182545360454034	1.00000261665001	1	11.8117373772527
66.	0.000298065362066668	1.00000123094764	1	11.8124069510974
67.	0.000169987266492644	0.999997360667753	1	11.8118775999801
68.	-3.36905921163311e-05	0.999999977121645	1	11.8117618018608
69.	-0.000161812795767213	1.00000273459585	1	11.8117809694734
70.	0.000443695210944228	0.999999111764715	1	11.8124691832795
71.	0.000150214674299209	0.999997187003949	1	11.8118309587265
72.	-5.07646526681782e-05	1.00000020945321	1	11.8117531691841
73.	-7.93216611745251e-05	1.00000168649293	1	11.8118288260205
74.	0.000372952240963120	0.999997846167817	1	11.8122489864926
75.	9.45968283175835e-05	0.999997530680011	1	11.8117686459908
76.	-3.69386097927027e-05	1.00000001157660	1	11.8117593521920

Train data of Phugoid mode oscillation pitch angle control

No	**Input data**			**Output data**
1.	1	0	0	0
2.	1	-1.99584545872826e-57	5.87353599499460e-71	7.88673519939994e-69
3.	1	-8.07817335019205e-06	1.58031315460360e-19	2.11137210420237e-11
4.	1	-0.000287903496868365	1.22234428712479e-15	4.52630593578531e-09
5.	1	-0.00730662688306313	4.38063412944130e-12	6.01121804012010e-07
6.	1	-0.142934154102349	1.23189151380499e-08	6.32999146571220e-05
7.	1	-0.440072815488554	4.34524083652489e-07	0.000454724050482076
8.	1	-0.713906161216534	3.17761380614953e-06	0.00127155795068557
9.	1	-0.912726212843842	1.41774454733001e-05	0.00259609439423775
10.	1	-1.00821724359818	4.59988906645413e-05	0.00433819007402848
11.	1	-1.02858789759512	0.000114391464036731	0.00624665386544296
12.	1	-1.01869075853840	0.000254792959769400	0.00841929127689239
13.	1	-1.00444492466130	0.000551576406813922	0.0110674370631199
14.	1	-0.997850246393458	0.00126770756924825	0.0147410964272438
15.	1	-0.997102508567987	0.00239634728814732	0.0183249417981142
16.	1	-0.995514226194304	0.00450529227909596	0.0227372553346432
17.	1	-0.990413438698573	0.00981237384448783	0.0296794918980249
18.	1	-0.982286156206973	0.0176250255676753	0.0362868895274301
19.	1	-0.973376571107114	0.0264864991534117	0.0417397455530583
20.	1	-0.962305340497345	0.0377307824900758	0.0471418812146898
21.	1	-0.940594859861127	0.0597523001178896	0.0552156311957352
22.	1	-0.915405908778712	0.0840317699099661	0.0620739977252936
23.	1	-0.897598952646809	0.102191146734649	0.0663748613038913
24.	1	-0.877567307327791	0.122482501135570	0.0706149281954389
25.	1	-0.842900675657875	0.157197763817235	0.0768889988957211
26.	1	-0.799358219883337	0.200342656501559	0.0835044307630851
27.	1	-0.765130545866358	0.234764447030050	0.0881264157395214
28.	1	-0.727925971069271	0.272144061672408	0.0926632092952959
29.	1	-0.675066960525175	0.324996100746191	0.0984273759348205
30.	1	-0.609577954653566	0.389911653498669	0.104725327684627
31.	1	-0.548917173499822	0.450829583759581	0.110034489803833
32.	1	-0.496829761536912	0.503589224275448	0.114255275435259
33.	1	-0.447878863160075	0.552138208241373	0.117869322508776
34.	1	-0.375468028199967	0.624296057696216	0.122799929650219
35.	1	-0.302523714290871	0.697485288104549	0.127281900389101
36.	1	-0.240524784936285	0.759634512870014	0.130671682606094
37.	1	-0.176400429192763	0.823580812527766	0.133732436016516
38.	1	-0.0716877747683167	0.927780919133615	0.137676494961578
39.	1	0.0148298532091511	1.01523785310510	0.139811545105079
40.	1	0.0700539250223173	1.07033408478238	0.140515235870370
41.	1	0.125790656897385	1.12576424978036	0.140637843504192
42.	1	0.219919931788320	1.21971721005776	0.139284319116528
43.	1	0.310023392288618	1.31024881458264	0.135730515463059
44.	1	0.371940103120458	1.37208892514018	0.131751570187246

45.	1	0.432593304388975	1.43255624309838	0.126379586198073
46.	1	0.524184810572548	1.52399407258099	0.114786963012783
47.	1	0.604634065509361	1.60518759153999	0.0998226038518159
48.	1	0.651392906381155	1.65155591905212	0.0885443560873526
49.	1	0.693915588823093	1.69385878813952	0.0758061877582847
50.	1	0.746071657222162	1.74600610398904	0.0552502207703372
51.	1	0.790974538086977	1.79133142291521	0.0289239891193736
52.	1	0.812442766739899	1.81253116766060	0.00912508731988111
53.	1	0.823686955063699	1.82358923291661	-0.0110542017430174
54.	1	0.822303243021194	1.82227152380768	-0.0346546520774661
55.	1	0.797463823863247	1.79797661860724	-0.0609992518780069
56.	1	0.756589836753728	1.75667413033237	-0.0800313488269539
57.	1	0.704407977467175	1.70383917098489	-0.0933237164184196
58.	1	0.650118974042613	1.65012919417706	-0.101137956317660
59.	1	0.554678240381818	1.55501869130488	-0.107352604498036
60.	1	0.454902848964248	1.45483233810728	-0.107585047709120
61.	1	0.356453138329342	1.35630413099412	-0.103836847132043
62.	1	0.249144771061925	1.24917689366035	-0.0967177967206104
63.	1	0.0724622419701209	1.07284459055833	-0.0804240590011487
64.	1	-0.0858300790355163	0.913673731575432	-0.0625774437824288
65.	1	-0.190281073233742	0.809500103056111	-0.0498639369871939
66.	1	-0.294931328803772	0.705112160296167	-0.0365412472484300
67.	1	-0.456233814136917	0.543893761963466	-0.0151157864598533
68.	1	-0.616596628941612	0.383093074210936	0.00710529698605548
69.	1	-0.722828569095654	0.277054138462807	0.0222603397769432
70.	1	-0.822785598454295	0.177271342749103	0.0370173007865679
71.	1	-0.948124834560481	0.0519527029191907	0.0565879542169812
72.	1	-1.06629656647358	-0.0668039301876792	0.0769630733344026
73.	1	-1.13470936322397	-0.134801128001998	0.0900581568741353
74.	1	-1.19203270414167	-0.191929619170766	0.102514035248183
75.	1	-1.24477259017096	-0.244753326618601	0.116289771579716
76.	1	-1.28803546347512	-0.288530717962116	0.132227244173637
77.	1	-1.30382762928939	-0.303870236155361	0.143852963897895
78.	1	-1.30301153353798	-0.302755150240182	0.150470791404899
79.	1	-1.29254876860184	-0.292551350596040	0.155985277883904
80.	1	-1.25271123154600	-0.253104469509937	0.162781318712505
81.	1	-1.19719609023232	-0.197046711253924	0.165499995092178
82.	1	-1.15350598700225	-0.153257751127493	0.165655357006283
83.	1	-1.10301727372012	-0.103028273192412	0.164691305163108
84.	1	-0.999330930788482	0.000389144799201085	0.160441576183318
85.	1	-0.890095022645344	0.110116611138568	0.153997722018495
86.	1	-0.815746258546175	0.184458214747793	0.148957701912854
87.	1	-0.737895783685782	0.262082358873251	0.143305402231988
88.	1	-0.599092519423858	0.400669973339058	0.132529325346682
89.	1	-0.465385163339811	0.534964812522093	0.121468092519869
90.	1	-0.381454132902109	0.618736485438844	0.114287611666443
91.	1	-0.298077508946816	0.701887889928411	0.106909958890112
92.	1	-0.164404589352135	0.835422779557274	0.0943692087480397

93.	1	-0.0395628835029054	0.960847737723851	0.0814347062592142
94.	1	0.0371095530392309	1.03725870142128	0.0727406022884300
95.	1	0.109517793427790	1.10946814419764	0.0637194797111573
96.	1	0.206319428780118	1.20623479191172	0.0499106171220674
97.	1	0.298200599144083	1.29862354817214	0.0339432189859598
98.	1	0.351700284090481	1.35180125329535	0.0228009576213126
99.	1	0.396982575666882	1.39690075713310	0.0115148062443206
100.	1	0.441225766504825	1.44119079263562	-0.00250491328643296
101.	1	0.475261031020419	1.47575115964919	-0.0187038575783502
102.	1	0.487721225022433	1.48787530487597	-0.0311971872617859
103.	1	0.485659259922596	1.48508519386405	-0.0400449189398744
104.	1	0.474139858163644	1.47413657599911	-0.0458167269784333
105.	1	0.442748700996719	1.44311757961231	-0.0516730867715793
106.	1	0.402091194151755	1.40204029469797	-0.0536072232872361
107.	1	0.358020229589689	1.35786420004644	-0.0527305333327826
108.	1	0.305915409325397	1.30593975125343	-0.0495205262763064
109.	1	0.209927958669457	1.21032638778696	-0.0399052328146121
110.	1	0.118686391934446	1.11822231989071	-0.0277594554363746
111.	1	0.0580329479835535	1.05778895024434	-0.0187438589638383
112.	1	-0.00429107420559405	0.995744444746003	-0.00881889564109262
113.	1	-0.108646363810497	0.891529778670420	0.00905958682309288
114.	1	-0.209720535868794	0.789980537356053	0.0276542961958587
115.	1	-0.277238808229939	0.722622340443261	0.0405382669558798
116.	1	-0.341700673579614	0.658345954337206	0.0532365827191847
117.	1	-0.428872041965230	0.571240046008933	0.0711485834215498
118.	1	-0.507446562308896	0.492064696691700	0.0883780412342086
119.	1	-0.552219595680650	0.447663774946040	0.0986632818996942
120.	1	-0.590093937388911	0.409980644559999	0.108001976746034
121.	1	-0.628262924876270	0.371775985246084	0.118574048258197
122.	1	-0.657417987344860	0.342136102482147	0.128967823760260
123.	1	-0.668393985902518	0.331383187240656	0.135898385270121
124.	1	-0.667314523891683	0.333261406549124	0.139951173781512
125.	1	-0.658384407050097	0.341630357464690	0.142234697038164
126.	1	-0.635318150120798	0.364395787839453	0.143976799881570
127.	1	-0.604046105826006	0.395976750862532	0.143994275314761
128.	1	-0.569208690918794	0.430944803902026	0.142852693929062
129.	1	-0.527841258051085	0.472135637666942	0.140727146371404
130.	1	-0.453064971022064	0.546416958843934	0.135714153881663
131.	1	-0.385631888897037	0.614804748183783	0.130264785386236
132.	1	-0.339443960948710	0.660820142203835	0.126276570450042
133.	1	-0.291582175837392	0.708386251065960	0.121913233842694
134.	1	-0.209920482206088	0.789890571349708	0.113895308234547
135.	1	-0.129665577095645	0.870593464013836	0.105244057537525
136.	1	-0.0740083095731786	0.926134709740513	0.0988202114955849
137.	1	-0.0193636820342975	0.980594259688879	0.0920733114264192
138.	1	0.0599658441649983	1.05982132327371	0.0812709451661209
139.	1	0.132957269934060	1.13347384091660	0.0698254973233444
140.	1	0.176719489749075	1.17685526935665	0.0622185790441051

141.	1	0.216636228997000	1.21657109419172	0.0544749031719593
142.	1	0.263889690183818	1.26383981312835	0.0438837321797289
143.	1	0.308329957878352	1.30873631599947	0.0315254847397415
144.	1	0.332627570080244	1.33270091840100	0.0231076194501271
145.	1	0.349780423887246	1.34964929751390	0.0152094725944553
146.	1	0.359923575061562	1.35991034301712	0.00733987985570983
147.	1	0.359185814744847	1.35972917050499	-0.000997215631274112
148.	1	0.348154478876063	1.34812901229793	-0.00600167131866516
149.	1	0.333864540278046	1.33363523142139	-0.00834679337070937
150.	1	0.314179393953547	1.31418990716984	-0.00957360431702206
151.	1	0.269653733356605	1.27000161725656	-0.00894826434537505
152.	1	0.220634496054630	1.22039531116767	-0.00545679280609054
153.	1	0.185867013608056	1.18563453629286	-0.00197966796684668
154.	1	0.148283309239412	1.14830323958807	0.00243378968695343
155.	1	0.0789185589347512	1.07915532979496	0.0120006416150956
156.	1	0.0105418330663589	1.01026159839238	0.0228974203477056
157.	1	-0.0342271912164586	0.965591563786420	0.0305385601317036
158.	1	-0.0788563339178686	0.921175281058352	0.0385316702377824
159.	1	-0.150478974578223	0.849718666317697	0.0521556349310793
160.	1	-0.214081625994491	0.785470116824773	0.0652190356388299
161.	1	-0.251475295874636	0.748357629091476	0.0731587717393823
162.	1	-0.285755222432139	0.714292122821717	0.0807676813638626
163.	1	-0.330265371602493	0.669827542498365	0.0913400481726583
164.	1	-0.368125104358592	0.631490639191521	0.101459256752243
165.	1	-0.388043842850895	0.611850384725752	0.107405834177911
166.	1	-0.402455270996175	0.597618053046238	0.112548742042558
167.	1	-0.412638539026961	0.587406781930519	0.117938003051651
168.	1	-0.412457033685504	0.587051388831638	0.122485369767127
169.	1	-0.403067210556913	0.596714958241515	0.124868158491930
170.	1	-0.389341880444856	0.611166965046552	0.125770946453999
171.	1	-0.372476100926021	0.627536435806502	0.125833514775704
172.	1	-0.341694511543127	0.658017994560406	0.124838562198118
173.	1	-0.307618609144470	0.692406705546044	0.122840355027620
174.	1	-0.274988544435341	0.725167679419899	0.120433099348807
175.	1	-0.239088386121811	0.760890046947257	0.117415465448680
176.	1	-0.177739794638015	0.821783366407018	0.111546890274552
177.	1	-0.125191821022766	0.875245113296150	0.105744540867566
178.	1	-0.0911081492549153	0.909156766325305	0.101768454866303
179.	1	-0.0568019319746090	0.943167378299284	0.0975344751417633
180.	1	-0.000349439606329716	0.999460203612233	0.0899358024583953
181.	1	0.0522125008125895	1.05246820097049	0.0819885146636092
182.	1	0.0871405747606155	1.08728469780785	0.0762564289699745
183.	1	0.120118136205722	1.12007688672672	0.0703868285546355
184.	1	0.165497390752515	1.16534775569333	0.0612901688616994
185.	1	0.203154331410961	1.20367415935177	0.0522467376584449
186.	1	0.223962159396347	1.22410113857906	0.0466080222143745
187.	1	0.241088472572210	1.24102475197987	0.0411752356584811
188.	1	0.258193322334442	1.25814138762377	0.0342400764171258

189.	1	0.268532971581191	1.26893352640212	0.0270860996183346
190.	1	0.270208694842127	1.27028439538697	0.0228694637938875
191.	1	0.266516281910032	1.26639095441820	0.0194942688135813
192.	1	0.255957645621288	1.25594206417689	0.0168442387099102
193.	1	0.233149825060569	1.23368666702051	0.0153482304890170
194.	1	0.208054568850080	1.20804376676975	0.0158063425583431
195.	1	0.186431460640031	1.18620023186731	0.0170813967211718
196.	1	0.161759280472159	1.16176873586473	0.0191287057367945
197.	1	0.114315848970956	1.11467584623722	0.0243407625568302
198.	1	0.0691280708403873	1.06889868235180	0.0305457428429525
199.	1	0.0396548520388956	1.03941795333131	0.0349897031149421
200.	1	0.00945522595609405	1.00947380173887	0.0398131554305953
201.	1	-0.0427405389350122	0.957501583096315	0.0488409751243759
202.	1	-0.0899347969016313	0.909798522543332	0.0578129037984243
203.	1	-0.119082002200788	0.880734541705783	0.0636000882911205
204.	1	-0.146790040313969	0.853240079049046	0.0693240559168213
205.	1	-0.188356371927042	0.811847734799746	0.0784930533068754
206.	1	-0.221236471733749	0.778326197610573	0.0866125236993944
207.	1	-0.238966332316836	0.760862281397831	0.0912449507511503
208.	1	-0.253710197462506	0.746335228723865	0.0954771081729882
209.	1	-0.269904632921784	0.730196387066711	0.101047966711008
210.	1	-0.278585933713883	0.721030747723139	0.105801775709923
211.	1	-0.280243717140533	0.719645969152521	0.108262218983482
212.	1	-0.277991459113992	0.722077118009093	0.110114379350482
213.	1	-0.269184015191031	0.730866187903963	0.111626515680936
214.	1	-0.250856479004091	0.748656874391731	0.112108751860430
215.	1	-0.229472906485205	0.770266133059160	0.111448779685385
216.	1	-0.209251489803760	0.791240585383842	0.110235952707807
217.	1	-0.188783693104409	0.811234430174514	0.108760707570655
218.	1	-0.156705028143343	0.843048787637573	0.105960644296812
219.	1	-0.123858360233797	0.876152901911687	0.102595896817435
220.	1	-0.0946194771431912	0.905537572884189	0.0992889381314614
221.	1	-0.0642755905674285	0.935704086385955	0.0956028988329799
222.	1	-0.0162759185879892	0.983171726335969	0.0892045661556996
223.	1	0.0205373269691522	1.02094997548595	0.0835390842982558
224.	1	0.0437038453013821	1.04397985305603	0.0798078169732569
225.	1	0.0661587605199885	1.06613084467858	0.0759795369532360
226.	1	0.101022116776440	1.10082289958652	0.0694103109256885
227.	1	0.130464358693745	1.13069890537842	0.0629972252378079
228.	1	0.148648859396067	1.14879606739892	0.0586190440822766
229.	1	0.164490022743898	1.16445156899238	0.0543668998827218
230.	1	0.183735698195353	1.18355952949448	0.0481298103235180
231.	1	0.194913560667146	1.19545519094996	0.0427283966290382
232.	1	0.199253873540444	1.19940826701570	0.0397688184251848
233.	1	0.200635108933930	1.20057615371640	0.0372048243866148
234.	1	0.197561998248861	1.19750134745060	0.0343556325326794
235.	1	0.186849381877964	1.18722119787202	0.0322985223354210
236.	1	0.175728831264855	1.17581321424740	0.0317094872785016

237.	1	0.161332038050031	1.16122605825150	0.0318560987619355
238.	1	0.140624618606749	1.14059869887201	0.0329554857639618
239.	1	0.110097765604121	1.11061574922242	0.0356297060740575
240.	1	0.0820489833844249	1.08210004633728	0.0389440519733075
241.	1	0.0606173535477624	1.06037902727468	0.0418331545245260
242.	1	0.0379084155315077	1.03791313929541	0.0450972109423282
243.	1	-0.00229560738627133	0.998124607316315	0.0514680096587486
244.	1	-0.0359708237069668	0.963843057076412	0.0575049250307514
245.	1	-0.0563419795509053	0.943398700797774	0.0613323274303281
246.	1	-0.0763355214280048	0.923676686999000	0.0651965762780946
247.	1	-0.109028172257368	0.891238513567630	0.0719622962210942
248.	1	-0.135288215611355	0.864508679075230	0.0780242197841245
249.	1	-0.150237740978797	0.849569890945309	0.0816814097395072
250.	1	-0.163475905922582	0.836547617062627	0.0851122400462394
251.	1	-0.181052186481768	0.819183891744832	0.0903199058339819
252.	1	-0.190962811850720	0.808647888014608	0.0944089241052823
253.	1	-0.194740398685020	0.805067210563990	0.0964904985879042
254.	1	-0.196311103273825	0.803726000563401	0.0982253563451097
255.	1	-0.193922262704751	0.806227989591882	0.100273887553335
256.	1	-0.185237877427585	0.814377939981225	0.101394185046040
257.	1	-0.177254425603688	0.822609898283803	0.101616290775582
258.	1	-0.167091686286312	0.832960402274583	0.101447479368808
259.	1	-0.148971000978715	0.851106716373348	0.100551732786308
260.	1	-0.124384071587179	0.875161947601517	0.0987164295108218
261.	1	-0.106612336761881	0.893291863738157	0.0970148357764336
262.	1	-0.0874622906701157	0.912628200962453	0.0949759515280494
263.	1	-0.0626304888485398	0.937396732807221	0.0920754060256714
264.	1	-0.0301978512269334	0.969306971748595	0.0879045043539214
265.	1	-0.00306585845238216	0.996833946876957	0.0839132346268743
266.	1	0.0149491741414927	1.01521043516909	0.0810393878466658
267.	1	0.0330890513990560	1.03309058376713	0.0780619337422993
268.	1	0.0634872504675649	1.06303861735317	0.0726023635202666
269.	1	0.0861601304334871	1.08627101827854	0.0678369266777519
270.	1	0.0988198127381843	1.09909210121664	0.0649406250599239
271.	1	0.110639513562386	1.11063293722331	0.0621023956353018
272.	1	0.128012272433016	1.12771236186642	0.0572755636544058
273.	1	0.138906380552269	1.13906463886090	0.0532291039590369
274.	1	0.143762748984086	1.14396884433203	0.0509199146408320
275.	1	0.147023784665080	1.14700601201237	0.0488526819526861
276.	1	0.148052623515220	1.14778895327565	0.0459298175038674
277.	1	0.143119715283619	1.14344756934351	0.0440580317462442
278.	1	0.138247665819905	1.13845560059888	0.0433592445895695
279.	1	0.131803627645202	1.13177402008784	0.0430081151830647
280.	1	0.117171453559142	1.11697485886464	0.0432197311765132
281.	1	0.0984880835697171	1.09885317745123	0.0443735792792015
282.	1	0.0853503635420145	1.08551152912036	0.0455953966537034
283.	1	0.0711250791209519	1.07108215614631	0.0471622454416458
284.	1	0.0475302890745584	1.04741497659968	0.0501597546769952

285.	1	0.0208329950176513	1.02126233415237	0.0539622651727288
286.	1	0.00360123451074301	1.00372076878463	0.0567631478066243
287.	1	-0.0136982848326819	0.986236422636786	0.0597346274952520
288.	1	-0.0365723474607459	0.963376891094838	0.0638887311770699
289.	1	-0.0623335904219156	0.938125975986521	0.0688537859228774
290.	1	-0.0781920615009044	0.921879161982440	0.0722959352793930
291.	1	-0.0927388093065964	0.907125891922261	0.0756314990227655
292.	1	-0.107069570489981	0.892921812212642	0.0791052357804767
293.	1	-0.122803675015309	0.877754819053055	0.0832908418580439
294.	1	-0.131269264146880	0.868677992866847	0.0863053038122252
295.	1	-0.135463531242249	0.864299614307291	0.0881289378867576
296.	1	-0.138448373049263	0.861562334820500	0.0897094864427757
297.	1	-0.139604260630706	0.860720726368754	0.0918383863160450
298.	1	-0.135637423153152	0.864133623116831	0.0930776219999214
299.	1	-0.131597118246201	0.868180603378563	0.0935117557236562
300.	1	-0.126395740453125	0.873624930326598	0.0936926880469481
301.	1	-0.114194707391397	0.886042162473045	0.0934214566891860
302.	1	-0.0987592866335536	0.900937042779818	0.0925158264837671
303.	1	-0.0881031592750019	0.911712502646782	0.0916307762071162
304.	1	-0.0766701534352648	0.923362483385084	0.0905242418832819
305.	1	-0.0560151241804836	0.944175950874353	0.0882424490815688
306.	1	-0.0340123528191630	0.965547162227528	0.0855640253653635
307.	1	-0.0204592946065828	0.979378864713437	0.0836606625440757
308.	1	-0.00680405858628430	0.993244150916053	0.0816265548227058
309.	1	0.0134455884757039	1.01353516066495	0.0784094879553250
310.	1	0.0350898632590413	1.03469602492046	0.0747154217046796
311.	1	0.0482513332875782	1.04814740035742	0.0721475878493760
312.	1	0.0605612713910704	1.06063741834075	0.0695763952580222
313.	1	0.0748403375546247	1.07488221357619	0.0663506016380793
314.	1	0.0894689571250912	1.08897742850626	0.0626863067358620
315.	1	0.0985737309576786	1.09837843296435	0.0597455253181206
316.	1	0.103467630483537	1.10399444738035	0.0575518347314464
317.	1	0.107104927756881	1.10711437384602	0.0559253662765998
318.	1	0.109421740879666	1.10910426950106	0.0538781204815382
319.	1	0.108119914590098	1.10815408652132	0.0524494883418805
320.	1	0.105209492375457	1.10536550823678	0.0516029437779516
321.	1	0.100847213708958	1.10082506958175	0.0510921386488640
322.	1	0.0907168526704655	1.09027553243637	0.0509904217050477
323.	1	0.0780689613682832	1.07851792015053	0.0515729469345744
324.	1	0.0698522465056719	1.07011118531584	0.0522384160107665
325.	1	0.0609896125969259	1.06095748183488	0.0531180750832709
326.	1	0.0444886863269499	1.04430292166710	0.0550343005766701
327.	1	0.0265165804474807	1.02678409651298	0.0573896985323434
328.	1	0.0141409918761573	1.01428347181502	0.0592511486934499
329.	1	0.00171588112182353	1.00167309652710	0.0612623464523476
330.	1	-0.0170206118995100	0.982841987656527	0.0645061692366426
331.	1	-0.0359191869074621	0.964590717315670	0.0679306913414013
332.	1	-0.0466117839320581	0.953520020454405	0.0701631541160686

333.	1	-0.0567461530915350	0.943187263837649	0.0723669098742127
334.	1	-0.0692679453554529	0.930684263736769	0.0752345310250415
335.	1	-0.0821372348569047	0.918277403219888	0.0784059250242788
336.	1	-0.0888010713534656	0.911269655196673	0.0804554052837867
337.	1	-0.0939701536592348	0.905892253406726	0.0822922877664019
338.	1	-0.0980287492250292	0.901960615408463	0.0840274282233475
339.	1	-0.100594397128945	0.899957706020989	0.0858171580440959
340.	1	-0.0990031165270126	0.900955321937015	0.0868767474599524
341.	1	-0.0966704418906774	0.903101692219494	0.0873854408520029
342.	1	-0.0936159696602082	0.906395557255419	0.0876894755417651
343.	1	-0.0857681852611860	0.914566918822453	0.0877371100231243
344.	1	-0.0754146308045226	0.924337487146533	0.0872861135472954
345.	1	-0.0683732812211514	0.931398959629715	0.0867772776710594
346.	1	-0.0608957229110517	0.939125526906946	0.0861070013165055
347.	1	-0.0465270328654229	0.953704683920999	0.0845999122455751
348.	1	-0.0310547148341259	0.968650825186857	0.0827993889174047
349.	1	-0.0212769144012429	0.978543815177439	0.0814805238571821
350.	1	-0.0114778527820744	0.988555261952950	0.0800537195716489
351.	1	0.00481433649476193	1.00500557490968	0.0775054797912953
352.	1	0.0208495287858564	1.02039127791836	0.0748788089221452
353.	1	0.0297693381435047	1.02960661739297	0.0731704542212039
354.	1	0.0382682581947205	1.03831752033215	0.0714508975350053
355.	1	0.0499706910797608	1.05005635307498	0.0689275073622140
356.	1	0.0614593210412008	1.06107319687122	0.0662516818108364
357.	1	0.0673971299155098	1.06729563720221	0.0645217859649014
358.	1	0.0722823748434138	1.07236079173074	0.0629070516035819
359.	1	0.0769618231413625	1.07700253131372	0.0610696422676811
360.	1	0.0803598653936660	1.07986360748034	0.0592359323846974
361.	1	0.0801367824689506	1.07995792954276	0.0580042144265429
362.	1	0.0778378156716939	1.07836664302950	0.0572623941096628
363.	1	0.0759249850746357	1.07593193983102	0.0568551666651815
364.	1	0.0708241866533069	1.07048363285647	0.0566015237827522
365.	1	0.0638605512931894	1.06390200990411	0.0567414766773482
366.	1	0.0571606780249423	1.05731712788750	0.0571241536451344
367.	1	0.0498803871372202	1.04985812144185	0.0577374662996516
368.	1	0.0368931066055376	1.03647874075556	0.0591595701535682
369.	1	0.0235683311345589	1.02402447993067	0.0607487276137031
370.	1	0.0158173144209590	1.01607230214336	0.0618795122080526
371.	1	0.00803397575879228	1.00800105089792	0.0631025953604948
372.	1	-0.00530201551550236	0.994514949863621	0.0653103885407923
373.	1	-0.0186682403370931	0.981606957997256	0.0676141558672106
374.	1	-0.0270366667794949	0.973104936079800	0.0692447472771909
375.	1	-0.0348898060944639	0.965066508486726	0.0708764852617898
376.	1	-0.0457524539605783	0.954116971498180	0.0732744963728910
377.	1	-0.0558925918240110	0.944611565726563	0.0755876400350242
378.	1	-0.0606469351708611	0.939480868848306	0.0769861902991195
379.	1	-0.0646921151405537	0.935239518587847	0.0782774450964869
380.	1	-0.0689060126437997	0.931048485976717	0.0798079609896287

381.	1	-0.0721002624281627	0.928322506714897	0.0813107532138505
382.	1	-0.0721803455987690	0.927955267325266	0.0822388237200284